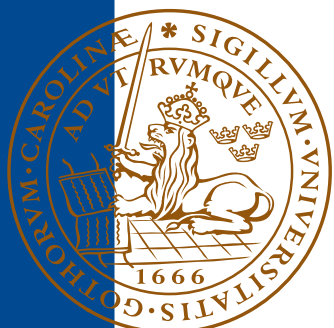
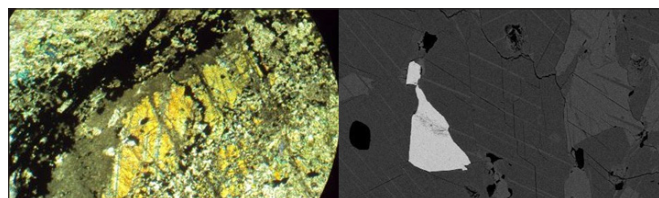


The alteration mineralogy of Svartliden, Sweden

Lawrence Nilsson

Dissertations in Geology at Lund University,
Master's thesis, no 336
(30 hp/ECTS credits)



Department of Geology
Lund University
2013

The alteration mineralogy of Svartliden, Sweden

Master's thesis
Lawrence Nilsson

Department of Geology
Lund University
2013

Contents

1 Introduction and aim	5
2 Ore geology– an introduction.....	5
2.1 Ore types	5
2.2 Alteration	5
3 Regional geology.....	6
4 Svartliden.....	7
4.1 History of Svartliden	7
4.2 Local geology	8
4.2.1 Bedrock description	8
4.2.2 Geology of Svartliden	8
4.2.3 Post ore forming processes at Svartliden and the appearance of the ore	9
5 Sampling & methods.....	9
6 Results.....	10
6.1 Results of all thin sections from both the optic microscope and the SEM	13
7 Discussion	23
8 Conclusions.....	26
9 Acknowledgements	26
10 References.....	27
11 Appendix.....	28

The alteration mineralogy of Svartliden, Sweden

LAWRENCE NILSSON

Nilsson, L., 2013: The alteration mineralogy of Svartliden, Sweden. *Dissertations in Geology at Lund University*, No. 336, 46 pp. 30 hp (30 ECTS credits).

Abstract:

Svartliden is an open gold deposit pit located in northern Sweden in the vicinity of the Skellefte mining district. The pit is located in the “Gold Line”, which is a tectonic zone containing gold mineralization's running from north-western Västerbotten to the Skellefte Field in south-eastern Västerbotten. Svartliden is of Paleoproterozoic age hosted by meta-greywacke, metavolcanics and the Revsund granitoid.

The aim of the study is to determine the alteration mineralogy that is typical for this type of deposit and to ascertain whether there are any significant changes in mineral composition and mineral chemistry within a restricted part of the alteration aureole. In order to do this, thin sections have been studied with optical and scanning electron microscopy.

The major minerals found within the studied drill core are amphibole, clinopyroxene, biotite, quartz, K-feldspar and epidote. Two types of amphibole are found: hornblende with a Mg/(Mg+Fe) atomic ratio ranging between 0.42 and 0.75 and actinolite with the Mg/(Mg+Fe) atomic ratio ranging between 0.36 and 0.89. The Al-contents vary between 0.88 and 2.21 Al-atoms calculated for 23 oxygen atoms for hornblende. The Na content varies from below the detectable limit to 0.43 and the K content from below the detectable limit to 0.09 atoms calculated for 23 oxygen atoms. For actinolite the Al content varies from below the detectable limit to 0.79 atoms and the Na content from below the detectable limit to 0.14 atoms calculated on 23 oxygen atoms. K content from below the detectable limit to 0.08 atoms calculated for 23 oxygen atoms. Actinolite appears to replace hornblende and diopside. Other, less common minerals are chlorite and chloritized biotite. The analysed plagioclase has a bytownitic composition. Retrograde metamorphism is indicated by replacement of biotite to chlorite and the mineral prehnite. The most common ore minerals are pyrrhotite and arsenopyrite. Amphibole has intergrowths of pyrrhotite and does not show any signs of chloritization. Löllingite is present and according to previous reports it is associated with gold. Calcic amphibole, diopside and calcic plagioclase are minerals common to both the Fäboliden and Svartliden deposits. The Fäboliden deposit is a gold bearing deposit approximately 20 kilometres from the Svartliden deposit that earlier has been studied more intensely.

In the studied samples the minerals seem to be of a similar composition; no zoning is recorded when approaching the ore perpendicular to the stratigraphy. The mineralization is epigenetic.

Keywords: Svartliden, alteration mineralogy, Fäboliden, amphibolite and granulite facies, Dragon Mining Sweden.

Supervisor: Anders Lindh

Lawrence Nilsson, Department of Geology, Lund University, Sölvegatan 12, SE-223 62 Lund, Sweden.
E-mail: nilsson.lawrence@gmail.com

Omvandlingsmineralogi typiskt för Svartliden, Sverige

LAWRENCE NILSSON

Nilsson, L., 2013: Omvandlingsmineralogi typiskt för Svartliden, Sverige. *Examensarbeten i geologi vid Lunds universitet*, Nr. 336, 46 sid. 30 hp.

Sammanfattning:

Svartliden är ett dagbrott som producerar guld och är beläget i närheten av Skelleftefältet i norra Sverige. Svartlidengruvan ligger i "The Gold Line", som är en tektonisk zon med guldminaliseringar som sträcker sig från nordvästra Västerbottens län till Skelleftefältet i sydost. Huvudbergarterna i Svartliden är metagråvacka, metavulkaniter och Revsundgranitoid.

Syftet med studien är att fastställa den typiska omvandlingsmineralogen för denna typ av fyndighet och att undersöka om det finns några signifikanta förändringar i mineralsammansättning och mineralalkemi inom en begränsat del av omvandlingsaureolen. För detta ändamål har tunnslip analyserats med hjälp av optisk mikroskop och svepelektronmikroskop.

Huvudmineralerna som påvisats i denna studie består av amfiboler både hornblände och aktinolit, klinopyroxen, biotit, kvarts, kalifältspat och epidot. Hornblände har ett $Mg/(Mg + Fe)$ atomförhållande mellan 0,42 och 0,75. För aktinolit är $Mg/(Mg+Fe)$ atomförhållandet mellan 0,36 och 0,89. Al-innehållet för hornblände varierar från 0,88 till 2,21 Al-atomer per 23 syreatomer. Na-innehållet för hornblände är upp till 0,43 Na-atomer per 23 syreatomer. K-innehållet för hornblende är upp till 0,09 K-atomer per 23 syreatomer. För aktinolit är Al-innehållet är upp till 0,79 och Na-innehållet upp till 0,14 joner allt räknat per 23 syreatomer. K-innehållet för aktinolit är upp till 0,08 K-atomer per 23 syreatomer. Den analyserade plagioclasen har en bytownitisk sammansättning. I de studerade tunnslipsporven syns ingen uppenbar mineralzonering. Andra mindre vanliga mineral är klorit och kloritiseras biotit. Kloritisering av biotit och närvaren av prehnit påvisar en retrograd metamorfos. De vanligaste malmminalerna är magnetkis, arsenikkis och i mindre grad löllingit. Amfibolerna kan samexistera med magnetkis. Amfibolmineralerna uppvisar inte några tecken på kloritisering. Löllengit har observerats och enligt tidigare rapporter är detta en indikator för guld förekomst. Kalciumrika amfiboler, plagioklas och diopsid i Svartliden liknar dem i Fäboliden. Fäbolidenförekomsten är en guldförekomst ungefär tjugo kilometer från Svartliden. Fäboliden har tidigare studerat mer intensivt.

I de studerade tunnslipen varierar mineralsammansättningen ytterst lite. Det finns ingen tydlig zonering i de individella kornen har kunnat påvisas vinkelrätt mot malmkroppens utsträckning. Mineraliseringen är epigenetisk.

Nyckelord: Svartliden, Fäboliden, amfibolit- och granulitfacies, Dragon Mining, Sverige.

Ämnesinriktning: Berggrundsgeologi.

Lawrence Nilsson, Geologiska institutionen, Lunds universitet, Sölvegatan 12, 223 62 Lund, Sverige.
E-post: nilsson.lawrence@gmail.com

1 Introduction

Svartliden is an open pit mine that has produced gold since 2005 with a total production of about 211000 ounces (\approx 6 ton; Dragon Mining Sweden AB 2010). Svartliden is located in northern Sweden in the vicinity of the Skellefte mining district (Fig. 1). The mine company is owned by Dragon Mining Ltd, an Australian based company. The pit is located in the “Gold Line” (Fig. 1), which is a tectonic zone that contains several gold mineralization's running from north-western Västerbotten to the Skellefte Field in south-eastern Västerbotten. The Gold Line was discovered from geochemical anomaly maps. Other elements associated with Au in the Gold Line are As, Sb and Te (Bark, 2008).

The Svartliden deposit is located in the Paleoproterozoic of the Baltic Shield (Grahn et al., 2002). The gold deposit is hosted by meta-greywacke and amphibolite. The metamorphic grade of the deposit is upper amphibolite facies (Grahn et al., 2002). The Svartliden deposit is similar to gold deposits in the Archean Yilgarn Craton, Western Australia, where some of the larger lode-vein gold deposits in the world occur. These deposits are found in amphibolite – to granulite facies terranes (Ridley, 1997).

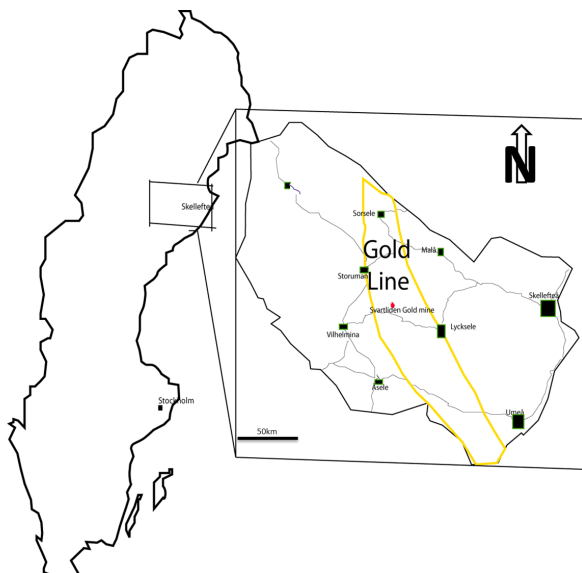


Fig. 1. Location of the Svartliden open pit and the Gold Line (Modified from Eklund, 2007 and Dragon Mining Sweden AB, 2010).

The aim of the study is:

- To determine the alteration mineralogy that is typical for this type of deposit.
- To ascertain, whether there are any significant changes in mineral composition and mineral chemistry within a restricted part of the alteration aureole.

The methods used are optical and scanning electron microscopy (SEM) together with Energy Dispersive X-ray analyses (EDS) on thin sections sampled from one drill core.

2 Ore geology – an introduction

2.1 Ore types

Ore is an economic term used to describe a valuable mineralization. This includes certain metallic elements but also gems. Ore can be classified according to several different schemes. One of these schemes classifies the ore with respect to its age relation to the host rock. Syngenetic ores are formed at the same time as their host rock and epigenetic ores are formed after their host rock.

Metasomatic mineralization's can be either hypogene or supergene. Hypogene mineralization's are formed from ascending hydrothermal solutions and supergene ones from descending solutions. The supergene process occurs due to weathering and it may be responsible for the *in situ* enrichment of ore minerals (Robb, 2005).

Orogenic gold associations occur in regional tectonic zones in epizonal, mesozonal, or hypozonal formations. Fig. 2 shows an example of how these associations are formed (Bark, 2008).

Hydrothermal deposits occur in epithermal, mesothermal or hypothermal settings. The epithermal deposits are formed at depths less than 1500 meters and temperatures between 50 and 200°C, the mesothermal ones between 1500 and 4500 meters and 200 and 400°C. The hypothermal deposits are formed at depths greater than 4500 meters and at temperatures of between 400 and 600°C (Robb, 2005).

Tectonic settings, in which hydrothermal ore deposits form, are convergent and divergent margins. The convergent margins in subduction zones have low geothermal gradients. When temperatures are reached, at which the hydrous metamorphic minerals become unstable, these minerals dehydrate. The rise of batholiths is a main energy source for the hydrothermal processes.

2.2 Alteration

The atlas of alteration (Eilu et al., 1999) divides the host rock alteration according to its metamorphic grade. This division goes beyond the concept of major facies, e.g. different alteration schemes are applied to the mid- and low-amphibolite facies. The alteration within a metamorphic facies is further divided into different alteration zones: distal, intermediate and

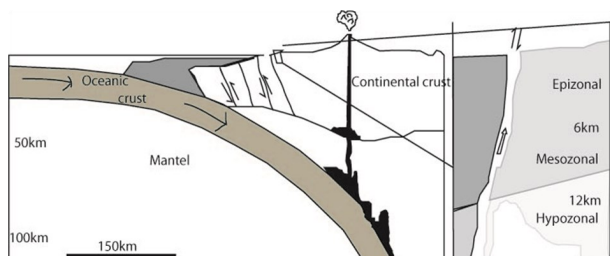


Fig. 2. The environment and the pressures of the epizonal, mesozonal and hypozonal zones of orogenic gold mineralizations (Modified from Bark, 2008).

proximal zones. This atlas of alteration is used as a guideline for identifying alterations. Ca-amphibole, diopside, plagioclase, biotite, garnet, scheelite, apatite and/or tourmaline should dominate altered, mafic rocks metamorphosed in the mid-amphibole facies. The distal and proximal zones are usually the detectable zones. However, most often, it is the proximal zone that can be clearly identified dependant on the alteration facies. As an example, in the amphibolite facies, distal alteration zones can be detected from their brownish colour, but this could be difficult in granitoids or sedimentary rocks. The zone can also be detected due to its stronger deformation compared to the unaltered rock. In higher metamorphic facies, the distal zone can be difficult to distinguish due to a low intensity of the biotitization or due to high amounts of biotite in the surrounding rocks. The proximal zone can be easier to detect due to strong banding, a diopside-enriched zone and sulphidization (Eilu et al., 1999).

Distal alteration zones are biotite dominated. Minerals found in distal alteration zones are biotite, plagioclase, hornblende, ilmenite and small amounts of pyrrhotite and quartz. Other minerals may occur, however, they are not prominent. In the lower-amphibolite facies, amphibole may be replaced by fine-grained chlorite or biotite. The rock colour in the amphibolite facies is brown due to biotitization. As described above, the distal zone can be difficult to detect (Eilu et al., 1999).

The intermediate alteration zones can be characterized by some of these minerals: biotite, pyrrhotite, diopside, tremolite, hornblende, calcite, quartz, plagioclase, ilmenite and titanite. Which of these that occur, depend on the metamorphic facies. In the lower-amphibolite facies, amphibole may be replaced by biotite (Eilu et al., 1999). The intermediate zone has not been localized at Svartliden.

The proximal alteration zone is the zone that is found immediately outside or within the ore zone. Grahn et al. (2002) call the zone highly mineralized. The most common sulphides found are pyrrhotite and arsenopyrite; löllingite may appear. Gold is found in this zone either in veins or disseminated in the wallrock. Major minerals found in this zone are diopside, pyrrhotite, arsenopyrite, biotite, hornblende, ilmenite and quartz, whereas pyrite is found only in small amounts or is totally absent (Eilu et al., 1999). The proximal zone at Svartliden compares well with this general description.

According to Grahn et al. (2002), the alteration at the Svartliden deposit can be summarized as:

- Biotite alteration; distal (10s of meters)
- Amphibole-pyrrhotite-silica; proximal (several meters)
- Amphibole-pyroxene-pyrrhotite-arsenopyrite-silica; mineralized zone
- Dark green amphibole-pyroxene-pyrrhotite-arsenopyrite-silica; highly mineralized zone

The mineralization at Svartliden is made up of pyrrhotite, arsenopyrite, löllingite and quartz (Grahn et al., 2002). This mineralization may also include graphite. This is the case in the surroundings of Svartliden, e.g. at Ekorråden (Fig. 4). Chalcopyrite is

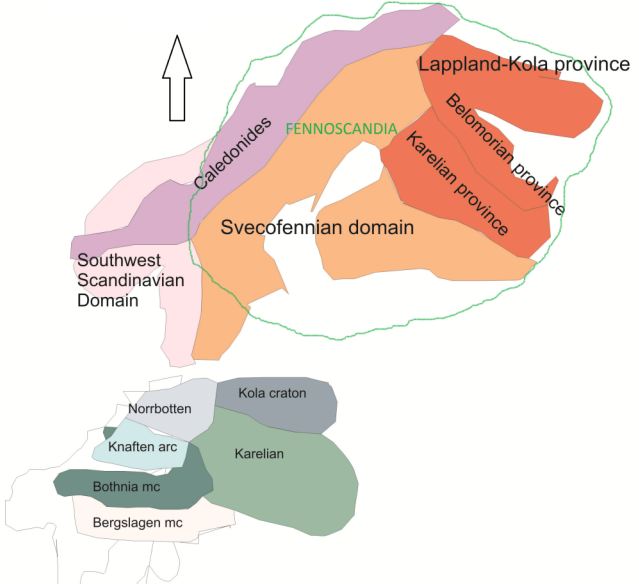


Fig. 3. The upper figure shows Fennoscandian Shield and how the Svecofennian domain is located within the shield. The figures below show the Norrbotten, Bothnian and Keitele micro-continents and the Knaften arc (modified from Lahtinen et al., 2005).

another ore mineral that occurs, however only in small quantities. The by far most common sulphide mineral is pyrrhotite (Bark, 2008).

3 Regional geology

The Svartliden gold deposit is found on the Fennoscandian Shield (Fig. 3). The Shield is divided into the Archean, Svecofennian and Southwest Scandinavian Domains. The Fennoscandian Shield forms part of the East European Craton and includes parts of Russia, Sweden, Finland and Norway (Fig. 3). The age of the Shield is about 3.4 Ga. Its main growth period is in the Paleoproterozoic. The Archean part of the Shield consists of the Kola, Belomorian and Karelian provinces (Fig. 3). The Karelian province is found in Russia and Finland and a small part occurs in northern Sweden. Its age is about 3.2 to 2.5 Ga (Lahtinen et al., 2005). The Svecofennian Domain is restricted to Finland and Sweden.

Lahtinen et al. (2005) have presented a model for the Paleoproterozoic history of the Fennoscandian Shield. Their model is based on a suggestion of several collisions of micro-continents. The Karelian Craton (Fig. 3) is characterized by rifting events; several of these took place between 2.5 and 1.95 Ga. Continental break-ups occurred on its western margin at 2.06 Ga. In the Lapland-Kola area, a back-arc basin was formed at 1.96 Ga as a result of a subduction event. This basin was eliminated by a collision between the Kola and the Karelian cratons between about 1.93 Ga and at 1.91 Ga. Another collision occurred between the Bothnian, Norrbotten and Keitele micro-continents (Lahtinen et al., 2005). The Norrbotten micro-continent (Fig. 3) had collided with the Knaften arc already before 1.92 Ga. At about 1.93 to 1.92 Ga

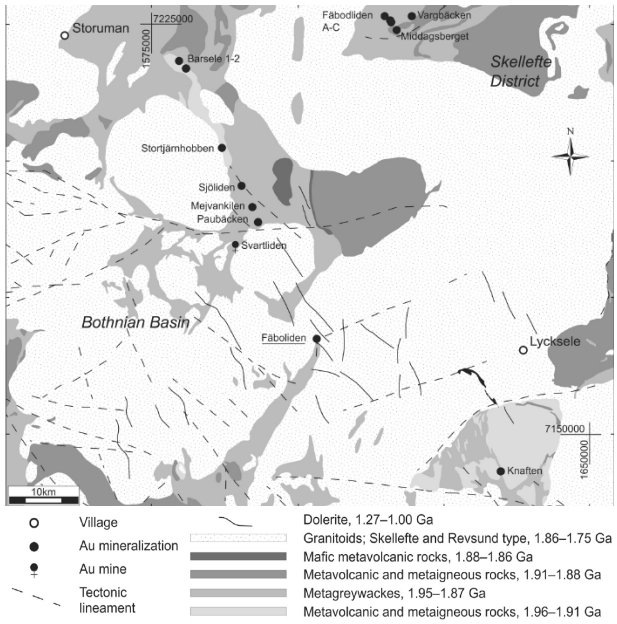


Fig. 4. Overview of the north-western Bothnian Basin, showing rock types and mineralizations found in the Gold Line (Bark, 2008). The location of Svartliden and Fäboliden is displayed. The distance between these two mines is 20km (Copied from Bark, 2008).

subduction magmatism was active on the Norrbotten micro-continent and in the Knaften arc. The collision between Bothnia and Norrbotten is suggested to have initiated the magmatism on the Bothnian micro-continent. This resulted in volcanism in the Skellefte district (Lahtinen et al., 2005). Ore formation is tied to these volcanic events. Between 1.89 and 1.87 Ga, several collisions occurred in the Fennoscandian Shield.

The Skellefte district is situated on the Fennoscandian Shield and is known for its Zn-Cu-Pb sulphide ores but also for the occurrence of gold. Gold is found both associated with the sulphide ore but also as discrete deposits. The latter occur in geological settings different from those of the sulphide mineralizations (Bark, 2008). The Skellefte district is the part of the Norrbotten micro-continent bordering on the Bothnian Basin. The major rocks in the district are rhyolite, dacite, andesite, basalt and metasediments. The metamorphic grade in the Skellefte deposits is of greenschist to lower amphibolite facies (Grahn et al., 2002).

The Skellefte-district deposits are different from the Svartliden deposit (Fig. 4). The metamorphic grade in the Skellefte district is of greenschist grade increasing towards the Bothnian Basin. The mineralization is associated with felsic and mafic rocks (Grahn et al., 2002). The major rocks in the Svartliden area consist of meta-greywacke and fine-grained mafic metavolcanics in the amphibolite to granulite facies (Bark, 2008). According to Bark (2008) the meta-morphism in the Fäboliden and Storuman areas occurred at temperatures between 500 and 580°C. At Enåsen, south of the Fäboliden area, the metamorphic temperature varies between 600 and 700°C (Bark, 2008). This indicates that the temperature in the Gold Line can fluctuate (Fig. 4).

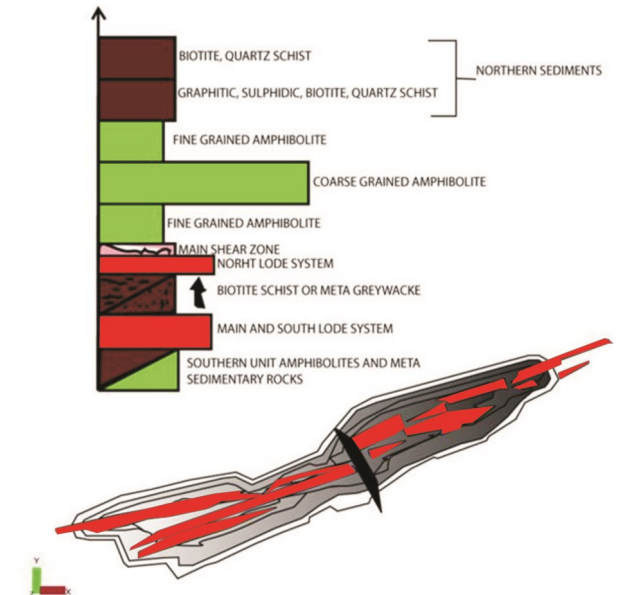


Fig. 5. The upper figure illustrates the rock formations and the location of the lodes relative to the other rocks. The middle figure shows the lode positions in the open pit. The black line indicates where the main shear zone cuts the pit. The lower figure shows how deep the pit was in 2009 (scale beside the figure) (Modified from Dragon Mining Sweden AB, 2010).

4 Svartliden

4.1 History of Svartliden

In the beginning of the 1970s, the Swedish Geological Survey was prospecting for zinc and copper sulphides in a region near Svartliden. Sulphide boulders were found. However, they were found rather far apart and according to the methods used and prevailing hypotheses of the time, the boulders were not thought to have a common origin. In the middle of the 1980s, Torbjörn Grahn, a former employee of SGU and later the founder of Lappland Goldminers, started to investigate the area east of Svartliden (Grahn et al., 2002).

Explored boulders in the Skellefte region have high amounts of sulphide and this is usually the key feature for a deposit. This was not the case at Svartliden, where the sulphide content in the boulders was rather low but the gold content rather high. A new prospecting method was applied: boulders with low amounts of sulphides were searched for. These boulders had a tendency to be associated with siliceous alteration. With this method, Grahn started to find mineralized outcrops at Fäboliden close to Svartliden (Fig. 4). However, the discovered outcrops were of low grade (<0.2ppm Au; Grahn et al., 2002).

A few amateur geologists discovered Svartliden when finding outcrops with gold mineralization. A drilling operation was initiated by Viking Gold, which resulted in four diamond drill-cores with up to 59 ppm Au. The finding was exceptional but for economical reasons, Viking Gold was sold to Dragon Mining (Johan Sjöberg, personal communication 2009).

Dragon Mining reviewed the project and noticed that Svartliden was a high temperature gold system similar to deposits in the Archean Yilgarn Craton in Western Australia. Many of the geologists in the company had previously worked in these deposits and were familiar with them. Later in 2004, production started at the pit and in February 2005 the first gold was produced. The average gold content is 5ppm, which is considered to be better than the world average (Johan Sjöberg, personal communication 2009). The world average changes depending on the strip ratio. Strip ratio is a mining term referring to the overburden that must be handled before getting to the ore. Open pit mines usually have <2ppm. In underground mines, the gold content can be between 1.5ppm up to 7ppm.

4.2 Local geology

4.2.1 Bedrock description

The main rocks at Svartliden are meta-greywacke, metavolcanite, Revsund granite and Härnö granite. The host rock for the mineralization is the supracrustal rocks.

Meta-greywacke

The meta-greywacke consists of quartz, plagioclase and biotite as major minerals. K-feldspar, muscovite and opaque minerals are found in small quantities. Apatite, epidote, chlorite and zircon occur as accessory minerals (Björk and Kero, 2001). Skarn is found as a minor rock type in the meta-greywacke and is suggested to have formed at the same time as the ore (Johan Sjöberg, personal communication 2009). The meta-greywacke is heterogeneous and at some places it appears as a banding of arenaceous and argillaceous rocks that have sedimented on the ocean floor (Björk and Kero, 2001). The meta-greywacke has a higher density than the metavolcanite because of quartz and feldspar phenocrysts occurring in the volcanic rocks (Bark, 2008). The meta-greywacke found at Svartliden most often show small-scale folding (Johan Sjöberg, personal communication 2009).

The meta-greywacke sequence is estimated to be up to ten kilometres thick within the Skellefte district (Bark, 2008). The rock may be strongly foliated. The foliation is defined by the mineral orientation of especially biotite. Shear zones can be seen in some outcrops (Bark, 2008).

Detratal zircon ages in the meta-greywacke fall into two groups: 2.93 to 2.65 Ga and 2.02 to 1.88 Ga (Claesson et al. 1993). This gives the upper age limit of the sedimentation at approximately 1.88 Ga (Claesson et al. 1993). The lower age limit is given by the age of Revsund granite (1.80 Ga) which indtruded the sediment.

According to Bark (2008) the Svartliden deposit is similar to the Fäboliden deposit. The country rock surrounding both deposits is in the mid-amphibolite facies.

Metavolcanite

At Svartliden, only mafic metavolcanite occurs (Johan Sjöberg, personal communication 2009). This is

different from the situation in the Skellefte Field, where also felsic volcanics is common. The major minerals found in this rock are plagioclase, biotite and amphibole; the accessory minerals are chlorite, calcite, epidote, apatite, and opaque minerals. The metavolcanite is homogeneous, fine-grained and slightly foliated. The colour varies from dark grey to black.

Revsund granitoid

The Revsund granite is named after a small village, Revsund, close to Östersund, Jämtland. It is a coarse-grained granitic rock with K-feldspar megacrysts, which occur as augens or euhedral crystals (Högdahl, 2004). The major minerals are quartz, plagioclase, K-feldspar and biotite (Björk and Kero, 2001).

In the Svartliden area, large areas are mapped as Revsund granite. This rock is heterogeneous concerning both grain size and chemical composition. The granitoid varies from medium to coarse grained and from granitic to granodioritic compositions. Age determinations have shown that rocks called Revsund granitoid belongs to at least two generations. According to Bark (2008) the Revsund granitoid has an age of about 1.77 to 1.80 Ga. The 1.77 to 1.80 Ga is the common age obtained for the Revsund granite. In the Bothnian Basin, the Revsund granite is dated to about 1.79 Ga by Wilson et al. (1985) and close to the village of Revsund the age of the granite is between 1.797 and 1.795 Ga (Högdahl, 2004).

Härnö granite

The term Härnö granite is normally used for muscovite bearing S-type granite, which is widespread in the Bothnian Basin. The granite varies in colour from white grey to light red (Björk and Kero, 2001).

The Härnö granite is one of the dominating rock types in the map sheet 22H Järvsjö NO, where Svartliden is located. It is a medium- and even-grained rock, which contains quartz, K-feldspar and plagioclase with the accessory minerals muscovite, chlorite, amphibole, garnet, epidote, titanite and zircon (Björn and Kero, 2001; Andersson, 2011). Högdahl et al. (2002) obtained 1.870 ± 0.007 Ga for Härnö granite sampled on Härnön, Härnösand.

4.2.2 Geology of Svartliden

The alteration at the Svartliden deposit can be divided into three types; ore/proximal alteration, intermediate alteration and distal alteration. Ore alteration implies Ca^{2+} -ions reacted with the host rock to form skarn. The intermediate alteration is a biotite alteration that occurs in veins but sometimes replaces the host rock. The biotite alteration often occurs close to the lode. Skarn veins also appear in the intermediate alteration zone. The distal alteration includes skarn veins that are found in the amphibolite (Dragon Mining Sweden AB, 2010). Bark (2008, page 200) has studied the Fäboliden deposit in detail. He describes it as: "the mineralization is commonly hosted in graphite-bearing quartz and sulphide veins, which parallel the main foliation, within the shear zone in the meta-greywacke host rock". The host rock is never mineralized but the mineralization is bounded to the veins. These veins

may be boudinaged in semi-ductile shear zones. The mineralization type is similar to the Svartliden deposit. Common sulphide minerals are arsenopyrite, löllingite, pyrrhotite and some chalcopyrite. They occur in semi-ductile shear zones (Bark, 2008).

The stratigraphy at Svartliden is not well understood, due to the lack of structures allowing up-and-down determinations. The occurrence of possible stratigraphic repetitions are not known (Bark, 2008). The mineralization is concentrated in a fold hinge. From north to south, the lithologies at Svartliden consist of the Northern Sediments (Fig. 5), which include biotite-quartz schist and graphite sulphidic biotite-quartz schist (Johan Sjöberg, personal communication 2009). Similar graphitic sulphidic rocks (Fig. 5) as those found at Svartliden are common in the Skellefte district. The Northern Sediments are followed by amphibolitic rocks. These are typically 40 meters wide. It is not known whether they constitute an intrusive or extrusive body, because the contacts are not possible to interpret. South of the amphibolite, there is a shear zone (Johan Sjöberg, personal communication 2009). To the south of the amphibolitic rocks, the Svartliden deposit follows (Fig. 5). The Svartliden pit contains three lode systems (Grahn et al., 2002). These are called the northern, main and southern lodes. The main and southern lodes occur rather close together, while the northern lode is separated from the others by a horizon of biotite schist to meta-greywacke (Fig. 5). At some places, a few lenses of amphibolite are preserved in the lodes; most of them are biotite altered. The schist is pure and without much quartz and is interpreted as a metasediment. Pseudomorphs after andalusite occur at Svartliden supporting the suggestion of the occurrence of meta-sedimentary rocks. The main and southern lodes are the largest ones. However, they are merely wide but shallow and will soon be exhausted. The width of the main lode is about 35m (Johan Sjöberg, personal communication 2009). The focus is now on the northern lode, which can be followed to larger depths. To the south of the deposit, amphibolite and metasedimentary rocks of the southern unit follow (Fig. 5).

The host-rock package of the Svartliden deposit consists of amphibolite and metasedimentary rocks. The chemistry and structures of the surrounding rock govern the mineralization.

South of the fine grained amphibolite and north of the northern lode follows the main shear zone. For the sake of simplicity, the sheared zone is called quartz mylonite (Fig. 6) by Dragon Mining Sweden AB. The reason is that it is strongly deformed and also hydrothermally altered. It is the most strongly deformed rock at Svartliden (Johan Sjöberg, personal communication 2009). This shear zone is conformable to the rock foliation. The main shear zone strikes NW–SE (Grahn et al., 2002; Johan Sjöberg, personal communication 2009).

The gold mineralization at Fäboliden was formed at 0.4 GPa and at around 520°C (Bark, 2008), Fäboliden is similar to Svartliden. The distance between the two occurrences is approximately 20km.

4.2.3 Post-ore forming processes at Svartliden and the appearance of the ore

The mineralized shear system is about 1km long and about 100m wide and deep. The lode is intruded by a granite body and in some areas the lodes appear both below and above the granite intrusion. The granite intrusion is younger than the mineralization. The granite is undeformed and displaces the ore at some places laterally up to 40m and vertically up to 50m (Grahn et al., 2002). According to Bark (2008), the Svartliden ore was formed in a deformation zone at high pressures and at temperatures around 500 to 600°C. The host rock already had a middle to upper amphibolite metamorphic grade. These temperatures are similar to the metamorphic temperatures at Fäboliden. These considerations suggest the peak metamorphism to have occurred between 1.85 and 1.80 Ga. The lower age limit is given by the intrusion of the Revsund granite, which this area is assumed to have taken place between 1.8 and 1.77 Ga. The Svartliden ore formation was followed by a retrograde hornfels metamorphism (Bark, 2008; Weihs et al., 1992). With a microprobe it has been possible to show the presence of gold both as electrum and as elemental gold (Eklund, 2007). The gold electrum is mostly associated with arsenopyrite or löllingite. Gold may appear together with amphibole or pyroxene, but never without the presence of ore minerals (sulphides and oxides) (Eklund, 2007).

5 Sampling and Methods

Core samples were collected at Dragon Mining's open pit at Svartliden from a core labelled SV09175. The samples were taken at depths from 219 to 244 meters (Table 1). Fig. 6 shows the rock types, through which the core was drilled and the positions of the collected samples. Fig. 7 shows a part of the core samples and how the core looks. Samples were collected according to mineral occurrence and rock type. This makes it difficult to take samples with a fixed distance; this is evident from table 1. When collecting the samples, aspects such as rock type, sulphide content, colour and mineralogy were used. This sampling scheme was used to obtain samples that were suitable for comparative studies and to ascertain a sufficient variation. Optical microscopy in transmitted and reflected light has been used to determine the ore and gangue minerals. The microscope used was a Nikon Eclipse E400 POL. All optical images are taken with crossed polarizers to display interference colours.

As a complement to the optical microscopy, scanning electron microscopy (SEM) was used. The backscatter electron detector (BSE) of the SEM allows imaging of atomic-number contrasts of the mineral assemblages and possible zoning in the crystals. The SEM used is a Hitachi S3400N equipped with an EDS (energy dispersive X-ray system) analytical device (Oxford instruments, INCA). The instrument is located at the Faculty of Science, Department of Geology in Lund. The acceleration voltage used was 15kV. Natural and synthetic mineral standards were used. A cobalt standard was used for instrument calibration.

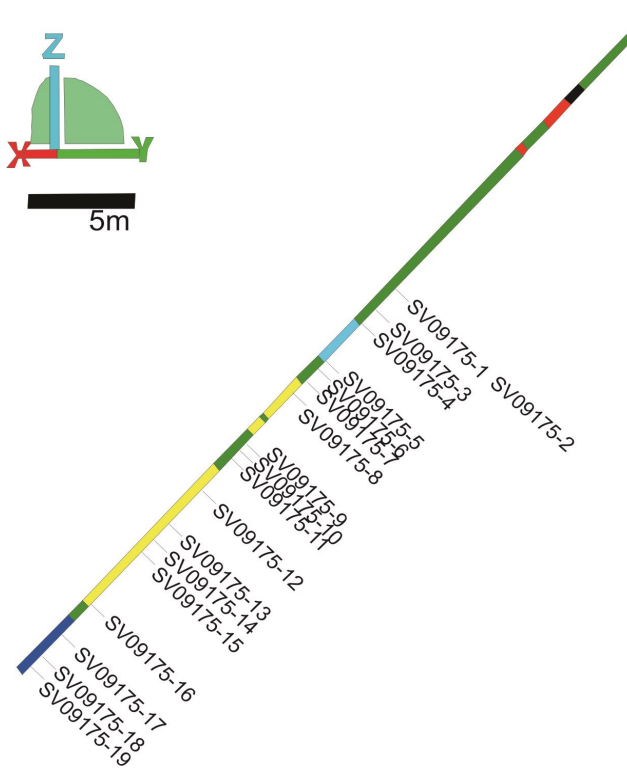


Fig. 6. The sampled core in detail. Sample length is 24.17m. The colours indicate; green= amphibolite, light blue= quartz mylonite, red= granite, yellow= skarn or ore alteration, dark blue= biotite schist. The x, y, z refer to easting, northing and elevation (Dragon Mining Sweden AB, 2010).



Fig. 7. Parts of the core SV09175 (Photo Lawrence Nilsson).

Oxygen was determined stoichiometrically. Carbonates will thus sum to about 50% (CO_2 is not reported). Magnifications of 100 times were used in

the optical microscopy and up to 550 times in the SEM.

Mineral analyses have been performed on amphibole, pyroxene and feldspars. Amphibole formula calculations were based on the EDS analyses using the scheme suggested by Leake et al. (1997). The data were imported into excel, which was used for the calculations. Pyroxene analyses were recast into end member compositions. The formulas, which have been used to determine the different mineral end-compositions are:

Wollastonite: $(\text{Ca}/(\text{Ca}+\text{Mg}+\text{Fe}^{2+}) \times 100)$,
Enstatite: $(\text{Mg}/(\text{Ca}+\text{Mg}+\text{Fe}^{2+}) \times 100)$ and
Ferrosilite: $(\text{Fe}^{2+}/(\text{Ca}+\text{Mg}+\text{Fe}^{2+}) \times 100)$.

Feldspar calculations were performed on the analysis results and put into an excel file, which was used for the calculations. The chloritized biotite are calculated on 22 oxygen.

In the appendix, the results from the SEM and EDS are presented together with overview images.

6 Results

Table 1 summarizes the results from the SEM and the optical microscopy studies. A combination of both methods is used to identify the minerals due to the difficulty to discriminate among opaque minerals with optical microscopy, e.g. to distinguish arsenopyrite from pyrrhotite.

Nineteen samples have been studied. Ten of these were selected for a more thorough investigation with the SEM and EDS techniques. These ten samples are marked in bold type in table 1. The number of points analysed in the sections varied. Samples analysed but not accompanied by any images are underlined and shown in bold in the table. The analytical results are given in the appendix. Analyses giving low total sums were regarded as unreliable; hence they do not appear in the appendix.

Mineral abbreviations in the photographs are: amf (amphibole), px (pyroxene), pyrr (pyrrhotite), qz (quartz), tita (titanite), rut (rutile), Ilm (ilmenite) epi (epidote), bi (biotite), chl (chlorite), feld (K-feldspar and plagioclase), carb (carbonates), and bi-chl (chloritized biotite). The letter P followed by a number has been used to refer to the points analysed with EDS (see appendix). Some of the opaque minerals that are analysed and supposed to be pyrrhotite show a large excess of S. The reason for this is not understood.

The major minerals found in the samples collected from the drill core (SV09175) are amphibole, pyroxene, quartz, biotite, epidote, K-feldspar and prehnite. The most common ore mineral is pyrrhotite. The sample SV09175-5 is strongly deformed and very fine grained. Thus, the mineral identification is difficult in this sample and a number of minerals are probably misidentified. The prefix SV09175 denoting the core number is omitted in the following text.

Amphibole appears in the samples 1 to 15 and 17 to 19. The shape of the mineral varies from angular to rounded except for sample 5, where the amphibole crystals are elongated. All analysed amphibole crystals are calcic. The Ca-ion content in the samples varies

between 1.7 and 2.0 when calculated on 23 oxygen atoms (water-free). The number of Al ions in P1, P9 and P17 is >1.0 whereas the rest of the analysed amphiboles have an Al content <1.0. Al-rich amphibole is classified as Fe- and Mg-hornblende and Al-poor amphibole as actinolite (Leake et al. 1997). Fig. 8 shows how the analysed amphiboles plot in a calcic-amphibole diagram. The amphiboles range from actinolite to hornblende. A trend can be visualised and that is that amphiboles from SV09175-17 and 19 (P33 and 34) plot mostly in the actinolite box and only a few in the magnesio-hornblende box. Samples collected higher up in the core, hence closer to the ore plot mostly in the magnesiohornblende box.

Pyroxene appears in samples 1, 3, 5 to 13 and 16 to 19. The analysed pyroxenes are plotted in a CaO-MgO-FeO diagram and they all plot in the diopside and hedenbergite field (Fig. 9). Among the analysed samples, diopside is found in samples 1 (P6), 11 and 18 (P29 and P32). Hedenbergite is found in sample 5. The pyroxene crystals are anhedral to subhedral. The

crystal size varies between 50µm and 200µm.

Quartz appears in samples 1, 3 to 5, 8, and 11 to 18. The amount of quartz is similar in all samples approximately between 20 and 40% except for sample 5, where quartz only appears in amounts less than 20%. Quartz appears as anhedral crystals.

Prehnite has been identified in samples 6 and 17.

K-feldspar appears in samples 1, 3 to 4, and 13 to 14 and 18 to 19. Tartan twinning is visible at some places. The analysed samples are plotted in a feldspar diagram (Fig. 10) and the samples plot as almost pure K-feldspar.

Plagioclase appears in samples 1 to 2, 5, 11 to 12, and 16. The shape of the mineral varies from subhedral to anhedral. The analysed plagioclase is plotted in Fig. 10. It plots as bytownite. The analysed plagioclase crystal has a perfect cleavage parallel to (001) (Fig. 10).

The criteria used for determining whether biotite is chloritized are: the total sum, which for chlorite, with its high H₂O content, is much lower than that for

Samples	From (m)	To (m)	Minerals found
SV09175-1	219.93	220.00	Amphibole (hornblende), clinopyroxene (diopside), K-feldspar, plagioclase, quartz, pyrrhotite, biotite.
SV09175-2	220.23	220.04	Amphibole (actinolite), carbonate, plagioclase, chlorite, biotite, pyrrhotite, titanite.
SV09175-3	221.05	221.15	K-feldspar, quartz, clinopyroxene, amphibole, carbonate.
SV09175-4	221.93	222.00	Quartz, amphibole, biotite, K-feldspar.
SV09175-5	224.35	224.43	Carbonate, clinopyroxene, amphibole (actinolite), plagioclase, pyrrhotite, chlorite, quartz.
SV09175-6	224.89	224.97	Clinopyroxene, amphibole (actinolite, hornblende), prehnite, epidote, biotite, carbonate, pyrrhotite.
SV09175-7	225.71	225.78	Clinopyroxene, chlorite, amphibole (actinolite), biotite, pyrrhotite, titanite.
SV09175-8	226.47	226.57	Quartz, clinopyroxene, amphibole (hornblende), biotite, pyrrhotite, zircon, apatite.
SV09175-9	229.72	229.80	Amphibole (actinolite), epidote, clinopyroxene, biotite, chloritized biotite, sillimanite, pyrrhotite, zircon.
SV09175-10	230.08	230.15	Clinopyroxene, amphibole (hornblende, actinolite), biotite, apatite, pyrrhotite, arsenopyrite
SV09175-11	230.48	230.56	Feldspar (k-feldspar, plagioclase), quartz, amphibole (hornblende, actinolite), clinopyroxene, biotite, apatite, lollingite, arsenopyrite, pyrrhotite.
SV09175-12	232.62	232.69	Quartz, clinopyroxene, amphibole, biotite, apatite, pyrrhotite, fluorapatite.
SV09175-13	234.90	234.98	Clinopyroxene, quartz, pyrrhotite, amphibole, K-feldspar, biotite, carbonate, chalcopyrite, zircon.
SV09175-14	235.82	235.91	Quartz, amphibole (actinolite), biotite, K-feldspar, apatite, pyrite, zircon.
SV09175-15	236.56	236.65	Quartz, biotite, amphibole (actinolite), pyrrhotite.
SV09175-16	240.00	240.09	Clinopyroxene, plagioclase, quartz, biotite, pyrrhotite.
SV09175-17	242.00	242.07	Muscovite, biotite, chloritized biotite, K-feldspar, amphibole (actinolite, hornblende), quartz, prehnite, carbonate, clinopyroxene, pyrrhotite, apatite, titanite.
SV09175-18	243.27	243.35	Clinopyroxene, K-feldspar, quartz, amphibole (actinolite), titanite, pyrrhotite.
SV09175-19	244.02	244.10	Amphibole (actinolite), biotite, chloritized biotite, quartz, clinopyroxene, K-feldspar, carbonate.

Table 1. Observations in the thin sections. Samples in bold were examined in the SEM. The minerals are enumerated in descending order of abundance.

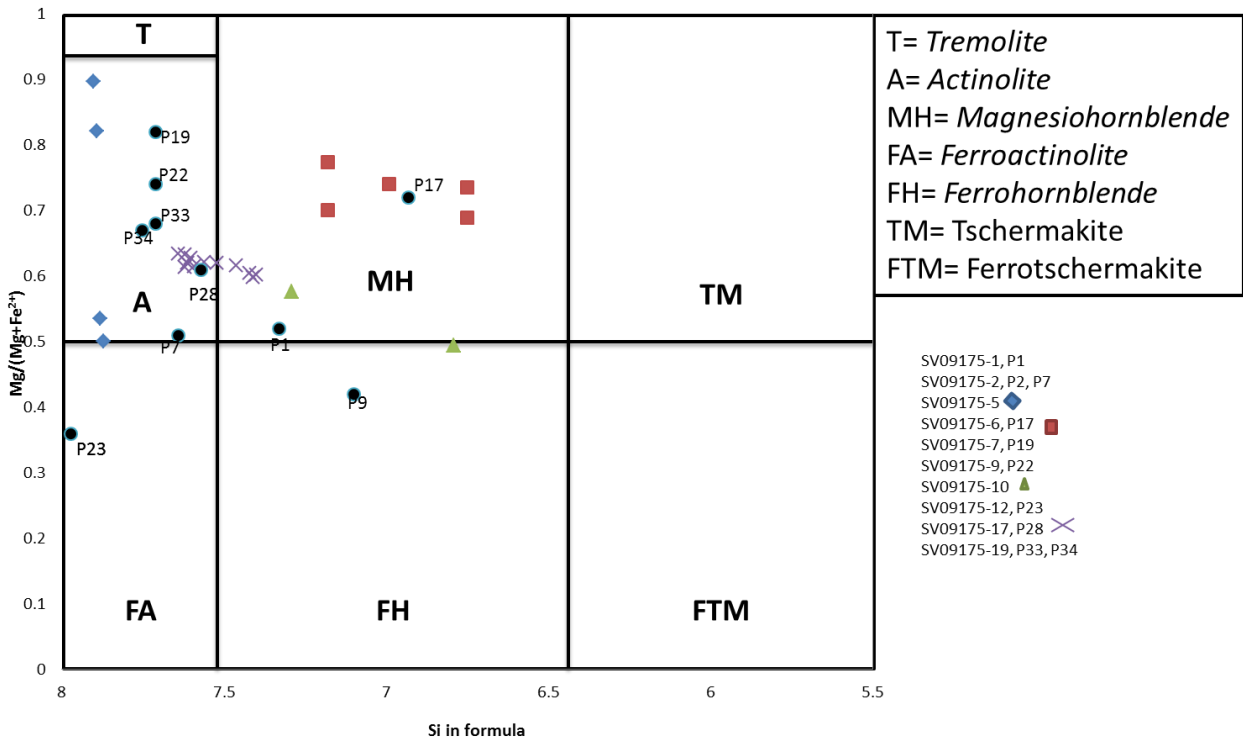


Fig. 8. The diagram shows the results from amphibole analyses plotted in a calic amphibole diagram. The points referred to as Point (P) are the analysed point associated with images (Modified from Leak et al. 2007).

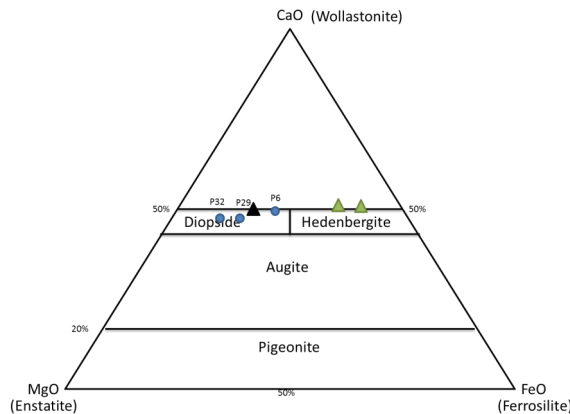


Fig. 9. The figure shows the results from pyroxene from the analysed samples. The green triangle is from SV09175-5 and the black are from SV09175-11 (modified from Morimoto et al. 1988).

biotite (= 96 to 97 wt% calculated dry). Chlorite is K-free, whereas biotite ideally should have two K-ions for every 22 oxygen atoms. According to experience, something like 85 to 90% of the possible K-positions in biotite are normally occupied. If the K occupancy is significantly lower, this is a clear indication of chloritization. As an example, comparing the total wt% and the amount of K for analyses P26 and P35, we find the total sum 90.7wt% and K= 0.73 for analysis P26 and 92.0wt% and K=1.32 for analysis P35, respectively. The degree of chloritization is thus higher in P26 than in P35. In P26 the Mg, Fe and Al is higher than in P35.

Chlorite appears in samples 2, 5 and 7. In sample 7

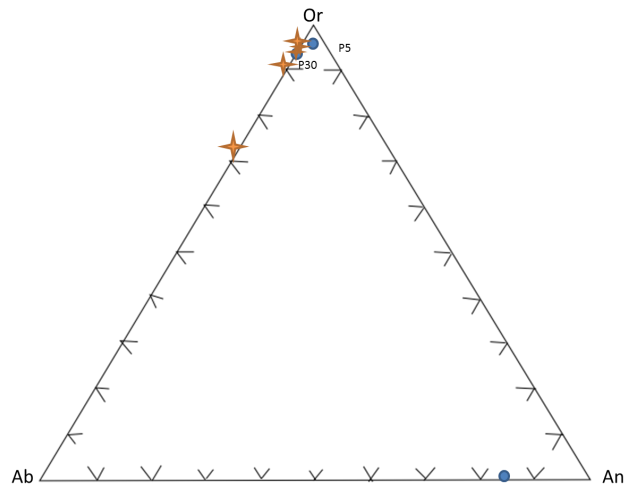


Fig. 10. The figure shows the chemical compositions of analysed feldspars from the analysed samples. The star shape points are from SV09175-17.

the chlorite appears in contact with amphibole and pyrrhotite. The chlorite occurs as crystals elongated parallel to (001) (Fig. 19).

Carbonates analysed contain mostly calcite and small amounts of magnesium.

Pyrrhotite is the most common ore mineral. It appears in samples 2, 5 to 13 and 15 to 19. The crystals are anhedral. Some of the observed pyrrhotite appears as inclusions in amphibole. This has been observed in samples 2 and 7. The pyrrhotite is pure and does not contain any Ni or other elements in detectable amounts. The Fe/S ratio is sometimes low.

6. 1 Results optical and electron optical microscopy

Sample SV09175-1 (amphibolite)

The sample is dominated by amphibole (*hornblende*). The shape of the amphibole crystals varies from rectangular to rounded and the size varying between 10 and 300 μm . K-feldspar, clinopyroxene and epidote are the second most common minerals. The shape of these two minerals is rectangular to rounded with sizes between 10 and 200 μm . The thin section is made up of both coarse and fine-grained crystals. The coarse crystals define a foliation (Fig. 17). Results from the EDS analyses are obtained from the points shown in Fig. 17. The amphibole P1 is an Al-rich Mg-hornblende. The Al content is 3.06 wt% and the ferric iron is 4% of the total iron according to Leak et al. (1997). The mineral at P2 is bytownitic plagioclase, at P3 and P4 pyrrhotite and at P5 K-feldspar. P6 is clinopyroxene (diopside).

Sample SV09175-2 (amphibolite)

The sample is dominated by amphibole, K-feldspar and calcite. There are also a few chlorite crystals and some pyrrhotite. Titanite and apatite are found as accessory minerals. Results from the SEM (Fig. 18) indicate that both actinolite, P7 (Al poor, 1.91wt%) and Al-rich (4.1wt%) Fe-hornblende, P9, occur. Approximately 1% of the total iron is ferric in the actinolite and 14% in the Fe-hornblende. The calculations are performed according to Leak et al. (1997)). The sizes of these minerals vary between 40 and 300 μm .

Sample SV09175-3 (amphibolite)

According to the optical microscopy study, amphibole and clinopyroxene megacrysts occur in the thin section SV090175-3. Further, the sample contains equigranular crystals of K-feldspar, quartz, amphibole and clinopyroxene. There are some carbonate crystals that are scattered all over the sample. The accessory minerals include apatite and zircon. The only opaque mineral found is chalcopyrite. Pyrrhotite has not been identified.

Sample SV09175-4 (amphibolite)

Results from the optical microscopy study show that the rock sample is equigranular and foliated/lineation. The major minerals are biotite and hornblende. There are some fractures filled with quartz, which crosscut the sample. A few black spots occur. It is hard to determine whether they are opaque minerals or some sort of fluid inclusions. Sizes of these black spots are <0.02mm.

Sample SV09175-5 (amphibolite/contact to quartz mylonite)

The sample is dominated by calcite, diopside, hedenbergite, and chlorite. The chlorite appears as elongated crystals in contact with carbonate at points P12 and P13. The size of the carbonate mineral is between 30 and 300 μm and the crystals are anhedral. The SEM analyses for the points in Figs. 18 and 19 give a total of 51wt% for the carbonate P11 and P14

(Mg, Ca and O); the reason is that carbon is not analysed. The results are reported as oxide percentages and CO₂ in a carbonate makes up almost 50% by weight.

Sample SV09175-6 (amphibolite)

The sample is dominated by clinopyroxene and amphibole. Prehnite and epidote are present. The amphibole (Fig. 13) is elongated with lengths varying between 10 and 100 μm and widths between 5 and 50 μm . The amphibole P17 is Mg-hornblende. It is difficult to determine the size and textural relation of the plagioclase since the crystals are very small and homogenous.

Sample SV09175-7 (amphibolite)

The sample is dominated by clinopyroxene, chlorite and amphibole. The grain size of the clinopyroxene and chlorite is between 50 and 300 μm . Amphibole most often occurs in contact with clinopyroxene. There is no apparent zoning. P19 in the sample is actinolite (Figs. 8 and 20).

Sample SV09175-8 (skarn)

Results from the optical microscopy study show that the minerals found in the sample include quartz, clinopyroxene, amphibole, biotite and some muscovite. The grain size of these minerals varies; amphibole and clinopyroxene are mostly megacrystic, whereas biotite, quartz and muscovite are matrix materials. There are micro-fractures that contain quartz, and plagioclase. The accessory minerals consist of zircon and apatite. The only opaque mineral in the sample is pyrrhotite.

Sample SV09175-9 (amphibolite)

Results from this sample are both from the EDS and optical microscopy. The sample is dominated by amphibole, clinopyroxene and epidote. Chloritized biotite is found in this sample. Mineral sizes vary between 30 and 300 μm . The shape of the minerals varies from angular to sub-rounded. The boundaries between the minerals are straight. The amphibole P22 (Fig. 20) is actinolite.

Sample SV09175-10 (amphibolite)

According to results from the optical microscopy study the minerals are fine grained. The minerals found are clinopyroxene (diopside), amphibole and biotite. Apatite is the only identified accessory mineral.

Sample SV09175-11 (amphibolite)

Results from the optical microscopy study show that the sample contains high amount of quartz and K-feldspar crystals. The size of the quartz grains varies from 1 to 2 mm. Assessor mineral is löllingite.

Sample SV09175-12 (skarn)

The sample contains mostly quartz, plagioclase and hornblende. The shape of the quartz crystals is angular to sub-angular and the size varies between 20 and 100 μm . There are also some clinopyroxene. The amphibole-quartz contacts are straight. The amphibole at P23 (Fig. 8) and P25 are ferroactinolite. P25 Si-

value is at 8.4 and there it does not plot in figure 8. Accessory minerals are apatite and titanite. Minerals in sample SV09175-12 (Figs. 15 and 21) are not oriented into a linear structures and this sample is located in the skarn alteration zone.

Sample SV09175-13 (skarn)

Results from the optical microscopy study show that the minerals found in the sample comprise pyroxene, quartz, amphibole, a few K-feldspar crystals, biotite and carbonates. Zircon is found in close contact with quartz. Pyrrhotite and zircon are identified as accessory minerals.

Sample SV09175-14 (skarn)

Results from the optical microscopy study show that the minerals found in the sample consist mostly of quartz. Other minerals are amphibole, and a few crystals of biotite and K-feldspar. Apatite is the only identified accessory mineral.

Sample SV09175-15 (skarn)

Results from the optical microscopy study show that the minerals found in the sample consist of biotite, quartz and some amphibole. Pyrrhotite is the only accessory mineral identified.

Sample SV09175-16 (skarn)

The results from the optical microscopy study show clinopyroxene crystals varying between 40 and 300 μm in size. Other minerals that occur in the sample are K-feldspar, quartz and some biotite. The biotite is elongated and flaky.

Sample SV09175-17 (biotite schist)

The sample contains mostly biotite and muscovite. It also contains; hornblende, actinolite, K-feldspar, prehnite, titanite, chalcopyrite, pyrrhotite, apatite and zircon. Many biotite crystals are chloritized. The size of both the muscovite and biotite crystals is between 40 and 80 μm . Amphibole appears as rather large crystals that are up to 500 μm long and 300 μm wide. The shape of the amphibole is rectangular. The amphibole P28 is actinolite (Fig. 8).

Sample SV09175-18 (biotite schist)

This sample is analysed both in optical microscopy and EDS. The sample (Figs. 16 and 22) contains mostly clinopyroxene and K-feldspar. These are similar in shape and size. The shape varies between angular and rounded and the size between 100 and 500 μm . The two clinopyroxene crystals P29 and P32 in Fig. 9 are diopside. There are also small amounts of titanite and pyrrhotite.

Sample SV09175-19 (biotite schist)

This sample has been studied in both optical microscopy and EDS. The sample (Fig. 16 and 22) contains mostly amphibole and biotite. These minerals are angular to sub-angular; they can also be sub-rounded in some areas. The size varies between 60 and 400 μm . Amphibole (P33 and P34; Fig. 8) is actinolite. There is some chloritized biotite, which is more brownish than the unaltered biotite and simultaneously

shows a more distinct cleavage. The size of these chloritized biotite crystals is between 20 and 100 μm . Zircon is the only accessory mineral identified.

SV09175-1(a)

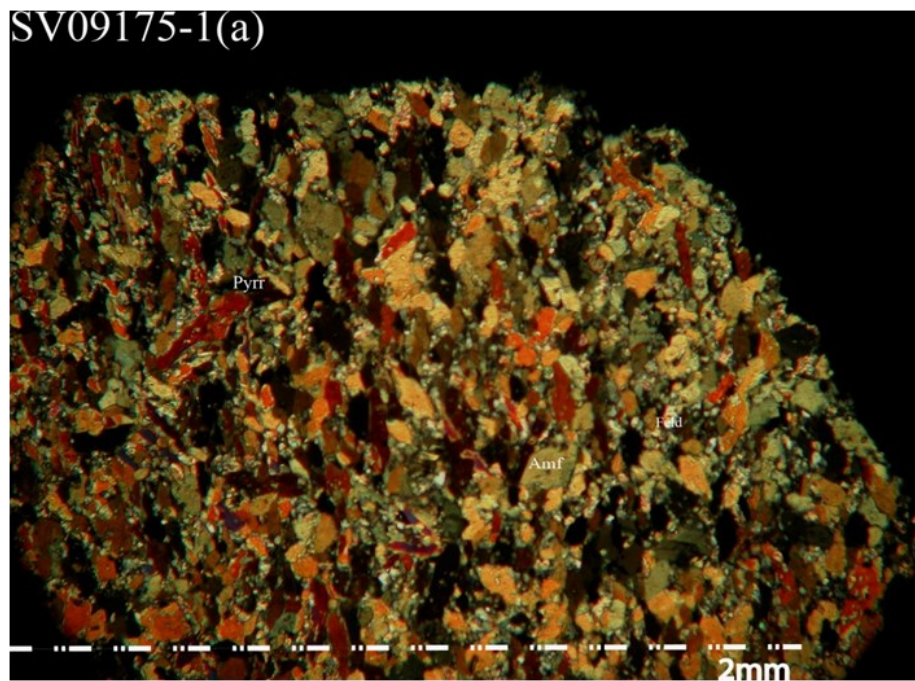
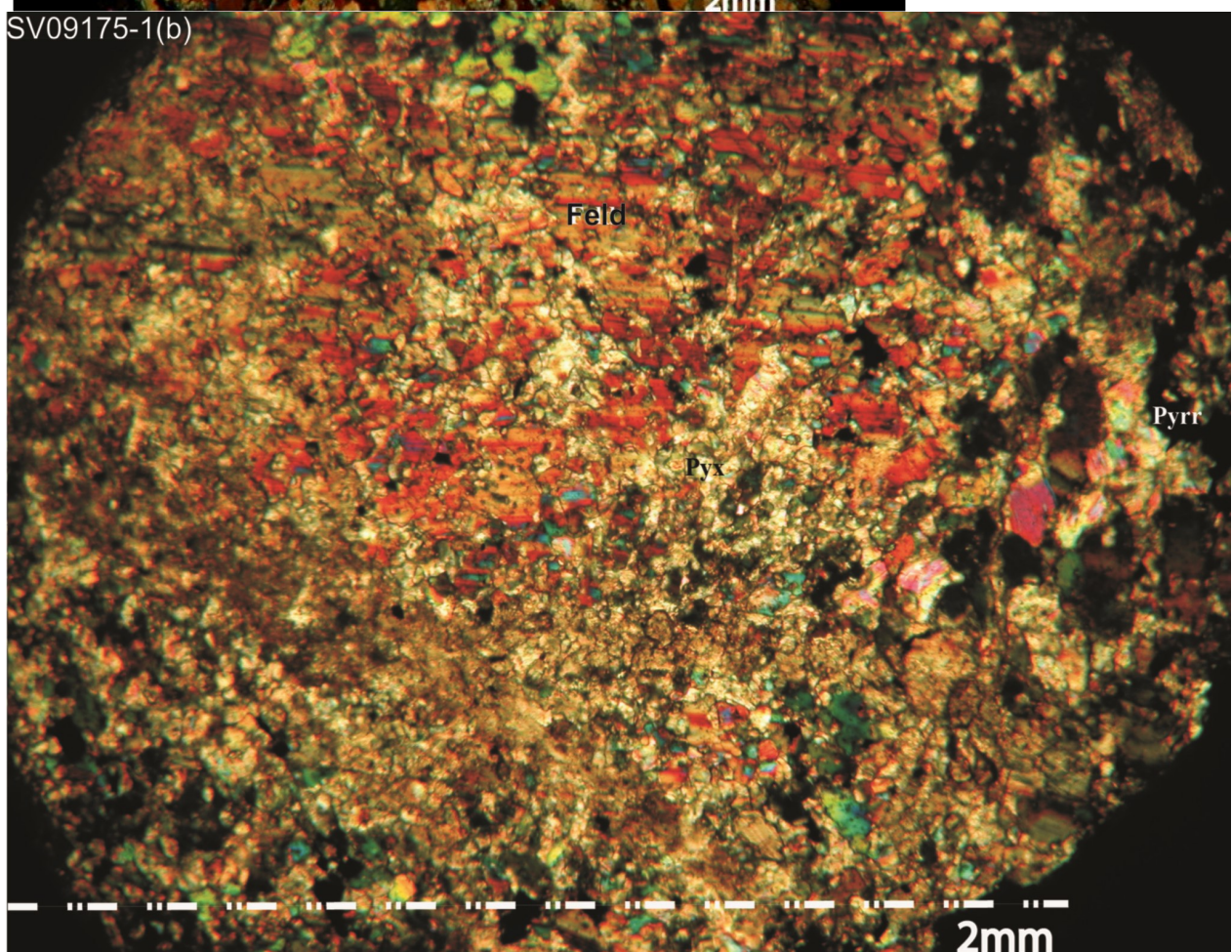


Fig. 11. Sample SV09175-1
Optical microscope images from different areas of the same thin section. Minerals found are feldspar, amphibole, pyroxene and pyrrhotite. A BSE image of this thin section is found in Fig. 17.

SV09175-1(b)



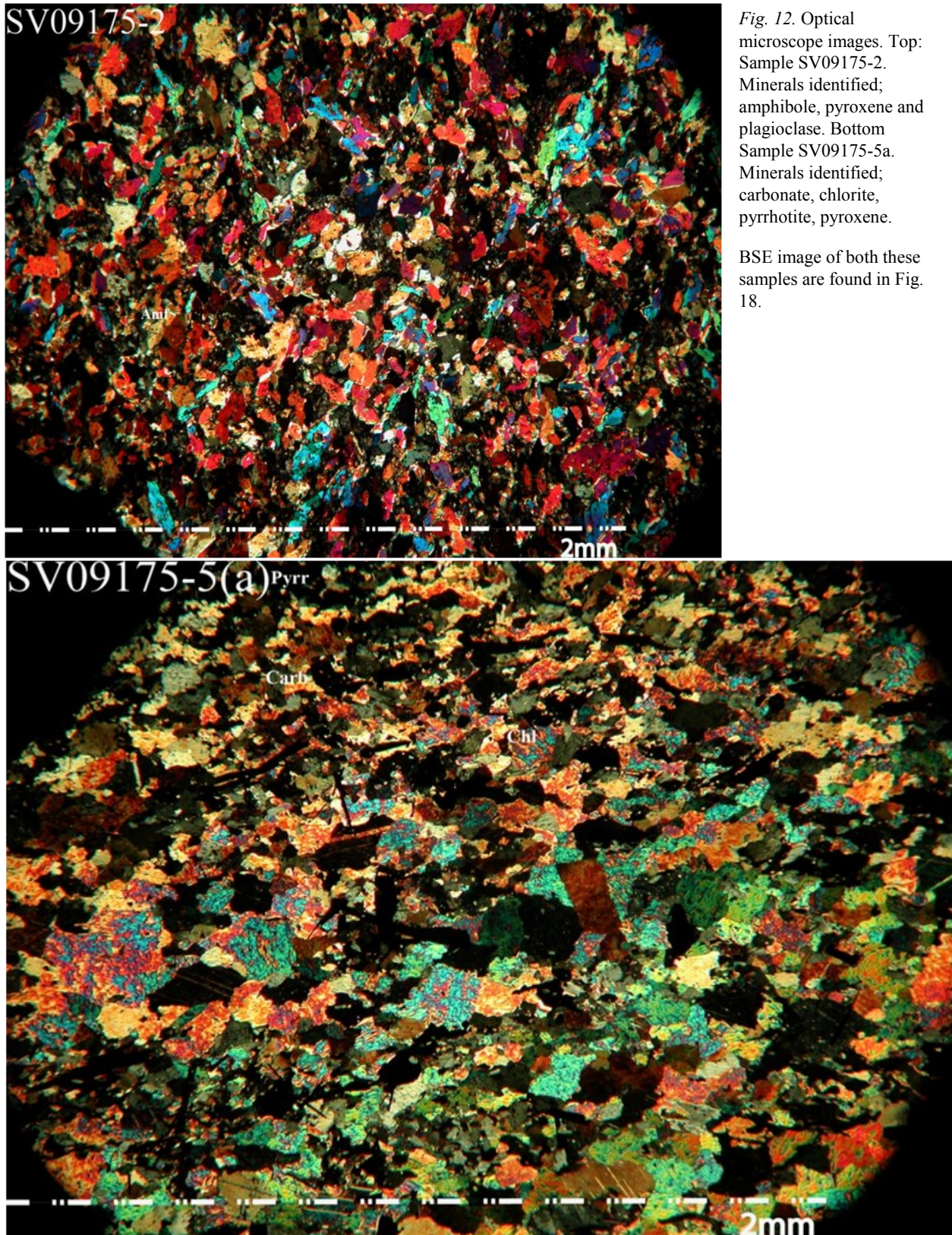


Fig. 12. Optical microscope images. Top: Sample SV09175-2. Minerals identified; amphibole, pyroxene and plagioclase. Bottom Sample SV09175-5a. Minerals identified; carbonate, chlorite, pyrrhotite, pyroxene.

BSE image of both these samples are found in Fig. 18.

SV09175-5(b)

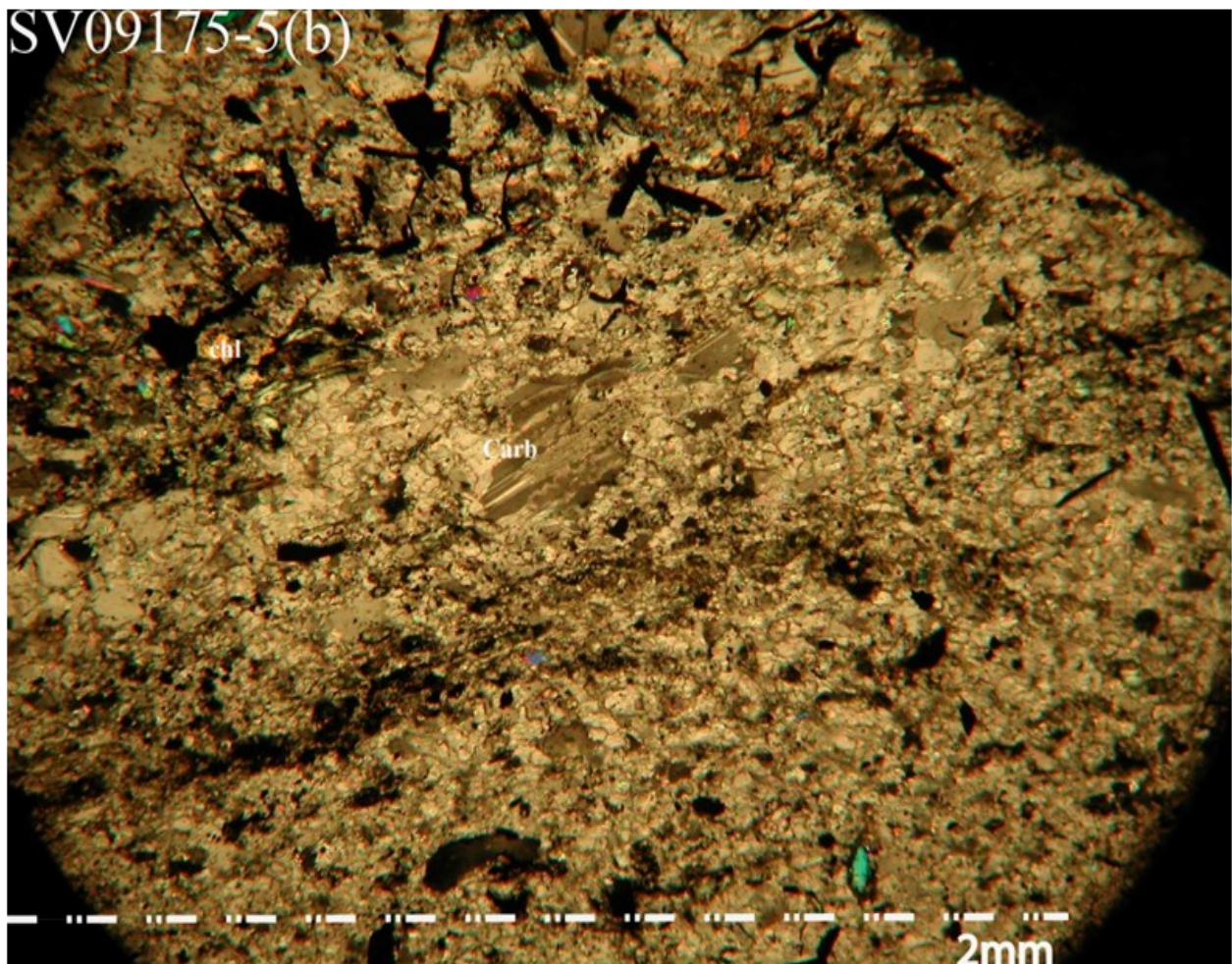
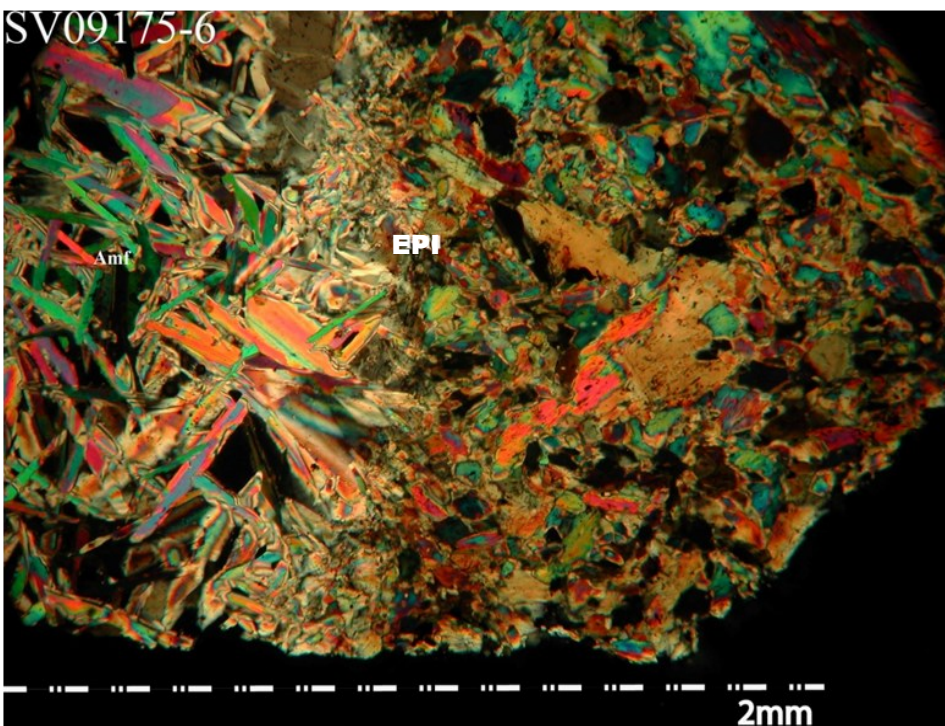


Fig. 13. Above: Optical microscope image. Sample SV09175-5b minerals identified; carbonate, chlorite. This section is similar to the one in Fig. 11. Below: Optical microscope image. Sample SV09175-6 minerals identified; Amphibole, epidote and pyroxene are identified. BSE images for both samples are found in Fig. 19.

SV09175-6



SV09175-7

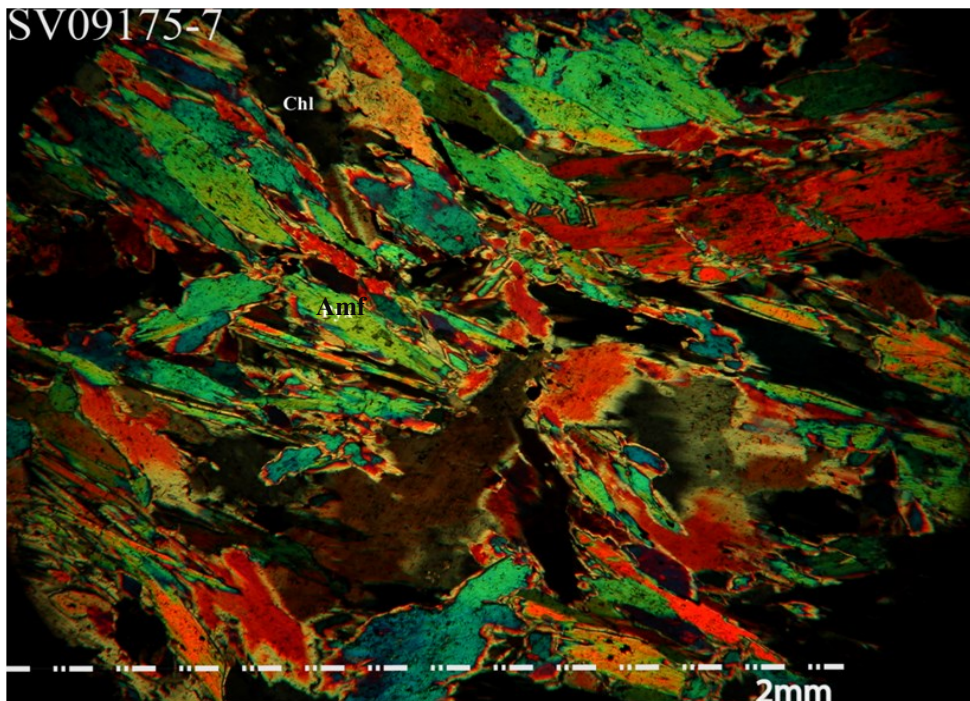
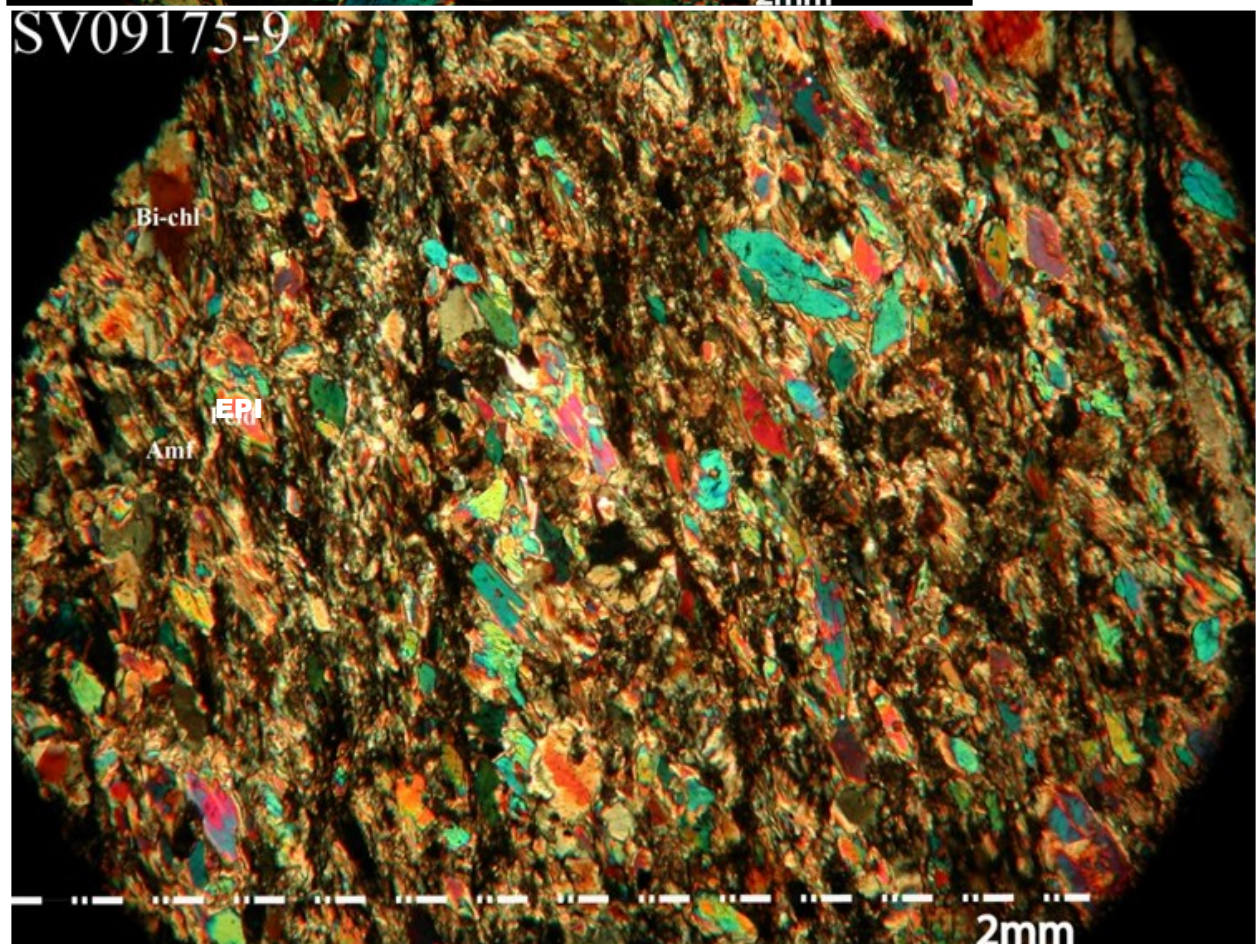


Fig. 14. Above: optical microscope image. Sample SV09175-7: Minerals identified are chlorite and amphibole. Fig. 20 shows the BSE image of the sample.

SV09175-9



Below: optical microscope image. Sample SV09175-9: Minerals identified are amphibole, chloritized biotite and epidote. Fig. 20 shows the BSE image.

SV09175-12

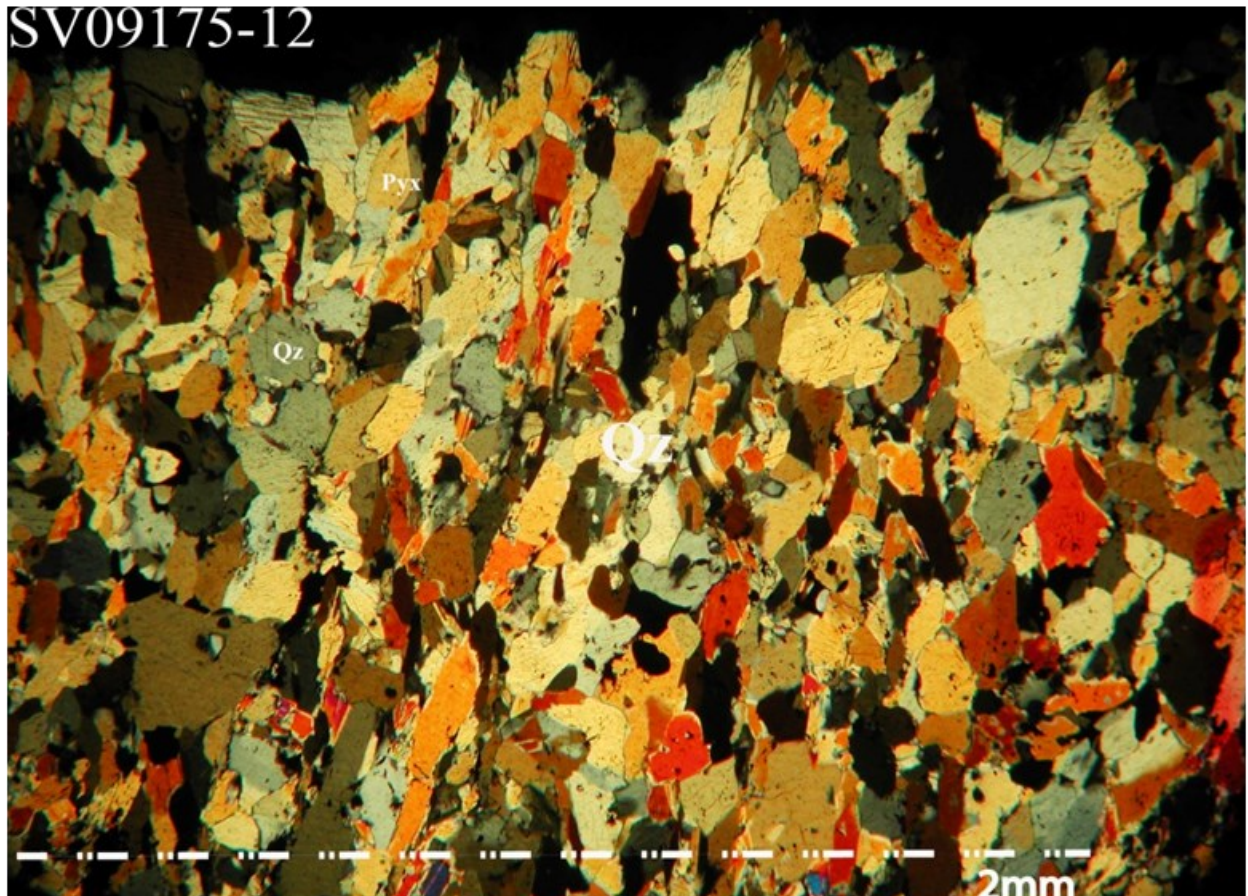
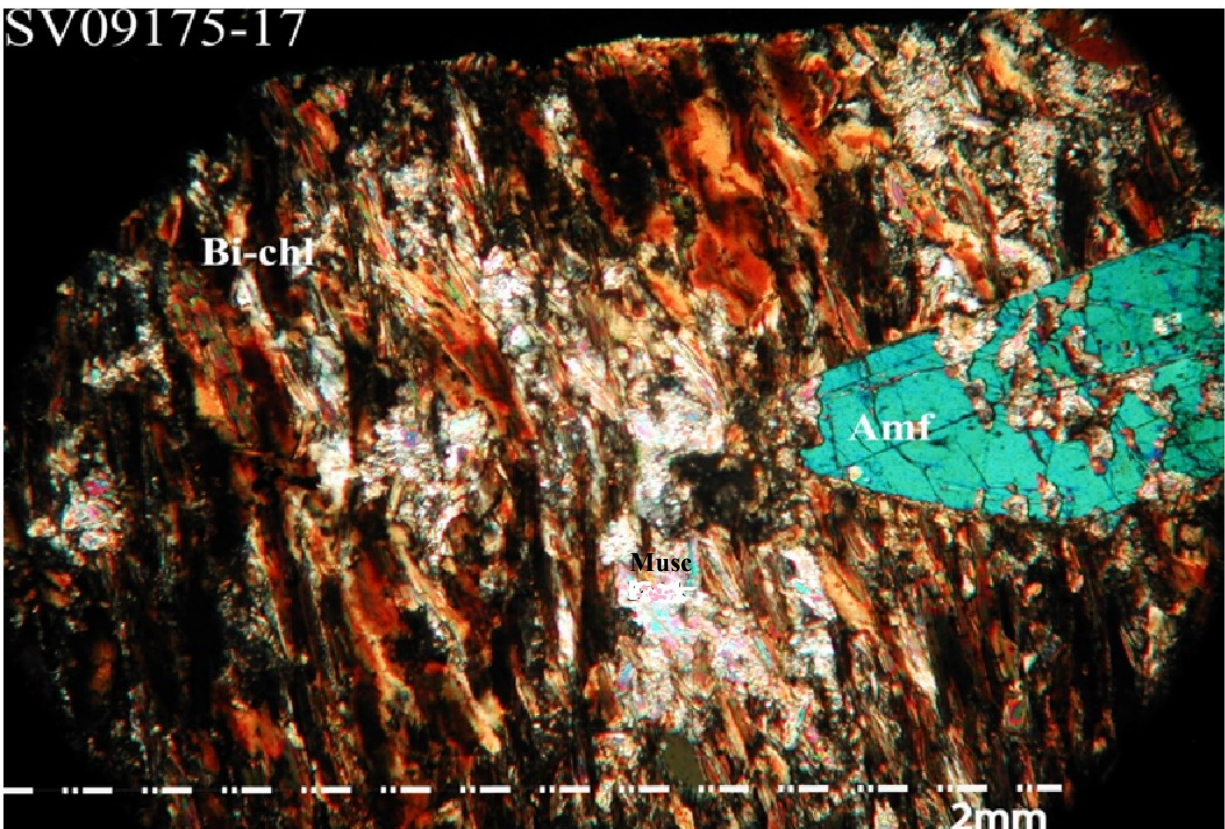


Fig. 15. Above: Optical microscope image of sample SV09175-12. Minerals identified are quartz and pyroxene. A BSE image of this sample is found in Fig. 21. Below is sample SV09175-17: Minerals identified in the optical microscope image are amphibole, chloritized biotite and muscovite. A BSE image for the sample is found in Fig. 21.

SV09175-17



SV09175-18

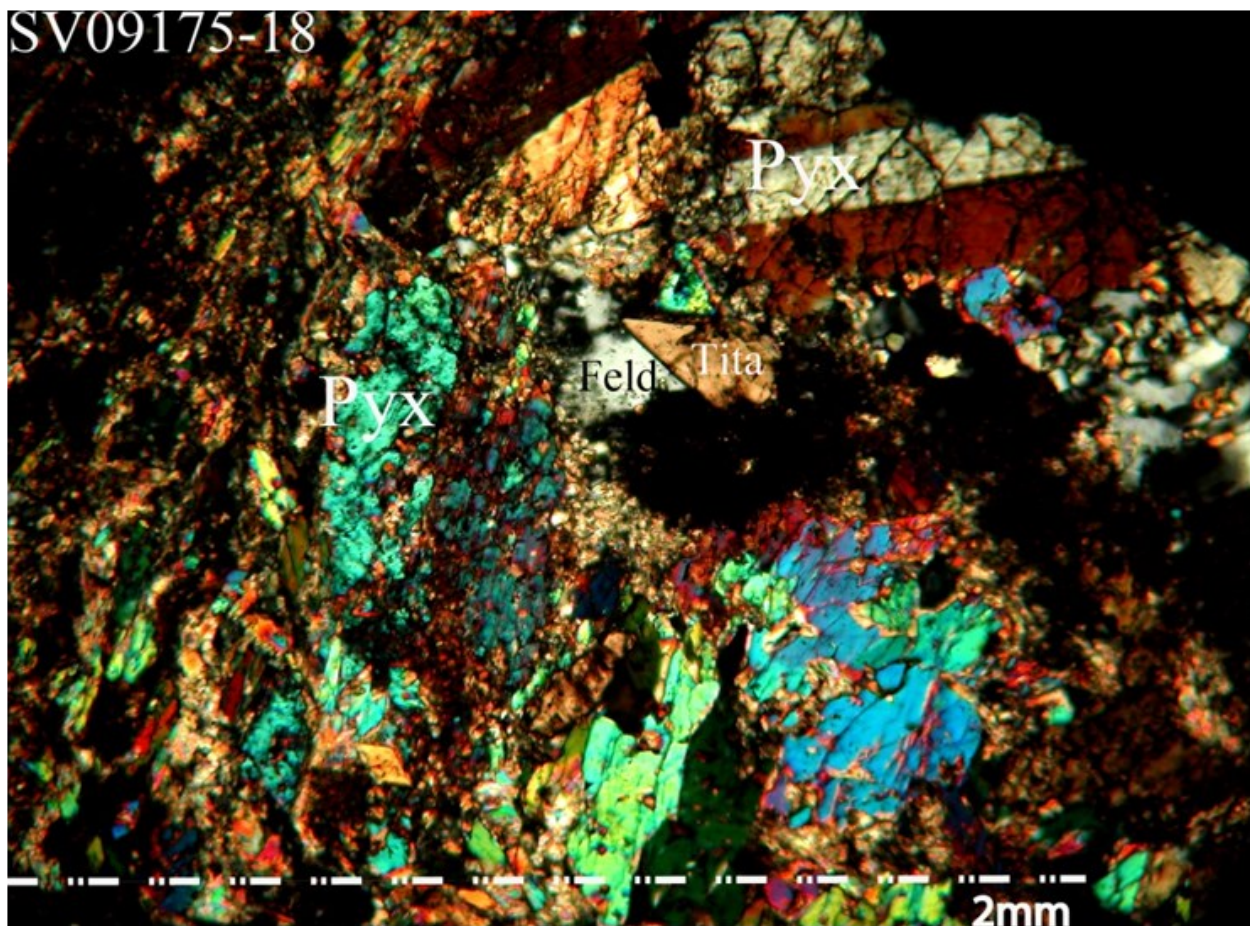
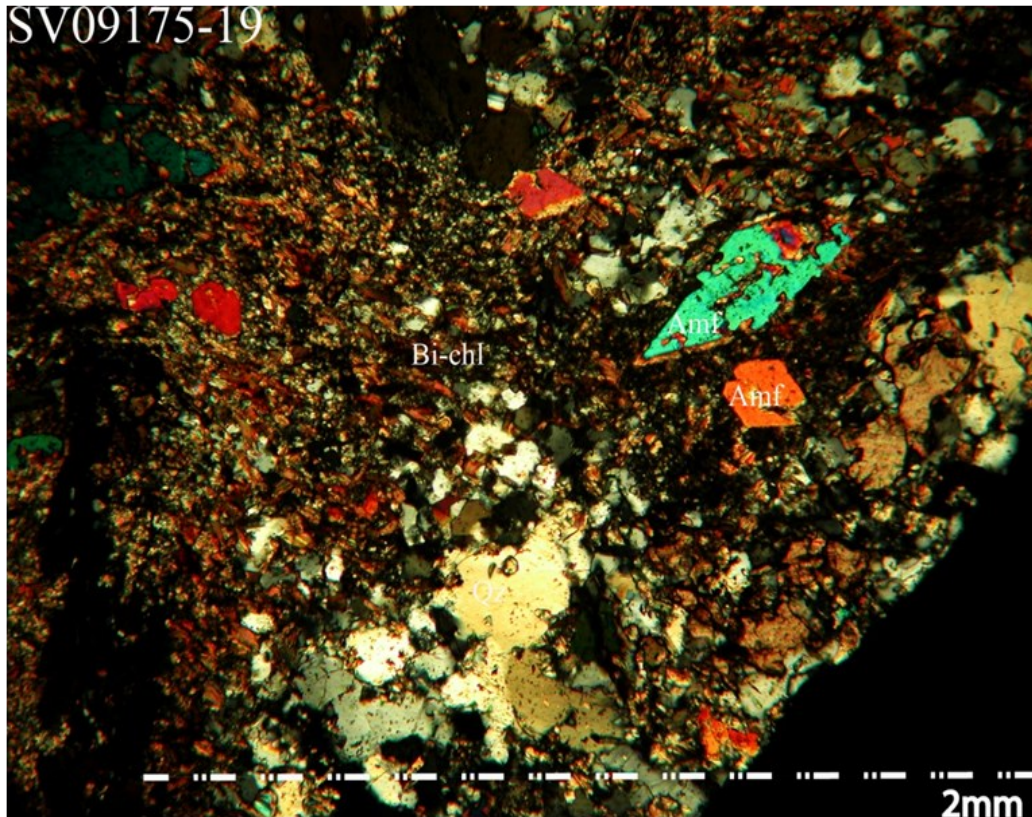


Fig. 16. Above: Optical microscope image of sample SV09175-18. Minerals identified are pyroxene, feldspar and titanite. Below: Optical microscope image of sample SV09175-19. Minerals identified are chloritized biotite, amphibole and quartz. BSE images for both samples are found in Fig. 22.

SV09175-19



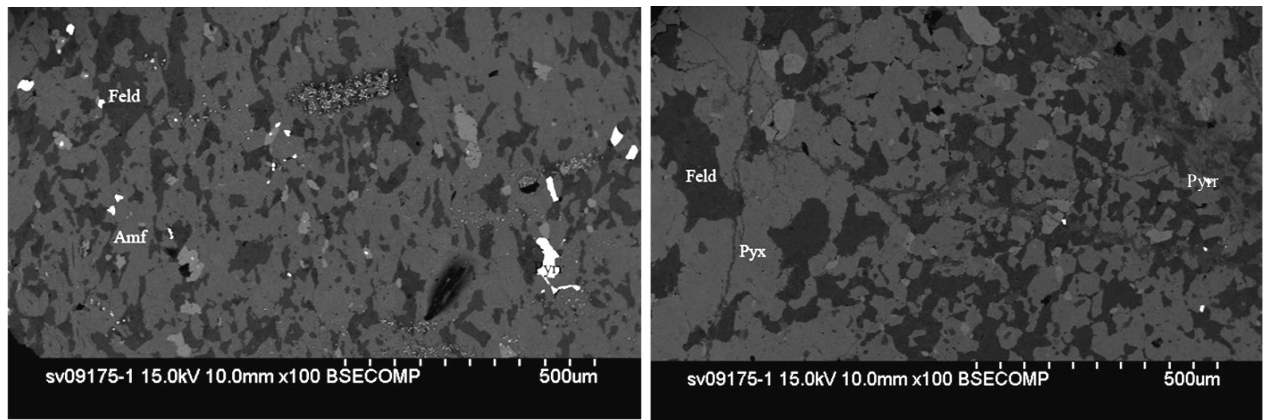


Fig. 17. Sample SV09175-1, left BSE image displaying feldspar, amphibole and pyrrhotite. P1 is hornblende, P2 anortite, P3 and pyrrhotite.

The BSE image to the right displays feldspar, pyroxene, pyrrhotite. P4 is pyrrhotite (white colour), P5 K-feldspar and P6 clino-pyroxene (diopside).

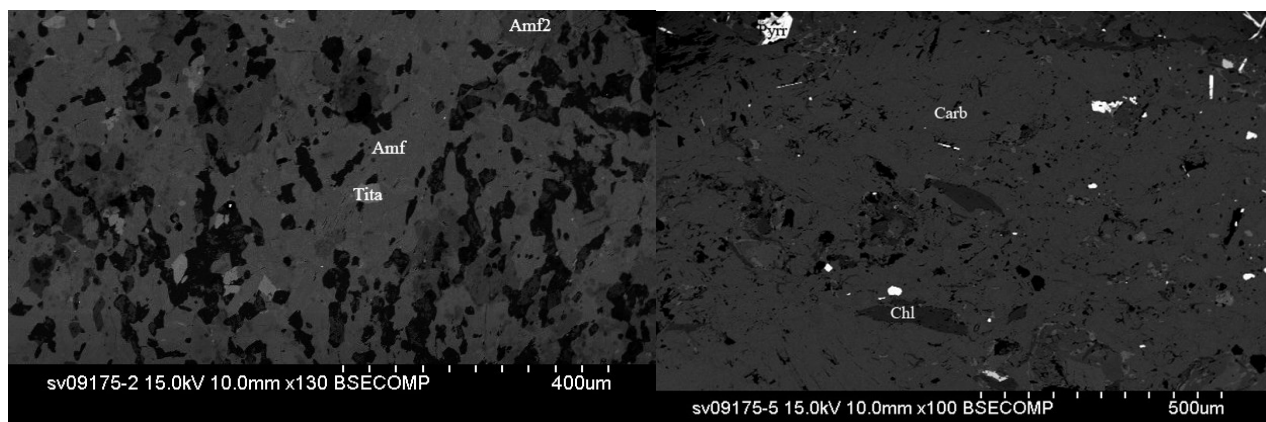


Fig. 18. The BSE image to the left (sample SV09175-2) displays amphiboles and titanite (P8). P7 is actinolite and P9 is hornblende. The BSE image to the right (sample SV09175-5) displays pyrrhotite (P10), carbonate (P11) and chlorite (P12).

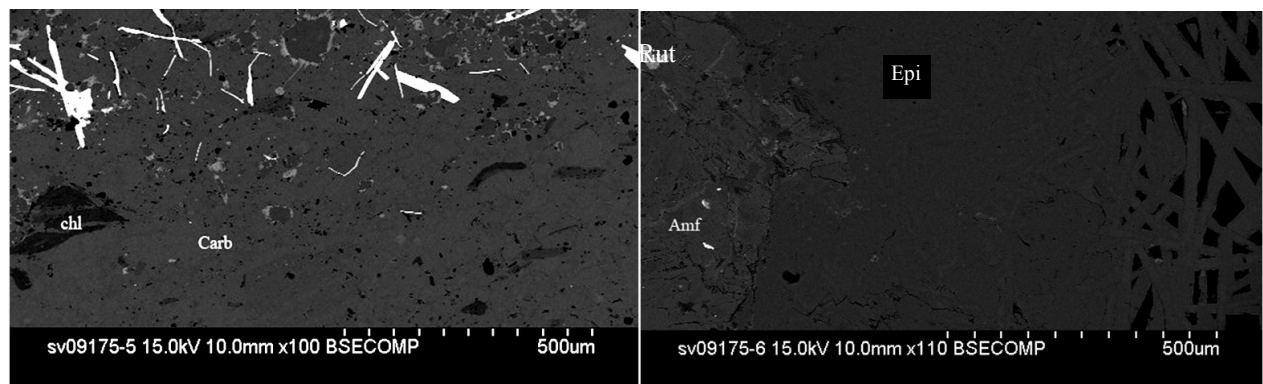


Fig. 19. Minerals identified in the BSE image (sample SV09175-5) to the left are chlorite (P13) and carbonate (P14). This image is from the same sample as Fig. 18 (right).

The BSE image to the right (sample SV09175-6) displays epidote (P16), rutile (P15) and amphibole (hornblende, P17).

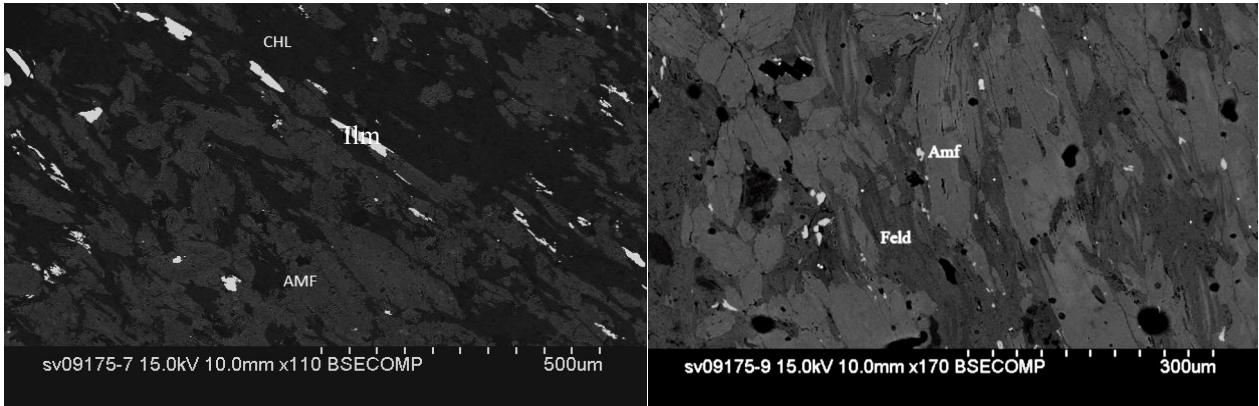


Fig. 20. Image to the left (sample SV09175-7) displays chlorite (P18), amphibole (P19), and Ilmenite (P20). The amphibole is actinolite and the titanite is the white coloured crystals. The image to the right (sample SV09175-9) displays amphibole (actinolite) (P22) and epidote (P21).

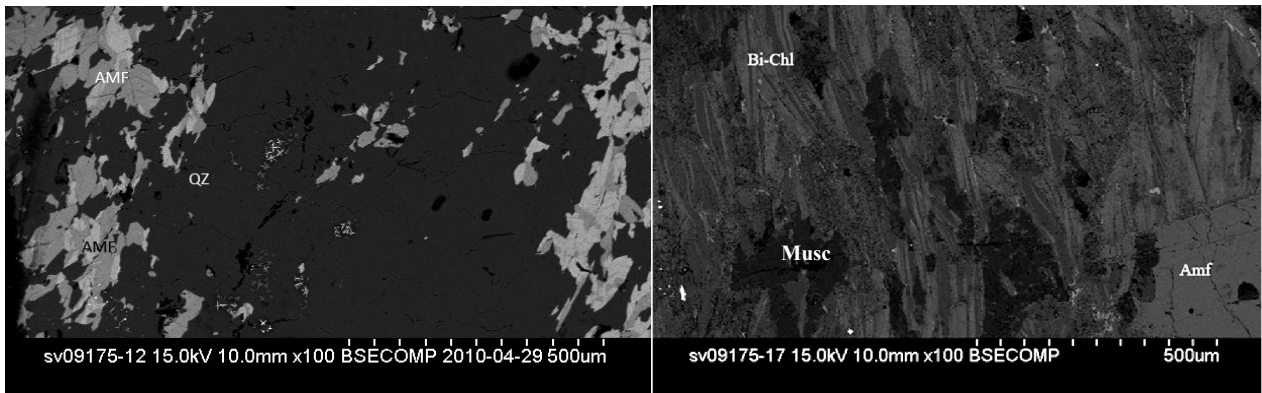


Fig. 21. The BSE image to the left (sample SV09175-12) displays quartz (P24), amphibole (P23 and 25). P23 is the amphibole in the upper and P25 is the amphibole in the lower part of the image. Both amphiboles are actinolite. The BSE image to the right (sample SV09175-17) displays chloritized biotite (P26), muscovite (P27) and amphibole (P28, actinolite).

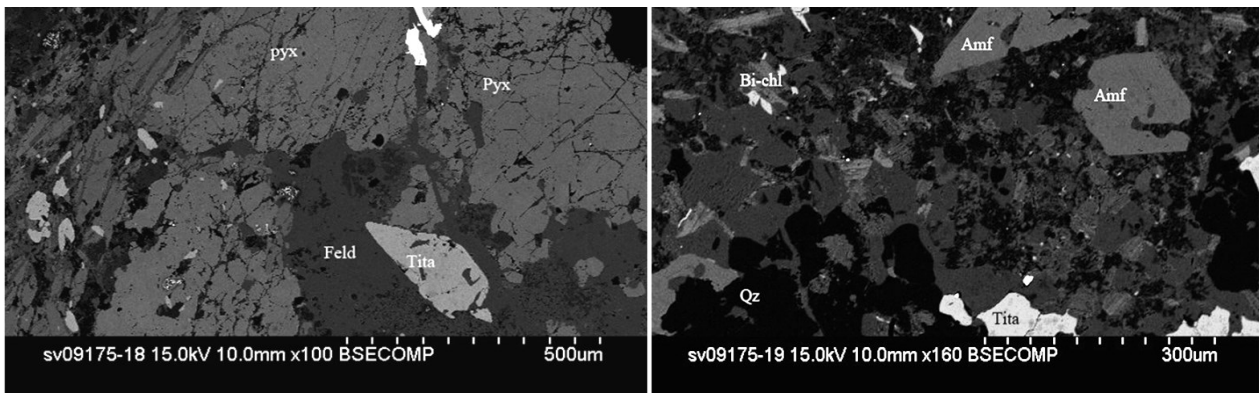


Fig. 22. The BSE image to the left (sample SV09175-18) displays clinopyroxene (P29 and 32), K-feldspar (P30), titanite (P31). The BSE image to the right (sample SV09175-19) displays actinolite (P33 and 34), chloritized biotite (P35), quartz (P36) and titanite (P37).

7 Discussion

This study is restricted to one drill core outside the current pit design from 2009. This leads to the question to what extent the results are wholly representative. However, they indicate how further studies should be focused.

The major minerals found in the collected core sample are amphibole (actinolite, hornblende), quartz, epidote, feldspars (plagioclase and K-feldspar), pyroxene (clinopyroxene; diopside and hedenbergite), biotite, prehnite, chlorite, chloritized biotite and muscovite. The accessory minerals are pyrrhotite, chalcopyrite, a carbonate mineral, apatite, löllingite, arsenopyrite, zircon and titanite. Their distribution varies irregularly within the core sample and the individual samples. The rock type referred to by Dragon Mining AB as amphibolite (Fig. 6) is the amphibole-richest rock, but amphibole is also found in the altered rock.

Deformational events

No evidence has been found suggesting that the granite at Svartliden is genetically associated with the host rock (Fig. 24). The granitic intrusion at Svartliden is younger than the ore and cuts and displaces the lodes (Grahn et al., 2002). Structures have not been mapped.

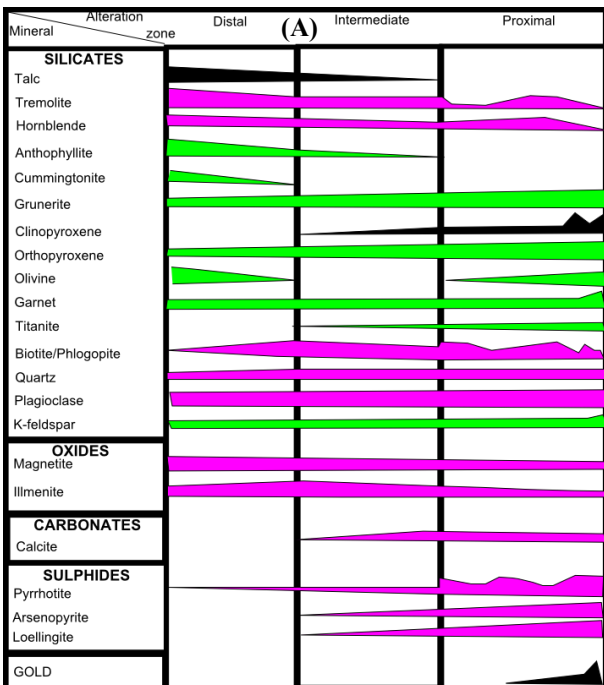
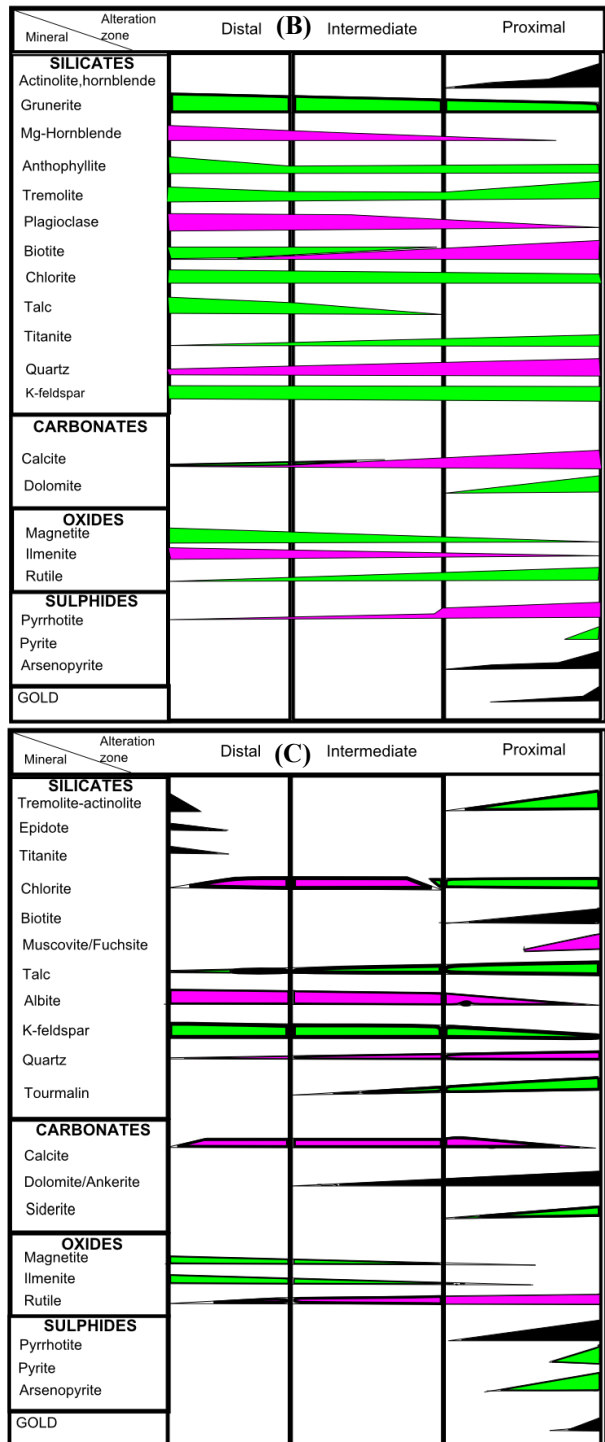


Fig. 23. The upper figure (A): Alteration scheme around lode-gold deposits in mid-amphibolite to lower granulite facies. The width shows how the relative proportions of a mineral change as a function of the distance from the ore. Upper figure to the right (B): The same information for the lower amphibolite facies Lower figure to the right (C): The same information for upper greenschist facies (Modified from Eilu et al., 1999). Colour code indicates common minerals to less common minerals. Black indicates most common, purple second most common and green less common. These schemes have been used as reference material for interpretation of the alteration.

Hence, the fold pattern of the area is not known. Mapping of structures was never part of the present investigation. If this pattern had been known, it would have been feasible to place the different samples into the stratigraphy. Thus, all the conclusions obtained in the present report are tentative, due to the poor structural control.

The host rock seems to have undergone more than one deformational event. The samples 4, 5, 7, 11, 12, 16 and 17 come from areas logged as: amphibolite, quartz mylonite, skarn or ore alteration and biotite schist (Fig. 6). The sampled rocks are lineated and fine-grained and occur in the contact regions within the sampled drill core. The quartz mylonite (Fig. 6)



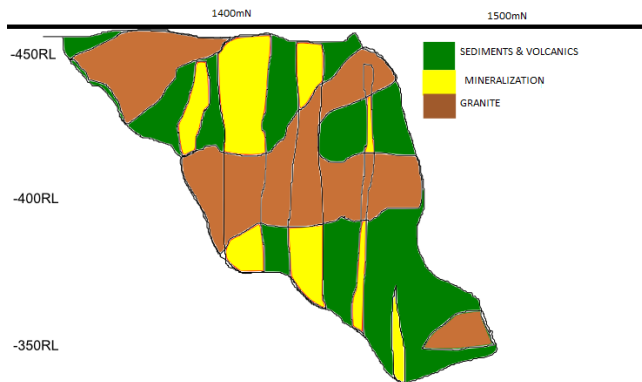


Fig. 24. Modified section from Svartliden, showing the granite that intrudes the sediments and the mineralization. RL= real level, level above sealevel (Modified from Grahn et al., 2002).

indicates a shear zone. There are no representative samples collected for the area logged as mylonite zone but the samples SV09175-4 and SV09175-5 (a and b) are the two sample closest to this zone. Sample 4 is strongly lineated suggesting shearing. However, no conclusive evidence is present to consider it as part of the Mylonite Zone. More sampling is needed to conclude whether the zone, from which sample 4 is taken represents a part of the mylonite zone.

Ore location within the lithological sequence

If the gold mineralization at Svartliden had been syngenetic, it would have been found not only in quartz or skarn veins but also in the host rock. Neither is there any positive evidence suggesting that the mineralization could have been syngenetic (Bark, 2008). Thus, the mineralization must be epigenetic.

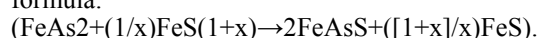
The core logging done by Dragon Mining shows from sample 1 to 19: amphibolite, quartz mylonite, amphibolite, skarn alteration, amphibolite, skarn alteration, amphibolite, skarn alteration, amphibolite and biotite schist (Fig. 6). Skarn alteration can be seen in several intervals within the core. The ore mineralization has migrated within the structures to be concentrated in a fold hinge. Shearing in Svartliden has provided the right environment for the mineralization. According to Johan Sjöberg (personal communication, 2009) the deformational events at Svartliden and Fäboliden are important for the ore alteration. The granite intrudes the mineralized zone and the amphibolite (Fig. 24). It is due to the deformation that fluids have been able to migrate and create the two lodes; the main and southern lodes are considered as one lode. It might be possible that gold deposition is due to a tectonic event that provided space for the fluids to migrate and at the same time prevented them from escaping and accumulating before reaching the fold hinge.

Metamorphism

The Svartliden deposit might have been exposed to more than one metamorphic event, since the mineral associations are not entirely consistent with the mid-amphibolite facies of the country rocks. Evidence that would support this possibility is: chloritization of biotite and the occurrence of minerals as epidote,

chlorite, actinolite, prehnite and diopside. Chlorite mineral and the chloritization phenomena are not common at mid-amphibolite facies conditions. A mineral paragenesis including chlorite, actinolite and diopside is typical for the greenschist facies. In the Yilgarn gold-mineralized areas, high-grade metamorphism is followed by a greenschist-facies event (Ridley et al., 2000). This is similar to what is suggested here for the Svartliden deposit. Replacement of biotite by chlorite is common in the Yilgarn Craton and is related to the retrograde metamorphism (Ridley et al., 2000); chlorite is interpreted as a secondary mineral. According to Ridley et al. (2000), chlorite and diopside are major minerals that may be found in mafic rocks associated with the retrograde assemblage. Prehnite that is found in samples SV09175-6 and -17 is a low grade mineral that is associated with retrograde metamorphism. The samples in which prehnite is found, are logged as amphibolite (sample 6) and biotite schist (sample 17; Fig. 6) by Dragon Mining. The sample SV09175-6 is interpreted to belong to the proximal zone whereas sample SV09175-17 belongs to the distal (table 2). The proximal zone is the mineralized zone. The presence of prehnite is considered evidence in favour of an epigenetic ore formation. According to Grahn et al. (2002), it is not clear whether the retrograde metamorphism at Svartliden is related to the granite intrusion (Fig. 24) or not. The contacts between the ore body and the granite are sharp and at some places mineralization traces are found in the granite intrusion. The mineralization traces could have been incorporated during intrusion or precipitated from still active circulation of ore solutions. Recent studies on garnet in Svartliden have indicated retrograde alteration. Some garnets are replaced by muscovite and chlorite that form pseudomorphs after garnet (Andersson, 2011).

Bark (2008) suggests that graphite could be a good indicator of post peak metamorphism. Eklund (2007) found graphite within the analysed samples from Svartliden. At lower temperatures, arsenopyrite replaces löllingite and gold is released (Eklund, 2007). According to Eklund (2007) arsenopyrite at the Svartliden deposit has crystallized at 360°C, which should be the approximate temperature of gold release. Tomkins and Mavrogenes (2001), who performed a series of tests on the behaviour of arsenopyrite, löllingite and gold in pro- and retrograde metamorphism found that gold is set free from decomposing löllingite. They also concluded that löllingite mineral composition changes during retrograde metamorphism. Löllingite desolves with decreasing temperature. In the beginning of the prograde metamorphism, arsenopyrite is rimmed by löllingite and when the metamorphism changes from prograde to retrograde conditions löllingite becomes rimmed within arsenopyrite. A possible reaction formula:



Eklund's (2007) results show that in the Svartliden deposit, gold is found in the löllingite rimmed with arsenopyrite. These considerations lead to the tentative suggestion that the retrograde metamorphism suggested from the chloritization phenomena and the

Samples	Logged as	Minerals Found	Interpreted alteration zone
SV09175-1	Amphibolite	Amphibole (hornblende), clinopyroxene (diopside), K-feldspar, plagioclase, quartz, pyrrhotite, biotite.	Proximal
SV09175-2	Amphibolite	Amphibole (actinolite), carbonate, plagioclase, chlorite, biotite, pyrrhotite, titanite.	Proximal
SV09175-3	Amphibolite	K-feldspar, quartz, clinopyroxene, amphibole, carbonate.	Proximal
SV09175-4	Amphibolite/quartz mylonite	Quartz, amphibole, biotite, K-feldspar.	Proximal
SV09175-5	Quartz mylonite	Carbonate, clinopyroxene, amphibole (actinolite) , plagioclase, pyrrhotite, chlorite, quartz.	Proximal
SV09175-6	Amphibolite	Clinopyroxene, amphibole (actinolite, hornblende), prehnite, epidote, biotite, carbonate, pyrrhotite.	Proximal
SV09175-7	Amphibolite	Clinopyroxene, chlorite, amphibole (actinolite), biotite, pyrrhotite, titanite.	Proximal
SV09175-8	Skarn/ore alteration	Quartz, clinopyroxene, amphibole (hornblende), biotite, pyrrhotite, zircon, apatite.	Mineralized
SV09175-9	Skarn/ore alteration	Amphibole (actinolite), epidote, clinopyroxene, biotite, chloritized biotite, sillimanite, pyrrhotite, zircon.	Mineralized
SV09175-10	Amphibolite	Clinopyroxene, amphibole (hornblende, actinolite), biotite, apatite, pyrrhotite, arsenopyrite	Mineralized
SV09175-11	Amphibolite	Feldspar (k-feldspar, plagioclase), quartz, amphibole (hornblende, actinolite), clinopyroxene, biotite, apatite, löllingite, arsenopyrite, pyrrhotite.	Mineralized
SV09175-12	Skarn/ore alteration	Quartz, clinopyroxene, amphibole, biotite, apatite, pyrrhotite, fluorapatite.	Mineralized
SV09175-13	Skarn/ore alteration	Clinopyroxene, quartz, pyrrhotite, amphibole, K-feldspar, biotite, carbonate, chalcopyrite, zircon.	Mineralized
SV09175-14	Skarn/ore alteration	Quartz, amphibole (actinolite), biotite, K-feldspar, apatite, pyrite, zircon.	Mineralized
SV09175-15	Skarn/ore alteration	Quartz, biotite, amphibole (actinolite), pyrrhotite.	Mineralized
SV09175-16	Skarn/ore alteration	Clinopyroxene, plagioclase, quartz, biotite, pyrrhotite.	Mineralized
SV09175-17	Biotite schist	Muscovite, biotite, chloritized biotite, K-feldspar, amphibole (actinolite, hornblende), quartz, prehnite, carbonate, clinopyroxene, pyrrhotite, apatite, titanite.	Distal
SV09175-18	Biotite schist	Clinopyroxene, K-feldspar, quartz, amphibole (actinolite), titanite, pyrrhotite.	Distal
SV09175-19	Biotite schist	Amphibole (actinolite), biotite, chloritized biotite, quartz, clinopyroxene, K-feldspar, carbonate.	Distal

Tabel 2. This table has data from table 1 and fig. 6. and the interpreted alteration is based on Grahn et al. 2002.

occurrence of diopside and prehnite is responsible for the ore formation at Svartliden. However, the present evidence is insufficient to unequivocally tie ore formation and alteration to the retrograde metamorphism. The retrograde metamorphism at Fäboliden is tied to the ore alteration and so are the quartz veins. At Fäboliden, quartz veins have been found within the metagraywacke sequence (Bark, 2008).

Mineral associations and chemistry

In the sampled core from Svartliden, chlorite occurs in association with biotite, amphibole (hornblende and actinolite), clinopyroxene and calcite. It has not been found in contact with quartz in the studied samples. As seen in sample SV09175-5 (Figs. 12 and 13), chlorite appears on carbonate minerals in the amphibolite zone (Fig. 6). No graphite has been

identified in the investigated samples. The mineral assemblage of the studied samples, which includes diopside, hornblende, actinolite, clinopyroxene, titanite, quartz, plagioclase, K-feldspar, carbonates, pyrrhotite and löllingite compares well with the proximal alteration zone scheme (Fig. 23) for both greenschist and mid-amphibolite facies. This scheme is a standard scheme to determine alteration facies. The results are similar to those obtained by Grahn et al. (2002), Eklund (2007) and Bark (2008) suggesting that the Svartliden host rocks belongs to the mid-amphibolite facies and that the dominating alteration zone is the proximal zone.

The Al-content varies significantly in the amphibole (Fig. 8). According to Bark (2008) the hydrothermal ore alteration at Fäboliden includes the formation of calcic amphibole, Ca-rich plagioclase and diopside. This is consistent with results obtained from the sample core

SV09175 (Fig. 8). Proximal alteration of the host rock around gold deposits in the Yilgarn Craton is similar to that at Svartliden (Fig. 23; Ridley et al. (2002). The amphibole shows signs of being altered or chloritized.

In the Yilgarn Craton, alteration zones around gold deposits include high-temperature minerals like amphibole and diopside. Pyrrhotite appears together with amphibole in these zones in the Yilgarn craton (Ridley, 1997).

Pyrrhotite may appear as inclusion in the amphibole in some areas. According to Eklund (2007), the gold appears together with arsenopyrite/löllingite, pyrrhotite, amphibole and diopside. No gold has been found in the skarn/ore alteration in the present drill core (table 2).

The present samples 1 to 7 agree with the expected minerals in the proximal zone: amphibole, pyrrhotite and quartz. Minerals in samples 8 to 16 correspond to the expected minerals in the mineralized zone: amphibole, pyroxene, pyrrhotite, arsenopyrite and quartz. Sample 11 contains löllingite, but this is the only record of löllingite among the analysed samples. No mineralogical interpretation of the highly mineralized zone can be performed from the analysis of these samples. Thus, samples 1 to 7 are considered to belong to the proximal zone, the samples 8 to 16 to the mineralized zone and samples 17 to 19 to the distal zone (table 2; after Grahn et al. 2002). The intermediate zone is difficult to distinguish and has not been identified in the present samples.

The data are insufficient to determine the metamorphic facies. Minerals that corresponds to both greenschist and mid-amphibolitic facies are found within the analysed core.

8 Conclusions

The main conclusions from the thesis about the alteration at Svartliden are:

- The most important minerals found in the core sample are: amphibole, clinopyroxene, biotite, quartz, diopside, K-feldspar, prehnite and epidote. Amphibole, clinopyroxene, K-feldspar and biotite show the most prominent alterations. Actinolite appears as a replacement of hornblende and

diopside. Chlorite and chloritized biotite together with prehnite are good indicators of retrograde metamorphism at Svartliden.

- According to structural and mineralogical evidence both the mineralization and the granite intrusion is younger than the host rock. Contrary to the mineralization, the host rock is metamorphosed in the amphibolite facies during the svecofennian event. Svartliden is an epigenetic deposit.
- The hydrothermal alteration at Svartliden is similar to that at Fäboliden indicated by the calcic amphibole, diopside and Ca plagioclase.
- The most common ore mineral in the studied sample is pyrrhotite followed by arsenopyrite and löllingite.
- No zoning in individual grains has been found in any of the samples.

Suggestions for further studies

More core samples should be investigated to provide better reference. Samples should be collected with more precision to determine the alteration facies and structural control.

9 Acknowledgements

I would like to express my gratitude to my supervisor at the Department of Geology in Lund, Anders Lindh. Anders has been patient, supportive, open for enthusiastic discussions, and has been approachable whenever I have needed feedback. Moreover thanks to Johan Sjöberg and Johan Söderhielm at Dragon Mining Sweden who agreed on this project. Special thanks to Sonja Pabst from University of Heidelberg, Germany for helping me with my amphibole calculations. In the end I would like to thank my family and friends their support. Especially my dad who has inspired me to be strong and to never give up.

10 References

- Andersson, J. 2011: The Svartliden granite: Petrography, whole rock geochemistry and stable isotope composition. Master thesis, Luleå University.
- Bark, G. 2008: On the origin of the Fäboliden orogenic gold deposit, Northern Sweden. Doctoral Thesis 2008:72, Luleå University of Technology.
- Best, M. G. 2003: *Igneous and metamorphic petrology*. 2. ed. Malden: Blackwell Publishers
- Björk, L., and Kero, L., (2001): *Berggrundskartan 22H Järvsjö NO skala 1:50000*. Sveriges Geologiska Undersökning, Ai nr.145.
- Claesson, S., Huhma, H., Kinny, P.D., Williams, I.S. (1993): Svecofennian detrital zircon ages - implications for the Precambrian evolution of the Baltic Shield. *Precambrian Research* 64: 109-130.
- Claesson, S and Lundqvist, T. 1995: Origins and ages of Proterozoic granitoids in the Bothnian Basin, central Sweden; isotopic and geochemical constraints. *Lithos* 36: 115-140.
- Eklund, D. 2007: Mineralogy of the hypozonal Svartliden gold deposit, northern Sweden, with emphasis on the composition and paragenetic relations of electrum.
- Eilu, K. P., Mathison, I. C., Groves, I. D., Allardyce, J. W. 1999: Atlas of alteration assemblages, styles and zoning in orogenic Lode-Gold deposits in a variety of host rock and metamorphic settings. University of Western Australia. Dept. of Geology and Geophysics ; no. 30.
- Grahn, T., Sjölund, E., Unée, Å.J., Searle, J. 2002: Good old fashioned prospection finds a West Australian Eastern Goldfields style of epigenetic lode style gold mineralisation in Sweden.
- Högdahl, K., Sjöström, H., Andersson, B. U. 2002: Tectonic units and correlation problematics in the central Svecofennian domain. Department of Geology, Lund University, Sölvegatan 12, 223 62 Lund.
- Högdahl, K (red.). 2004: The Transscandinavian Igneous Belt (TIB) in Sweden: a review of its character and evolution. Espoo: Geological survey of Finland.
- Lahtinen, R., Korja, A.-S., Nironen, M. 2005: Paleoproterozoic tectonic evolution, in Lahtinen, M., Nurmi, P. A., Rämö, O. T., (eds): Precambrian geology of Finland — key to the evolution of the Fennoscandian Shield, Elsevier B. V. 481-532.
- Leake, E. B., Woolley, R. A., Arps, E. S. C., Birch, D. W., Gilbert, M. C., Grice, D. J., Hawthorne, C. F., Kato, A., Kisch, J. H., Krivovichev, G. V., Linthout, K., Laird, J., Mandarino, A. J., Maresch, V. W., Nickel, H. E., Rock, M.S.N., Schumacher, C.J., Smith, C. D., Stephenson, C. N.N., Ungaretti, L., Whittaker, J. W. E., Youzhi, G. 1997: Nomenclature of amphiboles: Report of the subcommittee on amphiboles of the international mineralogical association, commission on new minerals and mineral names. *The Canadian Mineralogist*. Vol. 35, pp. 219-246.
- Morimoto, N., Fabries, J., Ferguson, K. A., Ginzburg, V. I., Ross, M., Seifert, A. F., Zussman, J., Aoki, K., Gottardi, G. 1988: Nomenclature of pyroxenes: Subcommittee on pyroxenes, commission on new minerals and mineral names, international mineralogical association. *American Mineralogist*. Vol. 73, pp1123-1133.
- Ridley, J., Groves, I. D., Knight, T. J. 2000: Gold deposits in amphibolite and graulite facies terranes of the Archean Yilgarn Craton, Western Australia: Evidence and implications of synmetamorphic mineralization. *Reviews in Economic geology* Vol. 11, Metamorphic and metamorphogenic ore deposits. *Economic geology*, chapter 12.
- Robb, L. 2005: Introduction to ore-forming processes. Malden: Blackwell Publishing.
- Tomkins, G. A & Mavrogenes, A. J. 2001: Redistribution of Gold within Arsenopyrite and Löllingite during Pro- and Retrograde Metamorphism: Application to Timing of Mineralization. *Economic Geology* vol. 96, 2001, pp. 525-534.
- Weihed, P., Bergman, J. and Bergström, U., 1992: Metallogeny and tectonic evolution of the Early Proterozoic Skellefte district, northern Sweden. In: G. Gaul and K. Schulz (Editors), *Precambrian Metallogeny Related to Plate Tectonics*. *Precambrian Res.*, 58: 143-167.
- Wenk, H-R & Bulakh, A. G. 2004: Minerals: their constitution and origin. Cambridge: Cambridge University Press.
- Wilson, M.R., Hamilton, P.J., Fallick, A.E., Aftalion, M. and Michard, A., 1985: Granites and early Proterozoic crustal evolution in Sweden: evidence from Sm-Nd, U-Pb and O isotope systematics. *Earth Planet. Sci. Lett.*, 72: 376-388.

Web sources:

- <http://www.dragon-mining.com.au/-Sweden-.html>(2010)
- <http://www.mindat.org/> (2010)

11 Appendix

Appendix A

Results from the different point analysed in the EDS. Sample numbers are marked in red.

SV09175-1 Amphibole (Hornblende)

P1

Element	Weight%		Oxide	Formula	Number of ions
	Weight%	sigma			
Na	0.54	0.08	0.56	0.73	Na
Mg	6.47	0.11	6.33	10.72	Mg
Al	3.06	0.09	2.70	5.78	Al
Si	22.63	0.17	19.19	48.41	Si
K	0.18	0.06	0.11	0.22	K
Ca	8.46	0.13	5.03	11.83	C
Ti	0.29	0.08	0.15	0.49	Ti
Fe	13.49	0.28	5.75	17.36	Fe
O	40.42	0.29	60.17		
Totals	95.53			23.00	

SV09175-2 Amphibole (actinolite)P7

P7

Element	Weight%		Oxide	Formula	Number of ions
	Weight%	sigma			
Na	0.33	0.08	0.34	0.45	Na
Mg	6.62	0.11	6.36	10.97	Mg
Al	1.91	0.07	1.66	3.61	Al
Si	24.1	0.17	20.06	51.56	Si
Ca	8.84	0.13	5.16	12.37	Ca
Ti	14.49	0.28	6.07	18.65	Fe
Fe					2.31
O	41.31	0.28	60.36		
Totals	97.61			23.00	

Cation sum 15.22 Cation sum 15.11

Plagioclase (anortite) P2

P2

Element	Weight%		Oxide	Formula	Number of ions
	Weight%	sigma			
Na	1.44	0.08	1.36	1.94	Na
Al	17.15	0.14	13.81	32.39	Al
Si	21.60	0.17	16.71	46.21	Si
Ca	12.27	0.15	6.65	17.16	Ca
O	45.26	0.25	61.47		
Totals	97.71			8.00	

Titanite P8

P8

Element	Weight%		Oxide	Formula	Number of ions
	Weight%	sigma			
Al	0.57	0.05	0.51	1.08	Al
Si	14.62	0.13	12.58	31.29	Si
Ca	20.72	0.18	12.49	28.99	Ca
Ti	23.53	0.24	11.87	39.25	Ti
Fe	0.46	0.12	0.20	0.60	Fe
O	41.29	0.28	62.35		
Totals	101.2			5.01	

Pyrrhotite P3

P3

Element	Weight%		Oxide	Formula	Number of ions
	Weight%	sigma			
S	38.14	0.22	54.29		
Fe	55.92	0.49	45.71		
Totals	94.05				

Cation sum 3.01

Pyrrhotite P4

P4

Element	Weight%		Oxide	Formula	Number of ions
	Weight%	sigma			
S	35.06	0.22	54.07		
Fe	51.86	0.47	45.93		
Totals	86.92				

Amphibole2 (hornblende) P9

P9

Element	Weight%		Oxide	Formula	Number of ions
	Weight%	sigma			
Na	0.62	0.08	0.66	0.84	Na
Mg	5.11	0.10	5.13	8.48	Mg
Al	4.10	0.09	3.71	7.75	Al
Si	21.31	0.16	18.51	45.58	Si
K	0.21	0.05	0.13	0.26	K
Ca	7.98	0.13	4.86	11.16	Ca
Fe	16.02	0.29	7.00	20.61	Fe
O	39.33	0.28	59.99		
Totals	94.69				23.00

Cation sum 15.34

K-feldspar P5

P5

Element	Weight%		Oxide	Formula	Number of ions
	Weight%	sigma			
Mg	0.15	0.05	0.14	0.25	Mg
Al	17.56	0.14	15.24	33.17	Al
Si	21.16	0.17	17.65	45.26	Si
K	8.86	0.13	5.31	10.67	K
Fe	0.68	0.12	0.28	0.97	Fe
O	41.92	0.25	61.38		
Totals	90.32			8.00	

SV09175-5 Pyrrhotite P10

P10

Element	Weight%		Oxide	Formula	Number of ions
	Weight%	sigma			
S	37.18	0.22	53.72		

Clinopyroxene (diopside) P6

P6

Element	Weight%		Oxide	Formula	Number of ions
	Weight%	sigma			
Mg	5.3	0.10	5.26	8.79	Mg
Al	0.15	0.05	0.14	0.29	Al
Si	23.47	0.17	20.15	50.21	Si
Ca	16.36	0.17	9.84	22.89	Ca
Fe	10.41	0.25	4.49	13.39	Fe
O	39.88	0.27	60.11		
Totals	95.57			6.00	

Carbonate P11

P11

Element	Weight%		Oxide	Formula	Number of ions
	Weight%	sigma			
Mg	0.27	0.05	0.61	0.45	Mg
Ca	36.28	0.24	49.39	50.77	Ca
O	14.66	0.15	50.00		
Totals	51.22			3.98	28.00

Cation sum 28.00

Totals 51.22

Cation sum 28.00

Chlorite P12

Element	Weight%			Oxide	Number of ions
	Weight%	sigma	Atomic%		
Mg	14.99	0.14	15.58	24.85	Mg
Al	9.83	0.13	9.21	18.57	Al
Si	13.75	0.15	12.37	29.41	Si
Fe	9.61	0.24	4.35	12.36	Fe
O	37.02	0.26	58.49		28.00
Totals	85.19				

Amphibole (hornblende) P17

Element	Weight%			Oxide	Number of ions
	Weight%	sigma	Atomic%		
Na	0.95	0.08	0.93	1.28	Na
Mg	8.86	0.12	8.15	14.69	Mg
Al	5.73	0.11	4.75	10.83	Al
Si	22.66	0.17	18.05	48.47	Si
K	0.27	0.06	0.15	0.32	K
Ca	8.96	0.14	5.00	12.54	Ca
Fe	7.55	0.22	3.02	9.71	Fe
O	42.87	0.28	59.94		23.00
Cation sum	19.87				
Totals	97.84				

Chlorite P13

Element	Weight%			Oxide	Number of ions
	Weight%	sigma	Atomic%		
Mg	16.25	0.15	16.43	26.94	Mg
Al	10.36	0.14	9.44	19.58	Al
Si	13.99	0.15	12.25	29.92	Si
Fe	7.70	0.22	3.39	9.90	Fe
O	38.04	0.27	58.48		28.00
Totals	86.33				

SV09175-7 Chlorite P18

Element	Weight%			Oxide	Number of ions
	Weight%	sigma	Atomic%		
Mg	14.17	0.14	15.10	23.50	Mg
Al	10.21	0.13	9.80	19.30	Al
Si	13.18	0.14	12.16	28.20	Si
Fe	9.53	0.24	4.42	12.26	Fe
O	36.16	0.26	58.53		28.00
Cation sum	19.88				
Totals	83.25				

Carbonate P14

Element	Weight%			Oxide	Number of ions
	Weight%	sigma	Atomic%		
Ca	38.13	0.24	50.00	53.35	Formula
O	15.22	0.15	50.00		Ca
Totals	53.35				23.00

Amphibole (actinolite) P19

Element	Weight%			Oxide	Number of ions
	Weight%	sigma	Atomic%		
Na	0.39	0.07	0.37	0.52	Na
Mg	11.92	0.13	10.91	19.77	Mg
Al	1.48	0.08	1.22	2.79	Al
Si	25.55	0.18	20.23	54.66	Si
Ca	8.42	0.13	4.67	11.78	Ca
Ti	1.40				Ti
Fe	5.71	0.21	2.28	7.35	Fe
O	43.40	0.27	60.33		23.00
Totals	96.86				

SV09175-6 Titanite P15

Element	Weight%			Oxide	Number of ions
	Weight%	sigma	Atomic%		
Al	0.21	0.05	0.21	0.40	Al
Si	1.32	0.06	1.23	2.83	Si
Ca	2.10	0.08	1.37	2.93	Ca
Ti	56.35	0.35	30.83	94.00	Ti
Fe	0.58	0.14	0.27	0.75	Fe
O	40.35	0.31	66.08		3.00
Totals	100.91				

Ilmenite P20

Element	Weight%			Oxide	Number of ions
	Weight%	sigma	Atomic%		
Ti	31.55	0.26	20.22	52.62	Ti
Mn	0.94	0.13	0.52	1.21	Mn
Fe	34.84	0.41	19.15	44.82	Fe
O	31.33	0.31	60.11		3.00
Totals	98.65				

Epidote P16

Element	Weight%			Oxide	Number of ions
	Weight%	sigma	Atomic%		
Al	12.69	0.13	10.43	23.97	Al
Si	21.42	0.17	16.93	45.83	Si
Ca	20.06	0.19	11.11	28.07	Ca
Fe	0.94	0.13	0.37	1.34	Fe
O	44.10	0.26	61.16		25.00
Totals	99.21				

SV09175-9 Epidote P21

Element	Weight%			Oxide	Number of ions
	Weight%	sigma	Atomic%		
Mg	0.53	0.06	0.50	0.88	Mg
Al	12.00	0.13	10.23	22.67	Al
Si	21.32	0.17	17.46	45.60	Si
K	1.29	0.07	0.76	1.55	K
Ca	16.27	0.17	9.34	22.77	Ca
Fe	1.17	0.14	0.48	1.67	Fe
O	42.57	0.26	61.22		25.00
Totals	95.14				

Cation sum 15.81

Amphibole (actinolite) P22

Element	Weight%		Oxide	Number of ions
	Weight%	sigma		
Na	0.35	0.08	0.34	0.47
Mg	10.14	0.12	9.14	16.81
Al	2.00	0.08	1.62	3.77
Si	25.98	0.18	20.28	55.58
Ca	9.09	0.14	4.97	12.72
Fe	8.12	0.23	3.19	10.45
O	44.12	0.28	60.46	
Totals	99.80			23.00

Amphibole (actinolite) P28

Element	Weight%		Oxide	Number of ions
	Weight%	sigma		
Na	0.13		Na	0.42
Mg	3.48		Mg	7.99
Al	0.62		Al	2.21
Si	7.71		Si	24.24
Ca	1.89		Ca	19.83
Fe	1.21		K	0.35
			Ca	5.00
			Fe	4.88
			O	11.86
			Totals	8.72
				60.23
			Cation sum	41.93
				23.00
				Totals
				15.04
				97.73

SV09175-12 Amphibole (actinolite)**P23**

Element	Weight%		Oxide	Number of ions
	Weight%	sigma		
Mg	5.06	0.10	4.87	8.39
Al	0.21	0.06	0.18	0.39
Si	25.19	0.17	20.99	53.90
Ca	8.53	0.13	4.98	11.93
Fe	20.17	0.32	8.45	25.95
O	41.40	0.29	60.54	
Totals	100.56			23.00

SV09175-18 clinopyroxene (diopside) P29

Element	Weight%		Oxide	Number of ions
	Weight%	sigma		
Mg	1.85		Mg	7.08
Al	0.07		Al	25.59
Si	7.97		Si	17.40
Ca	1.89		Ca	8.43
Fe	3.21		Fe	43.18
O	23.00		O	101.68
Totals	100.56		Totals	14.99

Quartz P24

Element	Weight%		Oxide	Number of ions
	Weight%	sigma		
Si	48.23	0.22	33.33	103.18
O	54.95	0.23	66.67	
Totals	103.18			23.00

K-feldspar P30

Element	Weight%		Oxide	Number of ions
	Weight%	sigma		
Si	11.50		Na	0.42
O	23.00		Al	9.47
Totals	103.18		Si	31.14
			K	13.50
			O	46.82
			Totals	11.5
				101.35

Amphibole (actinolite) P25

Element	Weight%		Oxide	Number of ions
	Weight%	sigma		
Na	0.26	0.07	0.28	0.35
Mg	4.17	0.10	4.22	6.91
Al	0.05	0.05	0.04	0.09
Si	25.45	0.17	22.32	54.44
Ca	7.22	0.12	4.44	10.11
Fe	17.20	0.31	7.59	22.13
O	39.68	0.28	61.1	
Totals	94.03			23.00

Titanite P31

Element	Weight%		Oxide	Number of ions
	Weight%	sigma		
Na	0.11		Mg	1.40
O	23.00		Al	14.63
Totals	94.03		Si	21.11
			Ca	40.85
			Ti	46.82
			O	101.35
			Totals	14.64
				99.72

SV09175-17 Chloritized biotite P26

Element	Weight%		Oxide	Number of ions
	Weight%	sigma		
Mg	3.22		Mg	8.62
Al	3.21		Al	8.57
Si	5.18		Si	13.71
K	0.73		K	17.25
Ti	0.20		Ti	32.84
Fe	2.85		Fe	1.95
O	22.00		Si	1.67
Totals	90.73		Ca	21.11
			Ti	1.40
			O	14.63
			Ca	25.73
			Fe	0.73
			O	17.70
			Totals	15.39
				101.74

Clinopyroxene (diopside) P32

Element	Weight%		Oxide	Number of ions
	Weight%	sigma		
Mg	7.71		Mg	7.02
Al	5.52		Al	12.79
Si	6.27		Si	25.73
K	1.89		K	20.27
Fe	0.16		Fe	55.05
O	22.00		O	24.77
Totals	94.97		Totals	13.84
				30

Muscovite P27

Element	Weight%		Oxide	Number of ions
	Weight%	sigma		
Al	18.62	0.15	15.41	35.19
Si	22.01	0.17	17.49	47.09
K	9.22	0.13	5.26	11.11
Fe	1.10	0.13	0.44	1.58
O	44.01	0.25	61.39	
Totals	94.97			22.00

Clinopyroxene (diopside) P32

Element	Weight%		Oxide	Number of ions
	Weight%	sigma		
Mg	7.71		Mg	0.57
Al	5.52		Al	2.88
Si	6.27		Si	7.57
K	1.89		K	0.08
Fe	0.16		Fe	1.91
O	22.00		O	1.66
Totals	94.97		Totals	23.00

SV01975-19 Amphibole (actinolite)

P33

Element	Weight%	Weight% sigma	Atomic %	Oxide wt%
Na	0.27	0.08	0.26	0.36
Mg	8.97	0.12	8.34	14.87
Al	1.82	0.08	1.52	3.44
Si	25.18	0.18	20.26	53.87
K	0.29	0.06	0.17	0.35
Ca	9.06	0.14	5.11	12.67
Fe	9.73	0.25	3.94	12.52
O	42.77	0.28	60.4	
Totals	98.09			

Amphibole (actinolite) P34

Element	Weight%	Weight% sigma	Atomic %	Oxide wt%
Na	0.28	0.08	0.28	0.38
Mg	9.15	0.12	8.44	15.18
Al	1.49	0.07	1.24	2.82
Si	25.46	0.18	20.33	54.46
K	0.18	0.06	0.10	0.22
Ca	9.17	0.14	5.13	12.83
Fe	10.18	0.25	4.09	13.10
O	43.07	0.28	60.38	
Totals	98.98			

Chloritized biotite P35

Element	Weight%	Weight% sigma	Atomic %	Oxide wt%
Na	0.28	0.07	0.31	0.38
Mg	8.02	0.12	8.18	13.30
Al	8.63	0.12	7.92	16.31
Si	16.71	0.16	14.74	35.76
K	5.53	0.11	3.51	6.67
Ti	0.93	0.09	0.48	1.56
Fe	14.03	0.29	6.22	18.05
O	37.87	0.29	58.64	
Totals	92.02			

Quartz P36

Element	Weight%	Weight% sigma	Atomic %	Oxide wt%
Na	0.21	0.06	0.18	0.28
Si	47.62	0.22	33.24	101.88
O	54.33	0.24	66.58	
Totals	102.16			

Titanite P37

Element	Weight%	Weight% sigma	Atomic %	Oxide wt%
Al	0.95	0.06	0.87	1.79
Si	14.58	0.14	12.80	31.19
Ca	20.27	0.18	12.47	28.37
Ti	22.34	0.24	11.50	37.26
O	40.47	0.28	62.37	
Totals	98.61			

Appendix B. Analytical results from samples SV09175-5, 6, 11 and 17 that are not combined with images. Some results have high total sums. The reason for this is probably a too low cobalt-standard reading.

SV09175-5**Contaminated pyrrhotite**

Element	Weight%	Weight% sigma	Atomic%
Na	0.10		
Mg	3.17		
Al	0.58		
Si	7.71		
K	0.06		
Ca	1.94		
Fe	1.50		
O	42.44	0.27	53.72
S	0.39	0.08	0.39
Cation sum	15.08		
Totals	103.55		

Pyrrhotite

Element	Weight%	Weight% sigma	Atomic%
Na	0.10		
Mg	3.22		
Al	0.47		
Si	7.75		
K	0.04		
Ca	1.95		
Fe	1.56		
O	30.27	1.21	50
S	42.22	0.27	55.22
Cation sum	15.09		
Totals	101.86		

Calcite

Element	Weight%	Weight% sigma	Atomic%	Oxide wt%	Formula	Number of ions
Na	0.11					
Mg	3.07					
Ca	2.97					
O	5.53					
Totals	50.73					

Calcite

Element	Weight%	Weight% sigma	Atomic%	Oxide wt%	Formula	Number of ions
Na	0.18	0.06	1.05	0.77	Mg	0.06
Mg	35.71	0.26	48.95	49.96	Ca	2.94
O	14.56	0.17	50.00			3.00
Totals	50.73					

Calcite

Element	Weight%	Weight% sigma	Atomic%	Oxide wt%	Formula	Number of ions
Na	0.18					
Mg	2.33					
Ca	36.84	0.26	48.94	51.55	Ca	2.94
O	15.03	0.17	50.00			3.00
Totals	52.35					

Cation sum 15.52

Chlorite

Element	Weight%			Oxide	Formula	Number of ions
	Weight%	sigma	Atomic%			
Mg	18.60	0.17	18.42	30.85	Mg	8.82
Al	8.40	0.14	7.49	15.87	Al	3.59
Si	15.39	0.17	13.19	32.92	Si	6.32
Ca	0.29	0.06	0.17	0.40	Ca	0.08
Fe	5.24	0.22	2.26	6.74	Fe	1.08
O	38.86	0.29	58.47			28.00
Totals	86.78					

Chlorite

Element	Weight%			Oxide	Formula	Number of ions
	Weight%	% sigma	Atomic%			
Mg	17.12	0.17	16.88	28.38	Mg	8.10
Al	10.44	0.15	9.28	19.73	Al	4.46
Si	14.06	0.16	12.01	30.08	Si	5.76
Ca	0.25	0.06	0.15	0.35	Ca	0.07
Fe	7.82	0.25	3.36	10.06	Fe	1.61
O	38.91	0.30	58.32			28.00
Totals	88.61					

Cation sum 19.89

Cation sum 20.01

Chlorite

Element	Weight%			Oxide	Formula	Number of ions
	Weight%	sigma	Atomic%			
Mg	18.62	0.17	18.41	30.88	Mg	8.82
Al	8.42	0.14	7.50	15.91	Al	3.60
Si	15.28	0.17	13.08	32.69	Si	6.27
Ca	0.35	0.06	0.21	0.50	Ca	0.10
Fe	5.55	0.22	2.39	7.14	Fe	1.14
O	38.88	0.29	58.41			28.00
Totals	87.11					

Pyrrhotite

Element	Weight%		
	Weight%	% sigma	Atomic%
S	43.32	0.28	55.28
Fe	61.03	0.57	44.72
Totals	104.36		

Pyrrhotite

Element	Weight%		
	Weight%	% sigma	Atomic%
S	43.08	0.27	55.07
Fe	61.23	0.57	44.93

Chlorite with biotite residue

Element	Weight%			Oxide	Formula	Number of ions
	Weight%	sigma	Atomic%			
Mg	18.64	0.17	18.46	30.90	Mg	8.85
Al	8.16	0.14	7.28	15.42	Al	3.49
Si	15.44	0.17	13.24	33.04	Si	6.35
K	0.19	0.06	0.12	0.22	K	0.06
Ca	0.24	0.06	0.15	0.34	Ca	0.07
Fe	5.44	0.22	2.35	7.00	Fe	1.12
O	38.81	0.29	58.41			28.00
Totals	86.93					

Actinolite

Element	Weight%			Oxide	Formula	Number of ions
	Weight%	% sigma	Atomic%			
Na	0.34	0.08	0.32	0.46	Na	0.12
Mg	13.12	0.15	11.71	21.76	Mg	4.46
Al	0.49	0.07	0.39	0.92	Al	0.15
Si	26.73	0.20	20.66	57.18	Si	7.87
Ca	9.57	0.15	5.18	13.38	Ca	1.97
Fe	3.58	0.20	1.39	4.60	Fe	0.53
O	44.48	0.29	60.35			23.00

Calcite

Element	Weight%			Oxide	Formula	Number of ions
	Weight%	sigma	Atomic%			
Mg	0.48	0.06	1.06	0.80	Mg	0.06
Ca	36.55	0.26	48.94	51.14	Ca	2.94
O	14.91	0.17	50.00			3.00
Totals	51.94					

Actinolite

Element	Weight%			Oxide	Formula	Number of ions
	Weight%	% sigma	Atomic%			
Na	0.37	0.09	0.36	0.50	Na	0.14
Mg	12.94	0.18	11.69	21.46	Mg	4.45
Al	0.45	0.08	0.37	0.86	Al	0.14
Si	26.52	0.24	20.74	56.73	Si	7.90
Ca	9.36	0.18	5.13	13.10	Ca	1.95
Fe	3.43	0.24	1.35	4.41	Fe	0.51
O	43.98	0.35	60.37			23.00

Chlorite

Element	Weight%			Oxide	Formula	Number of ions
	Weight%	sigma	Atomic%			
Mg	17.13	0.17	16.95	28.4	Mg	8.14
Al	10.33	0.15	9.21	19.51	Al	4.42
Si	14.03	0.16	12.02	30.01	Si	5.77
Ca	0.20	0.06	0.12	0.28	Ca	0.06
Fe	7.88	0.25	3.39	10.14	Fe	1.63
O	38.78	0.30	58.31			28.00
Totals	88.35					

Chlorite

Element	Weight%			Oxide	Formula	Number of ions
	Weight%	% sigma	Atomic%			
Mg	15.51	0.16	16.80	25.72	Mg	8.06
Al	9.88	0.14	9.64	18.66	Al	4.63
Si	12.61	0.15	11.82	26.99	Si	5.68
Fe	7.25	0.24	3.42	9.33	Fe	1.64
O	35.44	0.28	58.32			28.00
Totals	80.70					

Cation sum 20.01

Chlorite							Chlorite																
	Weight%			Oxide				Weight%			Oxide				Number								
Element	Weight%	Weight	Atomic%	Oxide	Formula	Number	Element	Weight%	% sigma	Atomic%	wt%	Formula	of ions										
Mg	15.93	0.16	17.02	26.42	Mg	8.18	Mg	17.08	0.2	17.33	28.33	Mg	8.32										
Al	9.83	0.14	9.46	18.57	Al	4.54	Al	8.40	0.17	7.68	15.87	Al	3.68										
Si	12.79	0.16	11.82	27.35	Si	5.68	Si	14.78	0.20	12.98	31.63	Si	6.23										
Fe	7.37	0.24	3.43	9.48	Fe	1.65	K	0.35	0.07	0.22	0.42	K	0.11										
O	35.90	0.28	58.28			28.00	Fe	7.79	0.30	3.44	10.02	Fe	1.65										
Totals	81.82				Cation sum	20.05	O	37.86	0.35	58.35			28.00										
							Totals	86.26															
Actinolite														Cation sum	19.98								
Element	Weight%	Weight	Atomic%	Oxide	Formula	Number	Pyrrhotite																
Mg	11.49	0.14	10.85	19.06	Mg	4.12	Weight																
Al	0.58	0.07	0.49	1.09	Al	0.19	Element	Weight%	% sigma	Atomic%													
Si	25.42	0.19	20.77	54.38	Si	7.89	S	38.44	0.31	55.5													
Ca	8.79	0.14	5.03	12.3	Ca	1.91	Fe	53.67	0.64	44.5													
Fe	5.74	0.23	2.36	7.39	Fe	0.90	Totals	92.11															
O	42.19	0.29	60.51			23.00	Pyrrhotite																
Totals	94.21				Cation sum	15.01	Weight																
Chlorite														Element	Weight%	Weight	Element	Weight%	% sigma	Atomic%			
Element	Weight%	Weight	Atomic%	Oxide	Formula	Number	Element	Weight%	% sigma	Atomic%	wt%	Formula	of ions	Element	Weight%	Weight	Element	Weight%	% sigma	Atomic%			
Mg	15.62	0.16	16.86	25.90	Mg	8.09	Mg	4.12	0.32	55.45													
Al	9.68	0.14	9.41	18.28	Al	4.52	Al	0.19	0.67	44.55													
Si	12.79	0.16	11.95	27.36	Si	5.74	Si	7.89	Totals	101.03													
Fe	7.35	0.24	3.45	9.46	Fe	1.66	Fe	0.90															
O	35.57	0.28	58.33			28.00	Calcite																
Totals	81.01				Cation sum	20.00	Weight																
Chlorite														Element	Weight%	Weight	Element	Weight%	% sigma	Atomic%			
Element	Weight%	Weight	Atomic%	Oxide	Formula	Number	Element	Weight%	% sigma	Atomic%	wt%	Formula	of ions	Element	Weight%	Weight	Element	Weight%	% sigma	Atomic%			
Mg	15.69	0.16	17.00	26.01	Mg	8.15	Mg	0.45	0.07	1.03	0.75	Mg	0.06										
Al	8.82	0.14	8.61	16.66	Al	4.13	Ca	35.58	0.30	48.97	49.78	Ca	2.94										
Si	13.31	0.16	12.48	28.46	Si	5.99	O	14.50	0.20	50.00													
Ca	0.25	0.06	0.16	0.35	Ca	0.08	Totals	50.53															
Fe	7.09	0.23	3.35	9.12	Fe	1.60	Chlorite																
O	35.46	0.28	58.39			28.00	Weight																
Totals	80.61				Cation sum	19.95	Element																
Calcite														Element	Weight%	Weight	Element	Weight%	% sigma	Atomic%			
Element	Weight%	Weight	Atomic%	Oxide	Formula	Number	Element	Weight%	% sigma	Atomic%	wt%	Formula	of ions	Element	Weight%	Weight	Element	Weight%	% sigma	Atomic%			
Ca	33.32	0.24	50.00	46.62	Ca	3.00	Mg	17.87	0.21	17.63	29.64	Mg	8.45										
O	13.30	0.15	50.00			3.00	Al	8.90	0.17	7.91	16.81	Al	3.79										
Totals	46.62				Cation sum		Si	15.07	0.20	12.87	32.25	Si	6.17										
							Fe	7.42	0.28	3.19	9.55	Fe	1.53										
							O	38.98	0.35	58.41												28.00	
Calcite														Element	Weight%	Weight	Element	Weight%	% sigma	Atomic%			
Element	Weight%	Weight	Atomic%	Oxide	Formula	Number	Element	Weight%	% sigma	Atomic%	wt%	Formula	of ions	Element	Weight%	Weight	Element	Weight%	% sigma	Atomic%			
Mg	0.43	0.08	0.98	0.72	Mg	0.06																	
Ca	35.77	0.31	49.02	50.05	Ca	2.94																	
O	14.56	0.20	50.00			3.00	Totals	50.76															

Pyrrhotite

Element	Weight		
	Weight%	% sigma	Atomic%
Si	0.25	0.07	0.36
S	43.69	0.33	55.72
Ca	0.32	0.09	0.32
Fe	59.52	0.68	43.59
Totals	103.77		

Chlorite

Element	Weight			Oxide
	Weight%	% sigma	Atomic%	wt%
Mg	18.43	0.21	18.3	30.56
Al	8.21	0.17	7.34	15.51
Si	15.25	0.20	13.11	32.62
Fe	6.62	0.28	2.86	8.51
O	38.70	0.35	58.39	
Totals	87.20			

Pyrrhotite

Element	Weight		
	Weight%	% sigma	Atomic%
S	41.15	0.32	54.92
Fe	58.82	0.67	45.08
Totals	99.97		

Clinopyroxene

Element	Weight			Oxide
	Weight%	% sigma	Atomic%	wt%
Mg	0.96	0.09	0.95	1.59
Si	23.58	0.22	20.26	50.45
Ca	16.28	0.22	9.80	22.78
Fe	20.51	0.44	8.86	26.38
O	39.88	0.37	60.13	
Totals	101.21			

Pyrrhotite

Element	Weight		
	Weight%	% sigma	Atomic%
S	42.66	0.33	55.49
Fe	59.58	0.67	44.51
Totals	102.24		

Clinopyroxene

Element	Weight			Oxide
	Weight%	% sigma	Atomic%	wt%
Mg	2.62	0.11	2.53	4.35
Si	24.20	0.22	20.24	51.78
Ca	16.65	0.23	9.76	23.30
Fe	17.46	0.41	7.34	22.46
O	40.95	0.36	60.12	
Totals	101.89			

Actinolite

Element	Weight			Oxide
	Weight%	% sigma	Atomic%	wt%
Mg	7.47	0.15	7.07	12.39
Si	25.23	0.23	20.68	53.98
Ca	10.03	0.19	5.76	14.03
Fe	14.94	0.39	6.16	19.22
O	41.95	0.36	60.34	
Totals	99.62			

Chlorite

Element	Weight			Oxide	Number of ions
	Weight%	% sigma	Atomic%	wt%	
Mg	17.82	0.21	18.44	29.55	Mg
Al	7.27	0.16	6.78	13.74	Al
Si	15.11	0.20	13.54	32.33	Si
Ca	0.30	0.08	0.19	0.42	Ca
Fe	5.75	0.27	2.59	7.40	Fe
O	37.18	0.34	58.46		28.00
Totals	83.44				

Chlorite

Element	Weight			Oxide	Cation sum
	Weight%	% sigma	Atomic%	wt%	
Mg	8.06	0.16	8.97	13.36	Mg
Al	8.79	0.16	8.82	16.61	Al
Si	13.19	0.19	12.71	28.21	Si
Ca	0.28	0.07	0.19	0.39	Ca
Fe	22.18	0.45	10.75	28.53	Fe
O	34.61	0.38	58.56		28.00
Totals	87.10				

Clinopyroxene

Element	Weight			Oxide	Cation sum
	Weight%	% sigma	Atomic%	wt%	
Mg	1.07	0.09	1.06	1.77	Mg
Si	23.46	0.22	20.13	50.18	Si
Ca	16.33	0.22	9.82	22.85	Ca
Fe	20.66	0.44	8.92	26.58	Fe
O	39.87	0.37	60.07		6.00
Totals	101.39				

Pyrrhotite

Element	Weight		
	Weight%	% sigma	Atomic%
S	43.59	0.33	56.27
Fe	59.01	0.67	43.73
Totals	102.60		

Pyrrhotite

Element	Weight		
	Weight%	% sigma	Atomic%
S	41.63	0.32	55.28
Fe	58.65	0.66	44.72
Totals	100.28		

Quartz

Element	Weight			Oxide	Number of ions
	Weight%	% sigma	Atomic%	wt%	
Si	45.57	0.28	33.33	97.49	Si
O	51.92	0.30	66.67		28.00
Totals	97.49				

Pyrrhotite

Element	Weight		
	Weight%	% sigma	Atomic%
S	43.28	0.33	55.76
Fe	59.80	0.67	44.24
Totals	103.09		

Calcite								Prehnite							
Element	Weight%	sigma	Atomic%	Oxide	Formula	Number of ions		Element	Weight%	sigma	Atomic%	Oxide	Formula	Number of ions	
Ca	36.23	0.31	50.00	50.69	Ca	3.00		Mg	0.53	0.08	0.49	0.87	Mg	0.09	
O	14.46	0.19	50.00			3.00		Al	12.29	0.17	10.34	23.22	Al	1.86	
Totals	50.69							Si	20.97	0.22	16.96	44.86	Si	3.05	
Calcite								Ca	18.79	0.24	10.65	26.29	Ca	1.92	
Element	Weight%	sigma	Atomic%	Oxide	Formula	Number of ions		Fe	1.22	0.19	0.50	1.57	Fe	0.09	
Ca	37.04	0.31	50	51.83	Ca	3.00		O	43.02	0.34	61.06			11.00	
O	14.79	0.20	50			3.00		Totals	96.81						
Totals	51.83												Cation sum	7.01	
Pyrrhotite								Prehnite							
Element	Weight%	sigma	Atomic%					Element	Weight%	sigma	Atomic%	Oxide	Formula	Number of ions	
S	42.05	0.32	55.52					Al	12.49	0.17	10.49	23.6	Al	1.89	
Fe	58.66	0.67	44.48					Si	21.25	0.22	17.14	45.46	Si	3.08	
Totals	100.71							Ca	19.40	0.24	10.97	27.15	Ca	1.97	
Pyrrhotite								Fe	0.53	0.17	0.22	0.68	Fe	0.04	
Element	Weight%	sigma	Atomic%					O	43.22	0.33	61.19			11.00	
S	42.18	0.32	55.08					Totals	96.89						
Fe	59.91	0.67	44.92										Cation sum	6.98	
Totals	102.08							Prehnite							
Calcite								Element	Weight%	sigma	Atomic%	Oxide	Formula	Number of ions	
Element	Weight%	sigma	Atomic%	Oxide				Mg	0.84	0.08	0.79	1.39	Mg	0.14	
Ca	36.81	0.31	50.00	51.51	Ca	3.00		Al	12.30	0.17	10.42	23.23	Al	1.88	
O	14.69	0.20	50.00			3.00		Si	20.67	0.22	16.82	44.22	Si	3.03	
Totals	51.51							Ca	18.24	0.24	10.41	25.53	Ca	1.88	
<u>SV09175-6</u>								Fe	1.34	0.19	0.55	1.72	Fe	0.10	
Prehnite								O	42.70	0.34	61.02			11.00	
Element	Weight%	sigma	Atomic%	Oxide				Totals	96.09						
Al	12.58	0.17	10.6	23.76	Al	1.90								Cation sum	7.03
Si	21.17	0.22	17.13	45.28	Si	3.08		Hornblende							
Ca	19.48	0.24	11.05	27.26	Ca	1.99		Element	Weight%	sigma	Atomic%	Oxide	Formula	Number of ions	
O	43.08	0.32	61.22			11.00		Mg	8.32	0.16	7.78	13.79	Mg	2.97	
Totals	96.30							Al	6.77	0.15	5.71	12.79	Al	2.18	
Chlorite								Si	21.83	0.22	17.68	46.71	Si	6.75	
Element	Weight%	sigma	Atomic%	Oxide				Ca	8.90	0.18	5.05	12.45	Ca	1.93	
Mg	11.42	0.18	11.54	18.94	Mg	5.48		Fe	8.61	0.31	3.51	11.08	Fe	1.34	
Al	10.41	0.18	9.47	19.66	Al	4.50		O	42.39	0.37	60.27			23.00	
Si	14.93	0.20	13.06	31.95	Si	6.20		Chlorite							
Ca	1.56	0.10	0.96	2.18	Ca	0.45		Element	Weight%	sigma	Atomic%	Oxide	Formula	Number of ions	
Cr	0.61	0.13	0.29	0.90	Cr	0.14		Mg	11.96	0.19	12.55	19.84	Mg	5.98	
Fe	12.98	0.36	5.71	16.70	Fe	2.71		Al	10.23	0.17	9.67	19.33	Al	4.61	
O	38.41	0.38	58.97			28.00		Si	14.02	0.19	12.73	29.98	Si	6.06	
Totals	90.33							Fe	13.74	0.37	6.28	17.68	Fe	2.99	
Hornblende								O	36.88	0.36	58.78			28.00	
Element	Weight%	% sigma	Atomic%	Oxide				Totals	86.83						
Na	0.61	0.11	0.59	0.82	Na	0.23								Cation sum	19.64
Mg	8.80	0.16	8.12	14.6	Mg	3.11									
Al	4.53	0.13	3.77	8.57	Al	1.44									
Si	23.52	0.23	18.78	50.31	Si	7.18									
K	0.28	0.08	0.16	0.33	K	0.06									
Ca	8.84	0.18	4.95	12.37	Ca	1.89									
Fe	8.69	0.31	3.49	11.18	Fe	1.33									
O	42.91	0.37	60.14			23.00									
Totals	98.18														
					Cation sum	15.24									

Chloritized biotite

	Weight			Oxide
Element	Weight%	% sigma	Atomic%	wt%
Mg	10.34	0.17	10.28	17.14
Al	11.30	0.18	10.12	21.34
Si	16.33	0.21	14.05	34.94
K	1.95	0.10	1.21	2.35
Fe	11.75	0.35	5.08	15.11
O	39.22	0.36	59.26	
Totals	90.88			

Prehnite

	Weight			Oxide
Element	Weight%	% sigma	Atomic%	wt%
Mg	3.82		Al	12.92
Al	3.76		Si	21.54
Si	5.22		Ca	19.96
K	0.45		Fe	0.66
Fe	1.89		O	44.18
	22.00		Totals	99.25

Titanit

	Weight			Oxide
Element	Weight%	% sigma	Atomic%	wt%
Al	0.48	0.08	0.45	0.91
Si	6.87	0.14	6.16	14.71
Ca	8.82	0.17	5.54	12.34
Ti	34.38	0.38	18.08	57.35
Mn	1.66	0.19	0.76	2.15
Fe	15.02	0.39	6.77	19.32
O	39.54	0.44	62.23	
Totals	106.77			

Prehnite

	Weight			Oxide
Element	Weight%	% sigma	Atomic%	wt%
Al	13.08	0.17	10.64	24.72
Si	21.87	0.23	17.08	46.78
Ca	19.97	0.25	10.93	27.95
Fe	0.37	0.17	0.15	0.48
O	44.63	0.34	61.20	
Totals	99.93			
	5.00			

Ilmenit

	Weight			Oxide
Element	Weight%	% sigma	Atomic%	wt%
Ti	33.47	0.36	20.25	55.83
Mn	3.07	0.23	1.62	3.97
Fe	34.67	0.55	18.00	44.61
O	33.19	0.44	60.13	
Totals	104.40			

Prehnite

	Weight			Oxide
Element	Weight%	% sigma	Atomic%	wt%
Al	13.04	0.17	10.56	24.64
Si	22.08	0.23	17.18	47.23
Ca	20.21	0.25	11.02	28.28
O	44.82	0.33	61.23	
Totals	100.14			
	3.00			

Apatite

	Weight			Oxide
Element	Weight%	% sigma	Atomic%	wt%
F	3.15	0.32	3.73	0.00
P	19.79	0.23	14.38	45.35
Ca	40.92	0.34	22.97	57.26
O	41.89	0.34	58.92	
Totals	105.76			

Prehnite

	Weight			Oxide
Element	Weight%	% sigma	Atomic%	wt%
F	0.80		Al	12.78
P	3.08		Si	21.34
Ca	4.92		Ca	19.34
O	12.62		O	43.40
Totals	96.86			
	1.99			

Apatite

	Weight			Oxide
Element	Weight%	% sigma	Atomic%	wt%
F	2.77	0.32	3.28	0.00
Al	0.13	0.06	0.11	0.25
P	20.04	0.23	14.56	45.91
Ca	40.49	0.34	22.74	56.65
O	42.15	0.34	59.31	
Totals	105.58			

Prehnite

	Weight			Oxide
Element	Weight%	% sigma	Atomic%	wt%
F	0.70		Al	11.79
Al	0.02		Si	20.86
P	3.11		Ca	19.53
Ca	4.86		Fe	2.21
O	12.68		O	42.69
Totals	97.09			
	13.42			

Prehnite

	Weight			Oxide
Element	Weight%	% sigma	Atomic%	wt%
Al	12.85	0.17	10.48	24.27
Si	21.56	0.22	16.89	46.12
Ca	20.35	0.25	11.17	28.47
Fe	1.00	0.17	0.39	1.28
O	44.40	0.34	61.07	
Totals	100.15			

Apatite

	Weight			Oxide
Element	Weight%	% sigma	Atomic%	wt%
Al	1.89		Si	3.04
Si	3.04		Ca	2.01
P	2.98		Fe	0.07
Ca	19.60		O	40.48
Fe	0.23		Totals	104.53
O	3.57			
Ca	44.91			
Fe	56.64			
O	59.02			
Totals	104.53			
	13.38			
	7.01			

Apatite

Element	Weight%	Weight	% sigma	Atomic%	Oxide wt%
F	2.62	0.30	3.15	0.00	
P	19.83	0.23	14.63	45.43	
Ca	40.05	0.33	22.83	56.03	
O	41.59	0.33	59.39		
Totals	104.09				

Chlorite

Element	Weight%	Weight	% sigma	Atomic%	Oxide wt%	Formula	Number of ions	Element	Weight%	Weight%	% sigma	Atomic%	Oxide wt%	Formula	Number of ions
F	2.62	0.30	3.15	0.00		Mg	0.67	Mg	14.17	0.19	14.79	23.49		Mg	7.090
P	19.83	0.23	14.63	45.43		Al	3.12	Al	10.94	0.18	10.29	20.67		Al	4.93
Ca	40.05	0.33	22.83	56.03		Si	4.88	Si	12.86	0.18	11.62	27.52		Si	5.57
O	41.59	0.33	59.39			Fe	12.69	Fe	10.82	0.33	4.92	13.93		Fe	2.36
Totals	104.09					O		O	36.81	0.35	58.38				28.00
						Cation sum	13.36	Totals	85.61					Cation sum	19.96

Chlorite

Element	Weight%	Weight	% sigma	Atomic%	Oxide wt%	Formula	Number of ions
Mg	13.49	0.19	13.86	22.36		Mg	6.64
Al	11.27	0.18	10.43	21.29		Al	5.00
Si	13.16	0.19	11.70	28.15		Si	5.61
K	0.22	0.07	0.14	0.26		Ca	0.07
Fe	12.20	0.34	5.46	15.69		Fe	2.61
O	37.43	0.35	58.42			O	42.63
Totals	87.75					Totals	95.26
						Cation sum	19.93

Prehnite

Element	Weight%	Weight	% sigma	Atomic%	Oxide wt%	Formula	Number of ions
Mg	12.71	0.16	10.82	24.02		Al	1.95
Si	20.78	0.21	17.00	44.46		Si	3.06
Ca	19.14	0.23	10.97	26.78		Ca	1.97
O	42.63	0.31	61.21				11.00
Totals	95.26						
						Cation sum	6.97

Chlorite

Element	Weight%	Weight	% sigma	Atomic%	Oxide wt%	Formula	Number of ions
Mg	13.39	0.19	13.74	22.21		Mg	6.59
Al	10.93	0.18	10.11	20.66		Al	4.85
Si	13.47	0.19	11.96	28.82		Si	5.74
K	0.65	0.08	0.42	0.78		K	0.20
Fe	12.01	0.34	5.36	15.45		Fe	2.57
O	37.46	0.35	58.41			O	43.72
Totals	87.92					Totals	98.95
						Cation sum	19.94

Hornblende

Element	Weight%	Weight	% sigma	Atomic%	Oxide wt%	Formula	Number of ions
Na	0.72	0.1	0.69	0.97		Na	0.26
Mg	10.27	0.16	9.30	17.03		Mg	3.56
Al	4.14	0.12	3.38	7.82		Al	1.29
Si	23.97	0.23	18.78	51.27		Si	7.18
Ca	8.50	0.17	4.67	11.9		Ca	1.79
Ti	0.11	0.09	0.05	0.18		Ti	0.02
Cr	0.61	0.13	0.26	0.9		Cr	0.10
Fe	6.91	0.28	2.72	8.88		Fe	1.04
O	43.72	0.37	60.15				23.00
Totals	98.95						
						Cation sum	15.24

Chlorite

Element	Weight%	Weight	% sigma	Atomic%	Oxide wt%	Formula	Number of ions
Mg	13.87	0.19	13.97	23.00		Mg	6.70
Al	11.65	0.18	10.57	22.00		Al	5.07
Si	13.25	0.19	11.55	28.34		Si	5.54
K	0.40	0.07	0.25	0.48		K	0.12
Fe	12.10	0.34	5.31	15.57		Fe	2.55
O	38.13	0.36	58.35			O	43.19
Totals	89.39					Totals	98.97
						Cation sum	19.98

Hornblende

Element	Weight%	Weight	% sigma	Atomic%	Oxide wt%	Formula	Number of ions
Na	0.90	0.10	0.87	1.22		Na	0.34
Mg	9.85	0.16	8.99	16.34		Mg	3.45
Al	4.46	0.13	3.67	8.43		Al	1.41
Si	23.05	0.22	18.21	49.31		Si	6.99
K	0.11	0.07	0.06	0.13		K	0.02
Ca	8.66	0.17	4.80	12.12		Ca	1.84
Ti	0.22	0.09	0.10	0.37		Ti	0.04
Cr	0.55	0.13	0.24	0.81		Cr	0.09
Fe	7.96	0.29	3.16	10.24		Fe	1.21
O	43.19	0.38	59.90				23.00
Totals	98.97						
						Cation sum	15.40

Chlorite

Element	Weight%	Weight	% sigma	Atomic%	Oxide wt%	Formula	Number of ions
Mg	14.31	0.19	14.76	23.73		Mg	7.07
Al	10.74	0.18	9.98	20.30		Al	4.78
Si	13.32	0.19	11.89	28.50		Si	5.70
Fe	10.97	0.33	4.93	14.12		Fe	2.36
O	37.29	0.35	58.44			O	42.65
Totals	86.64					Totals	97.64
						Cation sum	19.91

Hornblende

Element	Weight%	Weight	% sigma	Atomic%	Oxide wt%	Formula	Number of ions
Na	1.13	0.11	1.11	1.53		Na	0.43
Mg	9.01	0.16	8.32	14.95		Mg	3.20
Al	5.99	0.14	4.98	11.31		Al	1.91
Si	21.99	0.22	17.56	47.03		Si	6.75
K	0.23	0.07	0.13	0.28		K	0.05
Ca	8.86	0.17	4.96	12.40		Ca	1.91
Ti	0.36	0.10	0.17	0.59		Ti	0.06
Fe	7.42	0.29	2.98	9.55		Fe	1.15
O	42.65	0.37	59.80				23.00
Totals	97.64						
						Cation sum	15.46

Element	Weight%	Weight	% sigma	Atomic%	Oxide wt%	Formula	Number of ions
Mg	13.74	0.19	14.17	22.78		Mg	6.78
Al	11.49	0.18	10.68	21.71		Al	5.11
Si	13.02	0.18	11.63	27.86		Si	5.57
Fe	11.25	0.33	5.05	14.47		Fe	2.42
O	37.32	0.35	58.48			O	42.65
Totals	86.82					Totals	97.64
						Cation sum	19.88

SV09175-10**Chloritized biotite**

Element	Weight			Oxide wt%	Number of ions
	Weight%	% sigma	Atomic%		
Mg	7.54	0.24	7.79	12.50	Mg
Al	8.86	0.25	8.24	16.73	Al
Si	15.78	0.31	14.11	33.75	Si
K	4.50	0.20	2.89	5.42	K
Ti	1.00	0.16	0.53	1.67	Ti
Fe	17.32	0.61	7.79	22.28	Fe
O	37.36	0.57	58.66		
Totals	92.35			22.00	

Arsenopyrite

Element	Weight%	% sigma	Atomic%
S	19.67	0.11	31.29
Fe	32.74	0.22	29.90
Co	2.73	0.16	2.37
As	53.55	0.20	36.45
Totals	108.7		

Arsenopyrite

Element	Weight%	% sigma	Atomic%
S	20.49	0.11	32.18
Fe	34.30	0.23	30.93
Co	1.97	0.16	1.68
As	52.37	0.20	35.21
Totals	109.13		

Hornblende

Element	Weight			Oxide wt%	Number of ions
	Weight%	% sigma	Atomic%		
Na	0.67	0.15	0.69	0.90	Na
Mg	7.02	0.23	6.85	11.64	Mg
Al	3.81	0.18	3.34	7.19	Al
Si	22.61	0.34	19.09	48.37	Si
Ca	8.05	0.26	4.76	11.26	Ca
Fe	11.92	0.54	5.06	15.34	Fe
O	40.63	0.56	60.21		
Totals	94.70			23.00	

Arsenopyrite

Element	Weight%	% sigma	Atomic%
S	19.25	0.11	30.96
Fe	31.70	0.22	29.27
Co	3.30	0.17	2.89
As	53.60	0.20	36.89
Totals	107.86		

SV09175-11**Arsenopyrite**

Element	Weight		
	Weight%	% sigma	Atomic%
S	20.08	0.39	33.36
Fe	31.34	0.77	29.90
Co	2.20	0.51	1.99
As	48.88	0.73	34.75
Totals	102.5		

Löllingite

Element	Weight%	% sigma	Atomic%
S	0.42	0.06	1.08
Fe	14.08	0.23	20.93
Co	3.28	0.20	4.62
Ni	5.17	0.23	7.31
As	59.61	0.32	66.06
Totals	82.56		

Löllingite

Element	Weight			Oxide wt%	Number of ions
	Weight%	% sigma	Atomic%		
Na	0.78	0.16	0.82	1.05	Na
Mg	5.75	0.21	5.70	9.53	Mg
Al	5.88	0.21	5.25	11.12	Al
Si	20.60	0.33	17.67	44.07	Si
K	0.37	0.12	0.23	0.45	K
Ca	7.70	0.25	4.63	10.77	Ca
Fe	13.50	0.56	5.82	17.36	Fe
O	39.77	0.57	59.89		
Totals	94.35			23.00	

SV09175-17**Apatite**

Element	Weight			Oxide wt%	Number of ions
	Weight%	% sigma	Atomic%		
F	3.34	0.48	3.68	0.00	F
P	21.61	0.37	14.58	49.51	P
Ca	43.41	0.52	22.64	60.74	Ca
O	45.23	0.53	59.10		
Totals	113.59			12.70	

Element	Weight			Oxide wt%	Number of ions
	Weight%	% sigma	Atomic%		
S	45.00	0.33	55.87		
Fe	61.91	0.67	44.13		
Totals	106.91				

Cation sum	13.49
------------	-------

Pyrrhotite

Element	Weight%		
	Weight%	sigma	Atomic%
S	43.75	0.32	55.20
Fe	61.85	0.67	44.80
Totals	105.60		

Pyrrhotite

Element	Weight%		
	Weight%	sigma	Atomic%
S	44.13	0.33	55.40
Fe	61.87	0.67	44.6
Totals	106.00		

Pyrrhotite

Element	Weight%		
	Weight%	sigma	Atomic%
S	36.69	0.30	54.91
Fe	52.48	0.62	45.09
Totals	89.17		

Pyrrhotite

Element	Weight%		
	Weight%	sigma	Atomic%
S	44.4	0.33	55.46
Fe	62.1	0.68	44.54
Totals	106.5		

Pyrrhotite

Element	Weight%		
	Weight%	sigma	Atomic%
S	42.74	0.32	54.55
Fe	62.04	0.67	45.45
Totals	104.78		

K-feldspar

Element	Weight%			Oxide	Formula	Number of ions
	Weight%	sigma	Atomic%			
Na	0.31	0.08	0.28	0.42	Na	0.04
Al	9.69	0.15	7.31	18.3	Al	0.95
Si	32.23	0.25	23.37	68.95	Si	3.04
K	14.36	0.21	7.48	17.30	K	0.97
O	48.38	0.32	61.57			8.00
Totals	104.96					

Cation sum 4.99

Pyrrhotite

Element	Weight%		
	Weight%	sigma	Atomic%
S	43.86	0.33	55
Fe	62.51	0.68	45
Totals	106.36		

Titanite

Element	Weight%			Oxide	Formula	Number of ions
	Weight%	sigma	Atomic%			
Al	1.88	0.09	1.64	3.55	Al	0.13
Si	15.36	0.18	12.89	32.85	Si	1.04
Ca	21.44	0.24	12.61	30.00	Ca	1.01
Ti	21.69	0.31	10.67	36.18	Ti	0.86
O	42.21	0.36	62.19			5.00
Totals	102.58					

Cation sum 3.04

Hornblende

Element	Weight%			Oxide	Formula	Number of ions
	Weight%	% sigma	Atomic%			
Na	0.43	0.10	0.44	0.58	Na	0.17
Mg	7.89	0.15	7.60	13.08	Mg	2.91
Al	2.81	0.11	2.44	5.30	Al	0.93
Si	23.26	0.22	19.40	49.76	Si	7.42
K	0.33	0.08	0.20	0.39	K	0.07
Ca	8.18	0.16	4.78	11.45	Ca	1.83
Fe	11.90	0.34	4.99	15.31	Fe	1.91
O	41.08	0.36	60.15			23.00
Totals	95.88					

Cation sum 15.24

Hornblende

Element	Weight%			Oxide	Formula	Number of ions
	Weight%	% sigma	Atomic%			
Na	0.37	0.1	0.37	0.50	Na	0.14
Mg	8.18	0.15	7.66	13.56	Mg	2.93
Al	2.81	0.11	2.37	5.31	Al	0.91
Si	24.08	0.22	19.53	51.52	Si	7.46
K	0.43	0.08	0.25	0.52	K	0.10
Ca	8.50	0.17	4.83	11.90	Ca	1.85
Fe	11.76	0.34	4.80	15.14	Fe	1.83
O	42.30	0.36	60.20			23.00
Totals	98.44					

Cation sum 15.21

Actinolite

Element	Weight%			Oxide	Formula	Number of ions
	Weight%	% sigma	Atomic%			
Na	0.30	0.09	0.30	0.41	Na	0.11
Mg	8.40	0.15	7.84	13.92	Mg	2.99
Al	2.16	0.10	1.82	4.09	Al	0.69
Si	24.74	0.22	20.00	52.93	Si	7.62
K	0.29	0.08	0.17	0.34	K	0.06
Ca	8.77	0.17	4.97	12.28	Ca	1.89
Fe	11.20	0.34	4.56	14.41	Fe	1.74
O	42.51	0.36	60.34			23.00
Totals	98.38					

Cation sum 15.12

Actinolite

Element	Weight%			Oxide	Formula	Number of ions
	Weight%	% sigma	Atomic%			
Na	0.30	0.10	0.30	0.41	Na	0.11
Mg	8.51	0.15	7.90	14.11	Mg	3.01
Al	2.04	0.10	1.71	3.85	Al	0.65
Si	24.84	0.22	19.95	53.14	Si	7.61
K	0.33	0.07	0.19	0.40	K	0.07
Ca	8.58	0.17	4.83	12.01	Ca	1.84
Fe	12.00	0.34	4.85	15.44	Fe	1.85
O	42.75	0.36	60.28			23.00
Totals	99.35					

Cation sum 15.16

Clinopyroxene										Actinolite										
Element	Weight%	Weight% sigma	Atomic% sigma	Oxide wt%	Formula	Number of ions	Element	Weight% sigma	Atomic% sigma	Oxide wt%	Formula	Number of ions								
Mg	7.53	0.15	6.63	12.48	Mg	0.66	Na	0.24	0.10	0.24	0.33	Na	0.09							
Al	0.08	0.07	0.06	0.15	Al	0.01	Mg	8.80	0.16	8.14	14.59	Mg	3.11							
Si	26.43	0.23	20.16	56.54	Si	2.01	Al	1.90	0.10	1.58	3.58	Al	0.60							
Ca	17.91	0.23	9.57	25.06	Ca	0.96	Si	24.89	0.22	19.92	53.24	Si	7.60							
Fe	9.09	0.32	3.49	11.69	Fe	0.35	K	0.20	0.07	0.11	0.24	K	0.04							
O	44.89	0.36	60.09			6.00	Ca	8.71	0.17	4.89	12.19	Ca	1.86							
Totals	105.93						Fe	12.05	0.34	4.85	15.51	Fe	1.85							
							O	42.88	0.36	60.27			23.00							
							Cation sum	3.98												
Chalcopyrite										Cation sum										
Element	Weight%	Weight% sigma	Atomic% sigma																	
S	39.65	0.32	52.00																	
Fe	31.22	0.49	23.51																	
Cu	37.01	0.84	24.49																	
Totals	107.87																			
K-feldspar										Cation sum										15.16
Element	Weight%	Weight% sigma	Atomic% sigma	Oxide wt%	Formula	Number of ions	Element	Weight% sigma	Atomic% sigma	Oxide wt%	Formula	Number of ions								
Na	2.47	0.12	2.14	3.33	Na	0.28	Na	0.17	0.09	0.18	0.23	Na	0.07							
Al	9.96	0.15	7.34	18.82	Al	0.95	Mg	7.71	0.15	7.74	12.79	Mg	2.95							
Si	32.95	0.26	23.34	70.49	Si	3.03	Al	2.09	0.1	1.89	3.94	Al	0.72							
K	11.01	0.19	5.60	13.27	K	0.73	Si	22.82	0.21	19.81	48.81	Si	7.56							
O	49.51	0.33	61.57			8.00	K	0.29	0.07	0.18	0.35	K	0.07							
Totals	105.90						Ca	8.41	0.16	5.12	11.77	Ca	1.95							
							Mn	0.16	0.14	0.07	0.20	Mn	0.03							
							Fe	10.81	0.32	4.72	13.91	Fe	1.80							
							O	39.55	0.35	60.29			23.00							
							Totals	92.01												
Titanite										Cation sum										15.15
Element	Weight%	Weight% sigma	Atomic% sigma	Oxide wt%	Formula	Number of ions	Hornblende	Element	Weight% sigma	Atomic% sigma	Oxide wt%	Formula	Number of ions							
Al	0.95	0.08	0.81	1.79	Al	0.07	Na	0.47	0.09	0.48	0.64	Na	0.19							
Si	15.64	0.18	12.90	33.46	Si	1.03	Mg	7.63	0.15	7.36	12.64	Mg	2.82							
Ca	21.12	0.24	12.2	29.55	Ca	0.98	Al	2.90	0.11	2.52	5.48	Al	0.97							
Ti	23.63	0.32	11.43	39.42	Ti	0.92	Si	23.16	0.22	19.36	49.54	Si	7.40							
Fe	0.73	0.18	0.30	0.93	Fe	0.02	K	0.27	0.08	0.16	0.32	K	0.06							
O	43.09	0.38	62.36			5.00	Ca	8.39	0.17	4.91	11.74	Ca	1.88							
Totals	105.16						Mn	0.36	0.14	0.15	0.47	Mn	0.06							
							Fe	11.63	0.34	4.89	14.96	Fe	1.87							
							O	40.99	0.36	60.15			23.00							
							Totals	95.79												
Muscovite										Cation sum										15.24
Element	Weight%	Weight% sigma	Atomic% sigma	Oxide wt%	Formula	Number of ions	Hornblende	Element	Weight% sigma	Atomic% sigma	Oxide wt%	Formula	Number of ions							
Na	0.94	0.10	0.88	1.27	Na	0.31	Na	0.31	0.10	0.31	0.42	Na	0.12							
Mg	0.58	0.08	0.51	0.97	Mg	0.18	Mg	7.80	0.15	7.29	12.94	Mg	2.78							
Al	17.16	0.19	13.60	32.43	Al	4.89	Al	3.06	0.11	2.58	5.78	Al	0.98							
Si	24.24	0.24	18.46	51.86	Si	6.63	Si	24.01	0.22	19.41	51.36	Si	7.41							
K	8.71	0.17	4.76	10.49	K	1.71	K	0.41	0.08	0.24	0.49	K	0.09							
Fe	1.49	0.19	0.57	1.91	Fe	0.20	Ca	8.96	0.17	5.08	12.54	Ca	1.94							
O	45.8	0.34	61.22			22.00	Fe	12.05	0.34	4.90	15.50	Fe	1.87							
Totals	98.92						O	42.43	0.36	60.21			23.00							
							Cation sum	13.94												
							Totals	99.03												
																			15.20	

Actinolite							Actinolite						
Element	Weight%	Weight% sigma	Atomic%	Oxide wt%	Formula	Number of ions	Element	Weight%	Weight% sigma	Atomic%	Oxide wt%	Formula	Number of ions
Na	0.26	0.10	0.26	0.35	Na	0.10	Na	0.34	0.09	0.33	0.46	Na	0.13
Mg	8.35	0.15	7.80	13.84	Mg	2.98	Mg	8.70	0.15	8.07	14.43	Mg	3.08
Al	2.46	0.10	2.07	4.64	Al	0.79	Al	1.85	0.1	1.54	3.49	Al	0.59
Si	24.35	0.22	19.69	52.09	Si	7.52	Si	24.96	0.22	20.04	53.41	Si	7.64
K	0.37	0.08	0.22	0.45	K	0.08	K	0.19	0.07	0.11	0.23	K	0.04
Ca	8.72	0.17	4.94	12.20	Ca	1.89	Ca	8.80	0.17	4.95	12.31	Ca	1.89
Fe	11.76	0.34	4.78	15.13	Fe	1.83	Fe	11.57	0.34	4.67	14.88	Fe	1.78
O	42.43	0.36	60.24			23.00	O	42.79	0.36	60.29			23.00
Totals	98.70						Totals	99.20					
					Cation sum	15.18						Cation sum	15.15
Actinolite							Actinolite						
Element	Weight%	Weight% sigma	Atomic%	Oxide wt%	Formula	Number of ions	Element	Weight%	Weight% sigma	Atomic%	Oxide wt%	Formula	Number of ions
Na	0.31	0.09	0.30	0.42	Na	0.12	Na	0.36	0.10	0.36	0.49	Na	0.14
Mg	8.43	0.15	7.80	13.97	Mg	2.97	Mg	8.42	0.15	7.84	13.96	Mg	2.99
Al	1.99	0.1	1.66	3.77	Al	0.63	Al	1.92	0.10	1.61	3.62	Al	0.61
Si	24.93	0.22	19.97	53.32	Si	7.62	Si	24.75	0.22	19.94	52.94	Si	7.61
K	0.26	0.07	0.15	0.32	K	0.06	K	0.13	0.07	0.08	0.16	K	0.03
Ca	8.79	0.17	4.94	12.30	Ca	1.88	Ca	9.06	0.17	5.12	12.67	Ca	1.95
Fe	12.15	0.34	4.89	15.63	Fe	1.87	Fe	11.83	0.34	4.80	15.22	Fe	1.83
O	42.86	0.36	60.29			23.00	O	42.60	0.36	60.27			23.00
Totals	99.72						Totals	99.07					
					Cation sum	15.15						Cation sum	15.16
Actinolite							Pyrrhotite						
Element	Weight%	Weight% sigma	Atomic%	Oxide wt%	Formula	Number of ions	Element	Weight%	Weight% sigma	Atomic%	Oxide wt%	Formula	Number of ions
Na	0.29	0.09	0.29	0.39	Na	0.11	S	44.63	0.33	55.53			
Mg	8.39	0.15	7.78	13.90	Mg	2.97	Fe	62.25	0.67	44.47			
Al	2.05	0.10	1.71	3.87	Al	0.65	Totals	106.87					
Si	24.76	0.22	19.89	52.96	Si	7.59							
K	0.27	0.07	0.15	0.32	K	0.06							
Ca	8.93	0.17	5.03	12.49	Ca	1.92							
Fe	12.07	0.34	4.88	15.53	Fe	1.86							
O	42.72	0.36	60.27			23.00							
Totals	99.47												
					Cation sum	15.16							
Biotite							K-feldspar						
Element	Weight%	Weight% sigma	Atomic%	Oxide wt%	Formula	Number of ions	Element	Weight%	Weight% sigma	Atomic%	Oxide wt%	Formula	Number of ions
Mg	6.05	0.14	6.70	10.03	Mg	2.51	Na	0.46	0.08	0.40	0.62	Na	0.05
Al	7.37	0.14	7.35	13.93	Al	2.76	Al	9.85	0.15	7.42	18.62	Al	0.96
Si	15.96	0.19	15.29	34.14	Si	5.73	Si	32.23	0.25	23.32	68.96	Si	3.03
K	7.01	0.15	4.82	8.44	K	1.81	K	13.99	0.20	7.27	16.85	K	0.94
Ti	1.48	0.12	0.83	2.47	Ti	0.31	O	48.51	0.32	61.59			8.00
Fe	13.11	0.35	6.32	16.87	Fe	2.37	Totals	105.04					
O	34.90	0.35	58.69			22.00							
Totals	85.89												
					Cation sum	15.48							
Titanite							Titantite						
Element	Weight%	Weight% sigma	Atomic%	Oxide wt%	Formula	Number of ions	Element	Weight%	Weight% sigma	Atomic%	Oxide wt%	Formula	Number of ions
							Element	Weight%	Weight% sigma	Atomic%	Oxide wt%	Formula	Number of ions
							Al	0.70	0.08	0.62	1.33	Al	0.05
							Si	15.28	0.18	12.88	32.70	Si	1.03
							Ca	20.62	0.24	12.18	28.85	Ca	0.98
							Ti	23.53	0.32	11.63	39.25	Ti	0.93
							Fe	0.70	0.17	0.30	0.90	Fe	0.02
							O	42.19	0.37	62.41			5.00
							Totals	103.02					
												Cation sum	3.01

Chalcopyrite						
	Weight					
Element	Weight%	% sigma	Atomic%			
S	38.78	0.31	51.61			
Fe	30.81	0.48	23.54			
Cu	37.00	0.83	24.85			
Totals	106.60					
Pyrrhotite						
	Weight					
Element	Weight%	% sigma	Atomic%			
S	43.8	0.33	54.41			
Fe	63.93	0.68	45.59			
Totals	107.72					
Pyrrhotite						
	Weight					
Element	Weight%	% sigma	Atomic%			
S	45.37	0.33	56.03			
Fe	62.01	0.67	43.97			
Totals	107.38					
Pyrrhotite						
	Weight					
Element	Weight%	% sigma	Atomic%			
S	45.07	0.33	55.75			
Fe	62.32	0.67	44.25			
Totals	107.39					
Chalcopyrite						
	Weight					
Element	Weight%	% sigma	Atomic%			
S	39.82	0.32	52.03			
Fe	31.70	0.50	23.78			
Cu	36.70	0.84	24.20			
Totals	108.23					
Chloritized Biotite						
	Weight					
Element	Weight%	% sigma	Atomic%	Oxide	Number of ions	Biotite
Mg	8.44	0.16	8.16	13.99	Formula	Mg
Al	8.81	0.16	7.67	16.64		Al
Si	17.00	0.20	14.23	36.36		Si
K	5.49	0.14	3.30	6.61		K
Ti	1.58	0.13	0.78	2.64		Ti
Fe	17.22	0.39	7.25	22.16		Fe
O	39.87	0.38	58.6		22.00	O
Totals	98.41					Totals
						Cation sum
					15.54	
Titanite						
	Weight					
Element	Weight%	% sigma	Atomic%	Oxide	Number of ions	Biotite
Al	1.17	0.06	1.07	2.22	Formula	Mg
Si	14.62	0.13	12.82	31.29		Al
Ca	20.02	0.17	12.3	28.02		Si
Ti	21.94	0.23	11.28	36.6		K
Fe	0.45	0.12	0.20	0.58		Ti
O	40.48	0.27	62.32		5.00	Fe
Totals	98.70					Totals
						Cation sum
					3.02	

Biotite							Chloritized Biotite								
	Element	Weight%	% sigma	Atomic%	Oxide wt%	Formula	Number of ions		Element	Weight%	% sigma	Atomic%	Oxide wt%	Formula	Number of ions
Mg	Mg	6.89	0.15	6.73	11.42	Mg	2.53		Mg	7.84	0.16	8.01	13.01	Mg	3.01
Al	Al	8.26	0.15	7.28	15.61	Al	2.74		Al	9.18	0.16	8.45	17.35	Al	3.18
Si	Si	18.06	0.20	15.28	38.63	Si	5.75		Si	15.61	0.20	13.8	33.39	Si	5.19
K	K	8.19	0.16	4.98	9.87	K	1.87		K	4.43	0.13	2.81	5.34	K	1.06
Ti	Ti	1.12	0.12	0.56	1.87	Ti	0.21		Ti	0.92	0.11	0.48	1.54	Ti	0.18
Fe	Fe	15.69	0.38	6.68	20.19	Fe	2.51		Fe	17.74	0.39	7.89	22.82	Fe	2.96
O	O	39.38	0.37	58.49			22.00		O	37.72	0.37	58.55			22.00
Totals	Totals	97.59							Totals	93.44					Cation sum 15.57
							Cation sum 15.61								
Biotite							Biotite								
	Element	Weight%	% sigma	Atomic%	Oxide wt%	Formula	Number of ions		Element	Weight%	% sigma	Atomic%	Oxide wt%	Formula	Number of ions
Mg	Mg	7.04	0.15	6.87	11.67	Mg	2.58		Mg	6.41	0.14	6.27	10.62	Mg	2.33
Al	Al	9.03	0.16	7.95	17.07	Al	2.98		Al	9.88	0.16	8.71	18.67	Al	3.24
Si	Si	17.25	0.20	14.58	36.90	Si	5.47		Si	17.44	0.20	14.77	37.31	Si	5.50
K	K	6.32	0.15	3.84	7.61	K	1.44		K	4.28	0.13	2.60	5.15	K	0.97
Ca	Ca	0.56	0.09	0.33	0.79	Ca	0.13		Ca	4.05	0.14	2.40	5.66	Ca	0.89
Ti	Ti	1.42	0.12	0.70	2.37	Ti	0.26		Ti	0.61	0.11	0.30	1.02	Ti	0.11
Fe	Fe	16.61	0.39	7.06	21.36	Fe	2.65		Fe	13.82	0.36	5.88	17.77	Fe	2.19
O	O	39.54	0.38	58.67			22.00		O	39.73	0.37	59.06			22.00
Totals	Totals	97.78							Totals	96.21					Cation sum 15.25
							Cation sum 15.50								
Biotite							Biotite								
	Element	Weight%	% sigma	Atomic%	Oxide wt%	Formula	Number of ions		Element	Weight%	% sigma	Atomic%	Oxide wt%	Formula	Number of ions
Mg	Mg	7.00	0.15	6.85	11.61	Mg	2.57		Mg	6.69	0.15	6.44	11.10	Mg	2.42
Al	Al	8.64	0.16	7.62	16.33	Al	2.86		Al	8.70	0.16	7.55	16.44	Al	2.83
Si	Si	17.57	0.20	14.89	37.58	Si	5.59		Si	18.22	0.21	15.19	38.98	Si	5.70
K	K	7.26	0.15	4.42	8.75	K	1.66		K	8.39	0.16	5.02	10.10	K	1.88
Ti	Ti	1.37	0.13	0.68	2.29	Ti	0.26		Ti	1.55	0.13	0.76	2.58	Ti	0.28
Fe	Fe	16.31	0.39	6.95	20.98	Fe	2.61		Fe	15.37	0.38	6.44	19.77	Fe	2.42
O	O	39.39	0.38	58.59			22.00		O	40.05	0.38	58.6			22.00
Totals	Totals	97.54							Totals	98.97					Cation sum 15.54
							Cation sum 15.55								
Biotite							Biotite								
	Element	Weight%	% sigma	Atomic%	Oxide wt%	Formula	Number of ions		Element	Weight%	% sigma	Atomic%	Oxide wt%	Formula	Number of ions
Mg	Mg	7.07	0.15	6.98	11.72	Mg	2.62		Mg	6.66	0.15	6.51	11.04	Mg	2.44
Al	Al	8.72	0.16	7.76	16.47	Al	2.91		Al	8.70	0.16	7.66	16.44	Al	2.88
Si	Si	17.50	0.20	14.96	37.43	Si	5.62		Si	17.39	0.20	14.72	37.21	Si	5.52
K	K	7.48	0.16	4.59	9.01	K	1.73		K	7.46	0.16	4.53	8.98	K	1.70
Ti	Ti	1.12	0.12	0.56	1.87	Ti	0.21		Ti	1.87	0.13	0.93	3.11	Ti	0.35
Fe	Fe	15.36	0.38	6.60	19.76	Fe	2.48		Fe	16.57	0.39	7.05	21.31	Fe	2.65
O	O	39.02	0.37	58.55			22.00		O	39.45	0.38	58.6			22.00
Totals	Totals	96.26							Totals	98.09					Cation sum 15.54
							Cation sum 15.57								
Biotite							Biotite								
	Element	Weight%	% sigma	Atomic%	Oxide wt%	Formula	Number of ions		Element	Weight%	% sigma	Atomic%	Oxide wt%	Formula	Number of ions
Mg	Mg	7.14	0.15	6.91	11.83	Mg	2.60		Mg	7.02	0.15	6.86	11.64	Mg	2.57
Al	Al	8.74	0.16	7.62	16.51	Al	2.87		Al	8.94	0.16	7.87	16.90	Al	2.95
Si	Si	17.86	0.20	14.97	38.20	Si	5.64		Si	17.59	0.20	14.86	37.63	Si	5.58
K	K	8.19	0.16	4.93	9.86	K	1.86		K	7.32	0.15	4.44	8.82	K	1.67
Ti	Ti	1.04	0.11	0.51	1.74	Ti	0.19		Ti	1.26	0.12	0.62	2.10	Ti	0.23
Fe	Fe	15.78	0.38	6.65	20.30	Fe	2.51		Fe	15.87	0.39	6.74	20.42	Fe	2.53
O	O	39.70	0.37	58.41			22.00		O	39.50	0.38	58.60			22.00
Totals	Totals	98.45							Totals	97.51					Cation sum 15.54
							Cation sum 15.66								

Biotite						K-feldspar							
Element	Weight%	Weight % sigma	Oxide Atomic%	Oxide wt%	Number of ions	Element	Weight%	Weight % sigma	Oxide Atomic%	Oxide wt%	Formula	Number of ions	
Mg	7.00	0.15	6.78	11.6		Mg	2.55	Na	0.38	0.09	0.33	0.51	
Al	9.01	0.16	7.87	17.03		Al	2.96	Al	9.58	0.15	7.22	18.11	
Si	17.78	0.20	14.92	38.04		Si	5.60	Si	32.34	0.25	23.42	69.19	
K	7.46	0.16	4.50	8.99		K	1.69	K	14.33	0.20	7.45	17.26	
Ti	1.09	0.12	0.54	1.82		Ti	0.20	O	48.43	0.32	61.57	K	
Fe	16.15	0.39	6.82	20.78		Fe	2.56	Totals	105.07			0.97	
O	39.76	0.38	58.57		22.00						8.00		
Totals	98.26									Cation sum	4.99		
Chloritized Biotite						Cation sum	15.56	Titanite					
Element	Weight%	Weight % sigma	Oxide Atomic%	Oxide wt%	Number of ions	Element	Weight%	Weight % sigma	Oxide Atomic%	Oxide wt%	Formula	Number of ions	
Mg	7.73	0.15	7.77	12.82		Mg	2.92	Al	0.98	0.08	0.89	1.85	
Al	9.26	0.16	8.38	17.49		Al	3.15	Si	14.83	0.17	12.95	31.73	
Si	16.35	0.20	14.22	34.99		Si	5.34	Ca	20.30	0.23	12.42	28.40	
K	5.37	0.14	3.35	6.47		K	1.26	Ti	22.22	0.31	11.37	37.06	
Ti	0.85	0.11	0.43	1.42		Ti	0.16	O	40.71	0.35	62.38	Ti	
Fe	16.65	0.39	7.28	21.42		Fe	2.73	Totals	99.04			5.00	
O	38.39	0.37	58.58		22.00					Cation sum	3.02		
Totals	94.61												
Muscovite						Cation sum	15.56	Titanite					
Element	Weight%	Weight % sigma	Oxide Atomic%	Oxide wt%	Number of ions	Element	Weight%	Weight % sigma	Oxide Atomic%	Oxide wt%	Formula	Number of ions	
Na	1.19	0.10	1.12	1.61		Na	0.40	Al	1.12	0.08	0.99	2.11	
Mg	0.84	0.08	0.74	1.39		Mg	0.27	Si	14.75	0.17	12.62	31.55	
Al	15.44	0.18	12.40	29.18		Al	4.46	Ca	20.56	0.23	12.33	28.76	
Si	24.62	0.23	18.99	52.67		Si	6.83	Ti	22.87	0.31	11.47	38.15	
K	8.38	0.16	4.64	10.10		K	1.67	Fe	0.68	0.16	0.29	0.87	
Ca	0.46	0.09	0.25	0.64		Ca	0.09	O	41.47	0.36	62.29	Fe	
Fe	1.80	0.19	0.70	2.31		Fe	0.25	Totals	101.44			0.02	
O	45.16	0.34	61.15		22.00					Cation sum	5.00		
Totals	97.89												
Muscovite						Cation sum	13.97	Biotite					
Element	Weight%	Weight % sigma	Oxide Atomic%	Oxide wt%	Number of ions	Element	Weight%	Weight % sigma	Oxide Atomic%	Oxide wt%	Formula	Number of ions	
Mg	0.23	0.07	0.21	0.37		Mg	0.07	Al	16.56	0.13	13.93	31.29	
Al	17.80	0.19	14.66	33.63		Al	5.26	Si	22.77	0.17	18.40	48.71	
Si	22.76	0.23	18.02	48.70		Si	6.46	K	8.83	0.12	5.13	10.63	
K	9.42	0.17	5.35	11.34		K	1.92	Fe	1.44	0.13	0.58	1.85	
Fe	1.05	0.17	0.42	1.36		Fe	0.15	O	43.27	0.24	61.4	Fe	
O	44.14	0.33	61.34		22.00	Totals	93.46					0.21	
Totals	95.40									Cation sum	22.00		
Muscovite						Cation sum	13.87	Biotite					
Element	Weight%	Weight % sigma	Oxide Atomic%	Oxide wt%	Number of ions	Element	Weight%	Weight % sigma	Oxide Atomic%	Oxide wt%	Formula	Number of ions	
Mg	0.98	0.08	0.88	1.63		Mg	0.32	Al	0.86	0.06	0.85	1.43	
Al	16.79	0.18	13.59	31.72		Al	4.87	Si	12.55	0.12	11.09	23.71	
Si	23.86	0.23	18.55	51.05		Si	6.65	K	23.95	0.17	20.33	51.24	
K	9.05	0.17	5.06	10.91		K	1.81	Fe	9.39	0.13	5.73	11.32	
Fe	1.31	0.18	0.51	1.68		Fe	0.18	O	1.17	0.23	0.50	1.50	
O	44.99	0.33	61.41		22.00	Totals	89.20					Fe	
Totals	96.99									Cation sum	22.00		
						Cation sum	13.83						

Muscovite							Chloritized biotite						
Element	Weight%	Weight % sigma	Oxide Atomic%	Oxide wt%	Formula	Number of ions	Element	Weight%	Weight % sigma	Oxide Atomic%	Oxide wt%	Formula	Number of ions
Na	0.49	0.09	0.46	0.66	Na	0.16	Mg	8.71	0.12	8.67	14.44	Mg	3.26
Mg	0.66	0.08	0.58	1.09	Mg	0.21	Al	8.96	0.12	8.04	16.93	Al	3.02
Al	17.66	0.19	13.99	33.37	Al	5.03	Si	16.11	0.15	13.89	34.46	Si	5.22
Si	23.88	0.23	18.17	51.09	Si	6.53	K	4.06	0.09	2.52	4.90	K	0.95
K	9.16	0.17	5.01	11.04	K	1.80	Ti	1.03	0.09	0.52	1.72	Ti	0.20
Fe	1.49	0.18	0.57	1.92	Fe	0.21	Fe	17.94	0.30	7.78	23.08	Fe	2.92
O	45.82	0.34	61.22			22.00	O	38.71	0.28	58.59			22.00
Totals	99.17						Totals	95.52					
					Cation sum	13.94						Cation sum	15.55
Muscovite							Chloritized biotite						
Element	Weight%	Weight % sigma	Oxide Atomic%	Oxide wt%	Formula	Number of ions	Element	Weight%	Weight % sigma	Oxide Atomic%	Oxide wt%	Formula	Number of ions
Na	0.46	0.08	0.43	0.62	Na	0.16	Mg	8.47	0.12	8.69	14.05	Mg	3.26
Al	18.76	0.19	15.17	35.44	Al	5.45	Al	8.83	0.12	8.16	16.68	Al	3.06
Si	22.93	0.23	17.81	49.05	Si	6.40	Si	15.72	0.14	13.96	33.63	S	5.24
K	9.57	0.17	5.34	11.53	K	1.92	K	3.97	0.09	2.53	4.78	K	0.95
O	44.92	0.31	61.25			22.00	Ti	0.94	0.08	0.49	1.57	Ti	0.18
Totals	96.63						Fe	16.89	0.29	7.54	21.73	Fe	2.83
					Cation sum	13.92	O	37.62	0.27	58.63			22.00
							Totals	92.44					
												Cation sum	15.52
Muscovite							K-feldspar						
Element	Weight%	Weight % sigma	Oxide Atomic%	Oxide wt%	Formula	Number of ions	Element	Weight%	Weight % sigma	Oxide Atomic%	Oxide wt%	Formula	Number of ions
Mg	0.20	0.07	0.18	0.34	Mg	0.07	Na	0.79	0.07	0.72	1.07	Na	0.09
Al	18.58	0.19	15.05	35.10	Al	5.39	Al	9.92	0.11	7.62	18.74	Al	0.99
Si	22.93	0.23	17.84	49.05	Si	6.39	Si	31.29	0.18	23.10	66.93	Si	3.00
K	9.01	0.17	5.04	10.85	K	1.80	K	12.80	0.14	6.79	15.42	K	0.88
Fe	1.18	0.17	0.46	1.52	Fe	0.17	Fe	0.40	0.11	0.15	0.57	Fe	0.02
O	44.96	0.33	61.43			22.00	O	47.53	0.25	61.62			8.00
Totals	96.85						Totals	102.73					
					Cation sum	13.82						Cation sum	4.98
Titanite							Chloritized biotite						
Element	Weight%	Weight % sigma	Oxide Atomic%	Oxide wt%	Formula	Number of ions	Element	Weight%	Weight % sigma	Oxide Atomic%	Oxide wt%	Formula	Number of ions
Al	1.02	0.08	0.93	1.92	Al	0.07	Mg	8.58	0.12	8.43	14.22	Mg	3.16
Si	14.53	0.17	12.83	31.08	Si	1.03	Al	9.08	0.12	8.04	17.16	Al	3.02
Ca	19.78	0.23	12.25	27.68	Ca	0.98	Si	16.64	0.15	14.15	35.6	Si	5.31
Ti	22.00	0.31	11.39	36.70	Ti	0.91	K	4.69	0.10	2.86	5.64	K	1.07
Fe	0.56	0.17	0.25	0.72	Fe	0.02	Ti	1.12	0.09	0.56	1.86	Ti	0.21
O	40.21	0.36	62.35			5.00	Fe	17.10	0.29	7.31	22.00	Fe	2.74
Totals	98.10						O	39.28	0.28	58.63			22.00
					Cation sum	13.82	Totals	96.49					
												Cation sum	15.51
Apatite							Chloritized biotite						
Element	Weight%	Weight % sigma	Oxide Atomic%	Oxide wt%	Formula	Number of ions	Element	Weight%	Weight % sigma	Oxide Atomic%	Oxide wt%	Formula	Number of ions
F	3.28	0.36	4.00	0.00	F	0.86	Mg	9.03	0.12	9.30	14.97	Mg	3.48
P	19.19	0.21	14.34	43.96	P	3.08	Al	9.52	0.12	8.84	17.99	Al	3.31
Ca	39.19	0.32	22.64	54.83	Ca	4.86	Si	14.86	0.14	13.25	31.78	Si	4.96
Fe	0.64	0.17	0.26	0.82	Fe	0.06	K	1.64	0.07	1.05	1.98	K	0.39
O	40.60	0.33	58.75			12.62	Ti	0.74	0.08	0.39	1.24	Ti	0.15
Totals	102.90						Fe	18.73	0.30	8.40	24.10	Fe	3.15
					Cation sum	13.48	O	37.53	0.28	58.77			22.00
							Totals	92.06					
												Cation sum	15.44

Muscovite

Element	Weight		Oxide	
	Weight%	% sigma	Atomic%	wt%
Na	0.79	0.07	0.71	1.07
Mg	0.57	0.06	0.48	0.94
Al	17.96	0.15	13.75	33.93
Si	25.19	0.18	18.53	53.9
K	8.97	0.13	4.74	10.81
Fe	1.20	0.14	0.44	1.55
O	47.51	0.27	61.34	
Totals	102.20			

Chalcopyrite

Element	Number		Weight		
	Formula	of ions	Element	Weight%	% sigma
Na	0.26	S	39.62	0.32	52.05
Mg	0.17	Fe	30.93	0.49	23.33
Al	4.93	Cu	37.13	0.85	24.62
Si	6.65	K	1.70	Totals	
		Fe	0.16	107.69	
	22.00				

Zircon

Element	Weight		Oxide	
	Weight%	% sigma	Atomic%	wt%
Al	0.54	0.05	0.60	1.02
Si	14.02	0.13	15.00	30.00
Ca	2.08	0.09	1.56	2.91
Fe	0.99	0.14	0.53	1.27
Zr	49.89	0.52	16.44	67.39
O	35.07	0.36	65.87	
Totals	102.59			

Cation sum
13.87

Element	Number		Element	Weight	
	Formula	of ions		Weight%	% sigma
Al	0.04	Al	0.04	108.07	
Si	0.91	Si	0.91		
Ca	0.09	Ca	0.09		
Fe	0.03	Fe	0.03		
Zr	1.00	Zr	1.00		
O	4.00				
Totals	2.07				

Chalcopyrite

Element	Number		Element	Weight	
	Formula	of ions		Weight%	% sigma
S	39.66	S	39.66	0.32	51.93
Fe	31.48	Fe	31.48	0.49	23.66
Cu	36.93	Cu	36.93	0.85	24.41
Totals	107.74				

Chloritized biotite

Element	Weight		Oxide	
	Weight%	% sigma	Atomic%	wt%
Mg	8.65	0.12	8.68	14.34
Al	9.00	0.12	8.14	17.01
Si	16.12	0.14	14.00	34.49
K	4.20	0.09	2.62	5.05
Ti	1.04	0.08	0.53	1.73
Fe	16.93	0.29	7.40	21.79
O	38.47	0.28	58.64	
Totals	94.41			

Cation sum
2.07

Element	Number		Element	Weight	
	Formula	of ions		Weight%	% sigma
F	3.95	F	3.95	0.33	4.59
P	20.30	P	20.30	0.22	14.44
Ca	40.83	Ca	40.83	0.33	22.44
O	42.51	O	42.51	0.33	58.54
Totals	107.60				

Cation sum
13.69

Cation sum
15.51

Tidigare skrifter i serien
"Examensarbeten i Geologi vid Lunds universitet":

287. Lindskog, Anders, 2011: A Russian record of a Middle Ordovician meteorite shower: Extraterrestrial chromite in Volkovian-Kundan (lower Darriwilian) strata at Lynna River, St. Petersburg region. (45 hp)
288. Gren, Johan, 2011: Dental histology of Cretaceous mosasaurs (Reptilia, Squamata): incremental growth lines in dentine and implications for tooth replacement. (45 hp)
289. Cederberg, Julia, 2011: U-Pb baddelyit dateringar av basiska gångar längs Romeleåsen i Skåne och deras påverkan av plastisk deformation i Protoginzonern (15 hp)
290. Ning, Wenxing, 2011: Testing the hypothesis of a link between Earth's magnetic field and climate change: a case study from southern Sweden focusing on the 1st millennium BC. (45 hp)
291. Holm Östergaard, Sören, 2011: Hydrogeology and groundwater regime of the Stanford Aquifer, South Africa. (45 hp)
292. Tebi, Magnus Asiboh, 2011: Metamorphosed and partially molten hydrothermal alteration zones of the Akulleq glacier area, Paamiut gold province, South-West Greenland. (45 hp)
293. Lewerentz, Alexander, 2011: Experimental zircon alteration and baddeleyite formation in silica saturated systems: implications for dating hydrothermal events. (45 hp)
294. Flodhammar, Ingrid, 2011: Lövestads åsar: En isälvsavlagring bildad vid inlandsisens kant i Weichsels slutskede. (15 hp)
295. Liu, Tianzhuo, 2012: Exploring long-term trends in hypoxia (oxygen depletion) in Western Gotland Basin, the Baltic Sea. (45 hp)
296. Samer, Bou Daher, 2012: Lithofacies analysis and heterogeneity study of the subsurface Rhaetian–Pliensbachian sequence in SW Skåne and Denmark. (45 hp)
297. Riebe, My, 2012: Cosmic ray tracks in chondritic material with focus on silicate mineral inclusions in chromite. (45 hp)
298. Hjulström, Joakim, 2012: Återfyllning av borrhål i geoenergisystem: konventioner, metod och material. (15 hp)
299. Letellier, Mattias, 2012: A practical assessment of frequency electromagnetic inversion in a near surface geological environment. (15 hp)
300. Lindenbaum, Johan, 2012: Identification of sources of ammonium in groundwater using stable nitrogen and boron isotopes in Nam Du, Hanoi. (45 hp)
301. Andersson, Josefina, 2012: Karaktärisering av arsenikförorening i matjordsprofiler kring Klippans Läderfabrik. (45 hp)
302. Lumetzberger, Mikael, 2012: Hydrogeologisk kartläggning av infiltrationsvattentransport genom resistivitetsmätningar. (15 hp)
303. Martin, Ellinor, 2012: Fossil pigments and pigment organelles – colouration in deep time. (15 hp)
304. Rådman, Johan, 2012: Sällsynta jordartsmetaller i tungsand vid Haväng på Österlen. (15 hp)
305. Karlstedt, Filippa, 2012: Jämförande geokemisk studie med portabel XRF av obehandlade och sågade ytor, samt pulver av Karlshamnsdiabas. (15 hp)
306. Lundberg, Frans, 2012: Den senkambriska alunskiftern i Västergötland – utbredning, mäktigheter och faciestyper. (15 hp)
307. Thulin Olander, Henric, 2012: Hydrogeologisk kartering av grundvattenmagasinet Ekenäs-Kvarndammen, Jönköpings län. (15 hp)
308. Demirer, Kursad, 2012: U-Pb baddeleyite ages from mafic dyke swarms in Dharwar craton, India – links to an ancient supercontinent. (45 hp)
309. Leskelä, Jari, 2012: Loggning och återfyllning av borrhål – Praktiska försök och utveckling av täthetskontroll i fält. (15 hp)
310. Eriksson, Magnus, 2012: Stratigraphy, facies and depositional history of the Colonus Shale Trough, Skåne, southern Sweden. (45 hp)
311. Larsson, Amie, 2012: Kartläggning, beskrivning och analys av Kalmar läns regionalt viktiga vattenresurser. (15 hp)
312. Olsson, Håkan, 2012: Prediction of the degree of thermal breakdown of limestone: A case study of the Upper Ordovician Boda Limestone, Siljan district, central Sweden. (45 hp)

313. Kampmann, Tobias Christoph, 2012: U-Pb geochronology and paleomagnetism of the Westerberg sill, Kaapvaal Craton – support for a coherent Kaapvaal-Pilbara block (Vaalbara). (45 hp)
314. Eliasson, Isabelle Timms, 2012: Arsenik: förekomst, miljö och hälsoeffekter. (15 hp)
315. Badawy, Ahmed Salah, 2012: Sequence stratigraphy, palynology and biostratigraphy across the Ordovician-Silurian boundary in the Röstånga-1 core, southern Sweden. (45 hp)
316. Knut, Anna, 2012: Resistivitets- och IP-mätningar på Flishultsdeponin för lokalisering av grundvattenytör. (15 hp)
317. Nylén, Fredrik, 2012: Förädling av ballastmaterial med hydrocyklon, ett fungerande alternativ? (15 hp)
318. Younes, Hani, 2012: Carbon isotope chemostratigraphy of the Late Silurian Lau Event, Gotland, Sweden. (45 hp)
319. Weibull, David, 2012: Subsurface geological setting in the Skagerrak area – suitability for storage of carbon dioxide. (15 hp)
320. Petersson, Albin, 2012: Förrutsättningar för geoenergi till idrottsanläggningar i Kallerstad, Linköpings kommun: En förstudie. (15 hp)
321. Axbom, Jonna, 2012: Klimatets och människans inverkan på tallens etablering på sydsvenska mossar under de senaste århundradena – en dendrokronologisk och torvstratigrafisk analys av tre småländska mossar. (15 hp)
322. Kumar, Pardeep, 2012: Palynological investigation of coal-bearing deposits of the Thar Coal Field Sindh, Pakistan. (45 hp)
323. Gabrielsson, Johan, 2012: Havsisen i arktiska bassängen – nutid och framtid i ett globalt uppvärmningsperspektiv. (15 hp)
324. Lundgren, Linda, 2012: Variation in rock quality between metamorphic domains in the lower levels of the Eastern Segment, Sveconorwegian Province. (45 hp)
325. Härling, Jesper, 2012: The fossil wonders of the Silurian Eramosa Lagerstätte of Canada: the jawed polychaete faunas. (15 hp)
326. Qvarnström, Martin, 2012: An interpretation of oncoid mass-occurrence during the Late Silurian Lau Event, Gotland, Sweden. (15 hp)
327. Ulmius, Jan, 2013: P-T evolution of paragneisses and amphibolites from Romeleåsen, Scania, southernmost Sweden. (45 hp)
328. Hultin Eriksson, Elin, 2013: Resistivitetsmätningar för avgränsning av lak-vattenplym från Kejsarkullens deponis infiltrationsområde. (15 hp)
329. Mozafari Amiri, Nasim, 2013: Field relations, petrography and $^{40}\text{Ar}/^{39}\text{Ar}$ cooling ages of hornblende in a part of the eclogite-bearing domain, Sveconorwegian Orogen. (45 hp)
330. Saeed, Muhammad, 2013: Sedimentology and palynofacies analysis of Jurassic rocks Eriksdal, Skåne, Sweden. (45 hp)
331. Khan, Mansoor, 2013: Relation between sediment flux variation and land use patterns along the Swedish Baltic Sea coast. (45 hp)
332. Bernhardson, Martin, 2013: Ice advance-retreat sediment successions along the Logata River, Taymyr Peninsula, Arctic Siberia. (45 hp)
333. Shrestha, Rajendra, 2013: Optically Stimulated Luminescence (OSL) dating of aeolian sediments of Skåne, south Sweden. (45 hp)
334. Fullerton, Wayne, 2013: The Kalgoorlie Gold: A review of factors of formation for a giant gold deposit. (15 hp)
335. Hansson, Anton, 2013: A dendroclimatic study at Store Mosse, South Sweden – climatic and hydrologic impacts on recent Scots Pine (*Pinus sylvestris*) growth dynamics. (45 hp)
336. Nilsson, Lawrence, 2013: The alteration mineralogy of Svartlidens, Sweden. (30 hp)



LUND'S UNIVERSITET